30 F

SHORT RESIDENCE TIME PYROLYSIS AND HYDROPYROLYSIS OF BITUMINOUS COAL

by

Sharon Lee Szydlowski

B.S., University of Wisconsin-Milwaukee, 1978

A MASTER'S THESIS

submitted in partial fulfillment of the
requirements for the degree

Master of Science

Department of Mechanical Engineering
KANSAS STATE UNIVERSITY
Manhattan, Kansas

1980

Approved by:

Thomas W. Lester
Co-Major Professor

R. E. Cranz
Co-Major Professor

TABLE OF CONTENTS

LIST OF ILLUSTRATIONS

List of Illustrations - continued

List of Illustrations - continued

LIST OF TABLES

1.0 INTRODUCTION

National policy calls for the increasing replacement of petroleum and petroleum products by synthetic fuels. Coal, our most abundant fossil energy resource, is targeted as the feedstock for much of this synthetic fuel need. The product of slow decomposition of organic matter deposited in prehistoric times, coal consists of carbon, hydrogen, oxygen, nitrogen, and sulfur in various amounts. The extent of organic decomposition is reflected in the amount of carbon present, with pure carbon corresponding to complete decomposition. Hence coal varies from region to region, and can vary from seam to seam. Coal can meet energy needs by direct burning, gasification, or liquefaction. Unfortunately, the use of coal in any of these modes brings a host of technological problems, the most important being the potential for severe water and air pollution.

Conversion technology for coal has existed in this country for over a century. Synthetic oil production in the U.S. peaked in 1858. Led by the Downer Company of Boston, the industry produced about 900,000 gallons of "coal oil" in that year before the Drake oil well.[1] Nevertheless, the old processes are inefficient and environmentally unsound.[2] The availability and relatively inexpensive price of petroleum products caused research to be sharply curtailed in the production of synthetic fuels from coal during the sixties. The past decade, however, has seen a new surge in coal research. This investigation was conducted to determine the effects that residence time, temperature, and surrounding gaseous atmospheres had on product yields and product distributions obtained from the pyrolysis of a bituminous coal. Coal pyrolysis was carried out in argon and argon/hydrogen atmospheres at total reaction pressures of 10 ± 1 atm. Dis-

cussion of the experimental technique employed and results obtained follows a review of previous investigations on coal pyrolysis. The purpose of the accompanying discussion is to give the reader a brief overview of the current understanding of the kinetics and mechanism of coal conversion. The interested reader is referred to several recent review articles[3,4,5] for a more thorough coverage of this voluminous topic.

1.1 Pyrolysis: Kinetics and Mechanisms

Much research during the beginning of the seventies was directed toward developing a better understanding of the physical and chemical mechanism of pulverized coal combustion. Two conflicting theories on the ignition of a single coal particle in an oxidizing environment have been proposed; heterogeneous combustion and the "Faraday" mechansim.[6] The Faraday mechanism proposes ignition of the gas phase volatiles ejected from the coal during the early stages of heat up or continuously throughout the combustion process, while heterogeneous combustion proposes ignition on the particle surface followed by volatile release. In either event, it is obvious that volatile production and composition can be a controlling factor in ignition of coal particles. Research into the devolatilization of coal prior to ignition has contributed directly to our understanding of gasification and liquefaction. Most devolatilization research has concentrated on developing a global model of coal pyrolysis suitable for all coals. Typically, a first order decomposition mechanism has been proposed by various researchers, differing only in the Arrhenius rate constants. Unfortunately, these models have only been valid for a specific coal under the experimental conditions from which they were derived.[7]

An example of the studies in which ignition was a prime interest is that of Badzioch and Hawksley,[8] who studied the effect that pyrolysis of pulverized coal particles had on their subsequent ignition. Using

a laminar flow furnace, they investigated the pyrolysis of ten bituminous coals and one semianthracite coal over a temperature range of 400 to 1000 °C at heating rates of 2.5 to 5.0 x 10^4 °C/sec. The extent of thermal decomposition, (weight loss), was measured for times ranging from 30 to 110 milliseconds. The significant finding of this research was that the extent of thermal decomposition exceeded that of the ASTM proximate analysis[9] by factors ranging from 1.3 to 1.8, a result the authors attributed to the higher heating rates employed.

Badzioch and Hawksley's research is significant for the questions it raised about the pyrolysis mechanism, and not for the answers it supplied (as it turns out erroneously). Determining the volatile content of coal as stated in the ASTM handbook is a captive method, conducted at low heating rates, 15 °C/sec. A one gram sample of the coal is placed in a platinum crucible and covered with a close fitting lid. The crucible is then placed in a furnace, maintained at 950 °C, where it is heated for exactly seven minutes. The crucible is removed from the furnace, allowed to cool to room temperature, and then weighed. The percentage of volatile matter in the coal is the weight loss exclusive of that attributed to water. Badzioch and Hawksley, in their conclusions, did not discuss the fact that the coal particles in their experiment were dispersed in the nitrogen carrier gas, and therefore, acted independently of each other. Insofar as their particles (nominally 20 μm diameter) are conceivably much smaller than those used in the ASTM analysis, there may also have been some influence of particle size on the ultimate yield. This, in fact is the argument of Gray, et al.[10],

who argue that the increase in volatile production may not be due solely to heating rate, but may also be influenced by particle interactions. This question is dealt with in more detail by Wegener.[11]

Menster, et al.[12], was one of the first group of researchers to identify and quantify products of coal pyrolysis. Using four bituminous coals and one subbituminous coal, devolatilization by rapid heating was studied over a temperature range of 400 to 1150 °C. Twenty-five milligram coal samples were placed on pulse-heated wire screen cylinders, and heated under vacuum at a rate of 8250 °C/sec. The weight loss data were recorded, and mass spectrometry analysis performed on the gaseous products. The four bituminous coals showed a characteristic weight loss curve (Figure 1) showing volatile loss reaching a peak between 700 to 900 °C. It is of interest to note that the bituminous coals, regardless of volatile content, display the same temperature dependent behavior. After reaching a peak volatile loss, the two bituminous coals with higher aliphatic hydrogen contents, (assuming aliphatic hydrogen increases as coal rank decreases), display an anomalous behavior in which the weight loss decreases with increasing temperature over a range of approximately 400 °C. The higher rank bituminous coals (numbers 3 and 4 on Figure 1) also display this behavior, but not to the same extent. The overall weight loss behavior of the bituminous coals under conditions of rapid heating varies considerably from that observed under conditions of slow heating. During slow heating, weight loss increases monotonically with increasing temperature.[13] The subbituminous coal showed no peak production, but exhibited a plateau

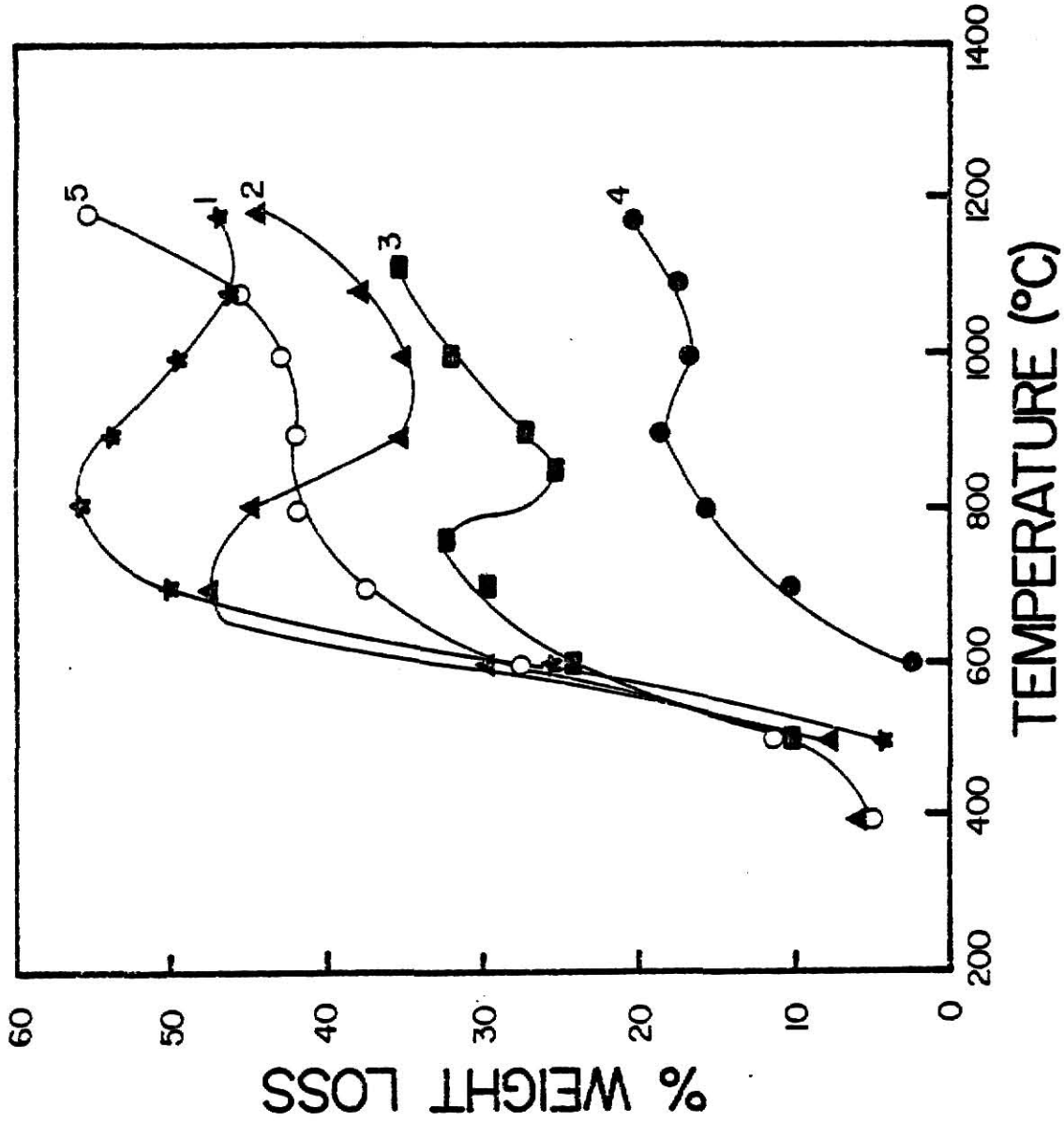

Fig. 1. Percent weight loss as a function of temperature for four bituminous and one subbituminous coals (from 12). Numbers 1 through 4 represent bituminous coals, in order of decreasing aliphatic hydrogen content, number 5 denotes the subbituminous coal.

between 800 to 1000 °C. (See Figure 1.) This plateau can be attributed to the competition for aliphatic hydrogen from the hydroxyl groups that should be more numerous in the subbituminous coal.[14] The principal stable products in the pyrolysate were H_2, CH_4, and CO. Menster found that tar formation was favored over gaseous products at low decomposition temperatures and that tar was the main pyrolysis product at all temperatures up to 1000 °C.† No acetylene was detected in the gaseous products, very likely because of the relatively low temperatures over which this study was conducted. As in previous work, Menster found the volatile yield to be greater than that determined from the ASTM standard test. However, in this instance the enhanced yields were attributed to the temperature dependence of decomposition reactions and to recombination reactions. From the appearance of the weight loss curves, Menster speculated that competitive reactions are occurring between bond cleavage and recombination of fragments. Bond cleavage reactions, that produce the initial decomposition fragments, may be more strongly temperature dependent than recombination reactions which can form more stable molecules or lead to repolymerization to coke. Figure 2 shows the product yield versus temperature for a bituminous coal as measured by Menster. It can be seen that above 1000 °C, the increase in gaseous yields appears to be at the expense of the tar yields.

In contrast to the conditions of the above two studies is that of Campbell,[15] who investigated the pyrolysis of a subbituminous

†In this investigation, tar is defined as all products in the liquid phase under experimental conditions.

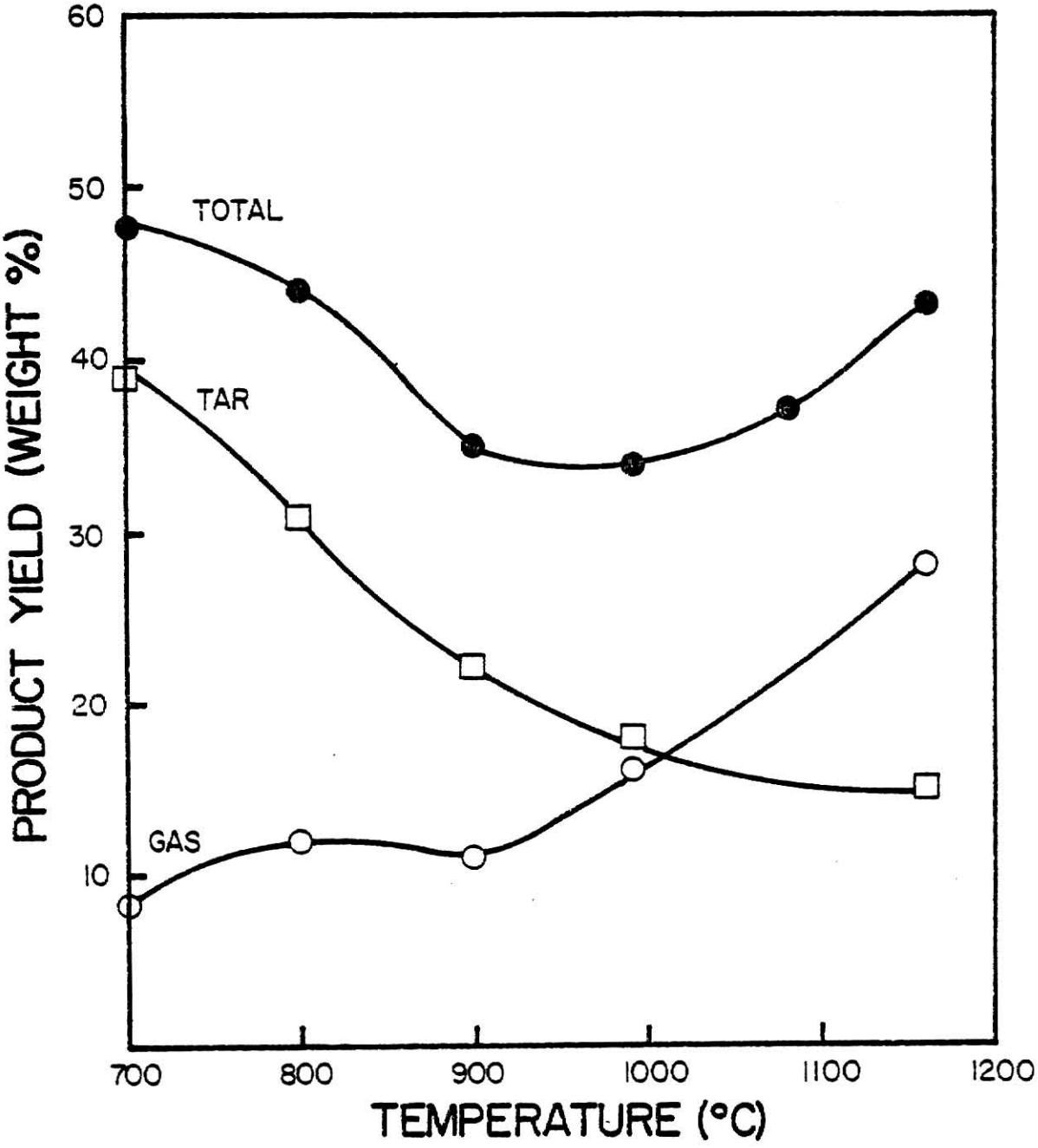

Fig. 2. Percent yield of tar and gas versus temperature for the pyrolysis of a bituminous coal (from 12).

coal. Concerned with enhancing the yields from the underground gasification of subbituminous coal, Campbell investigated coal pyrolysis under slow heating rates, 0.055 °C/sec. The evolution of pyrolysis products was studied over the temperature range of 110 to 1000 °C. The coal used in this study had a size distribution of 1.65 to 3.55 mm, two orders of magnitude larger than used in the preceding two studies.

The coal sample (50 to 60 grams) was loaded into a stainless steel mesh basket, and placed in the reactor on a mass of ceramic balls. The reactor, enclosed by a furnace which was linearly programmed to increase the temperature, was purged continuously with argon at .1 MPa (1 bar). The ceramic balls served to preheat the argon gas flow, and a thermocouple, centered in the coal sample, was used to monitor the pyrolysis temperature.

Campbell, like Menster,[12] discovered that water and tar were the main pyrolysis products at low temperatures; in this study they began evolving at 297 °C and were the major products up to 497 °C.[†] At these temperatures, water comprised 75% of the pyrolysate. Carbon dioxide, the evolution of which began at 250 °C, had two local maxima, one at 520 °C, the other at 750 °C. The CO_2 evolution declined to zero by 850 °C. Campbell postulated that the first maxima was due to carboxylic acid decomposition, while the second maxima resulted from carbonate decomposition of the mineral matter in the coal. Carbon monoxide

---

[†]Tars were defined as all evolved products condensible at 0 °C at 1 MPa.

evolved similarly to CO_2 in that its evolution also displayed two maxima between 497 to 547 °C and 697 to 747 °C. The first maxima is believed due to the rupture of ether and ketone linkages; the second maxima is believed due to degradation of heterocyclic compounds, and/or the product of the Boudouard[16] reaction:

$$CO_2 + C_{(s)} \rightarrow 2CO. \qquad (1.1)$$

At higher temperatures, hydrogen was the major pyrolysis gas, representing nearly 40% (by volume) of the total gas evolved. The volume percentage of hydrogen increased from below detectable amounts at 350 °C, reached a maximum at 827 °C, and declined to near zero by 1000 °C. Most of the hydrogen is presumably formed from the dehydrogenation of the coal, the balance from reactions in the char.

A number of light hydrocarbons, principally C_1 and C_2 species, were produced and displayed individual maxima in the temperature range of 500 to 630 °C. The evolution of hydrocarbon gases results primarily from dealkylation; however, methane evolution at higher temperatures appears to be from char-auto hydrogenation reactions.

Campbell calculated global activation energies and Arrhenius rate constants for the gaseous products evolved using a decomposition reaction, first order in the remaining functional group to be evolved. Except for the evolution of hydrogen, consecutive first order reactions were required to describe the gas evolution. The technique of consecutive first order reactions has also been employed by Suuberg.[17,18]

Global activation energies and Arrhenius rate constants as determined by Campbell are given in Table 1.

It is noteworthy that Campbells weight loss mirrors that of Menster.[12] Over a temperature range of approximately 200 °C, from 540 to 727 °C, there exists a constant rate of gas evolution. Figure 3 shows the combined evolution of CH_4, CO and CO_2 versus temperature. Although the relative proportions of the gases change, the total amount remains the same. Also of note is the distinct evolution of CH_4 as seen in Figure 4. From Figure 4 it can be deduced that CH_4 evolution is temperature dependent and independent of coal rank.

Although Campbell's kinetic data on gaseous pyrolysis products is an important contribution to the understanding of pyrolysis phenomena, his work with liquid and solid residue is of equal value. Studying the char formed at various temperatures, Campbell found that sulfur was preferentially released during tar formation, but that nitrogen is retained in the char matrix until tar evolution ceases. Surface area of the char was also measured, and found to increase to a maximum at 730 °C, before decreasing with increasing temperature. The percent of products as liquids reached a maximum value at 500 °C and remained constant at this value with increasing temperature.

Campbell's work provides a plausibly conceptual framework of the mechanism of gaseous and liquid product formation during very slow heating rates. Although Campbell did not use functional groups in evaluating his kinetic parameters, he did identify which functional groups he felt were contributing to product formation at various temperatures. The observation of different partitioning of sulfur

Table 1. Global activation energies and Arrhenius rate constants*.

Investigator	Campbell		Solomon		Suuberg	
Component	Activation energy	Pre-exponential factor	Activation energy	Pre-exponential factor	Activation energy	Pre-exponential factor
H_2	93.4	20	26.8	3600	376	10^{17}
CH_4	130	1.7×10^5	20.5	2300	230	10^{13}
	130	2.8×10^4			272	10^{13}
	148	3.0×10^4				
C_2H_4	140	2.3×10^6	--	--	230	10^{13}
					272	10^{13}
C_2H_6	140	1.7×10^6	--	--	230	10^{13}
C_3H_8	147	7.3×10^6	--	--	167	10^{13}
					184	10^{13}
					272	10^{13}
CO	75.4	55	21.7	7000	230	10^{13}
	126	2.5×10^3	25.3	890	272	10^{13}
CO_2	81.6	550	8.4	6	167	10^{13}
	96.3	230			272	10^{13}
light liquids	--	--	--	--	167	10^{13}
					230	10^{13}
tars	--	--	16.9	750	--	--
H_2O	--	--	10.4	15	73.8	10^{13}

*Activation energies are in kJ/mol; pre-exponential factors are sec^{-1}. Multiple values reflect in the use of consecutive reactions to describe devolatilization behavior.

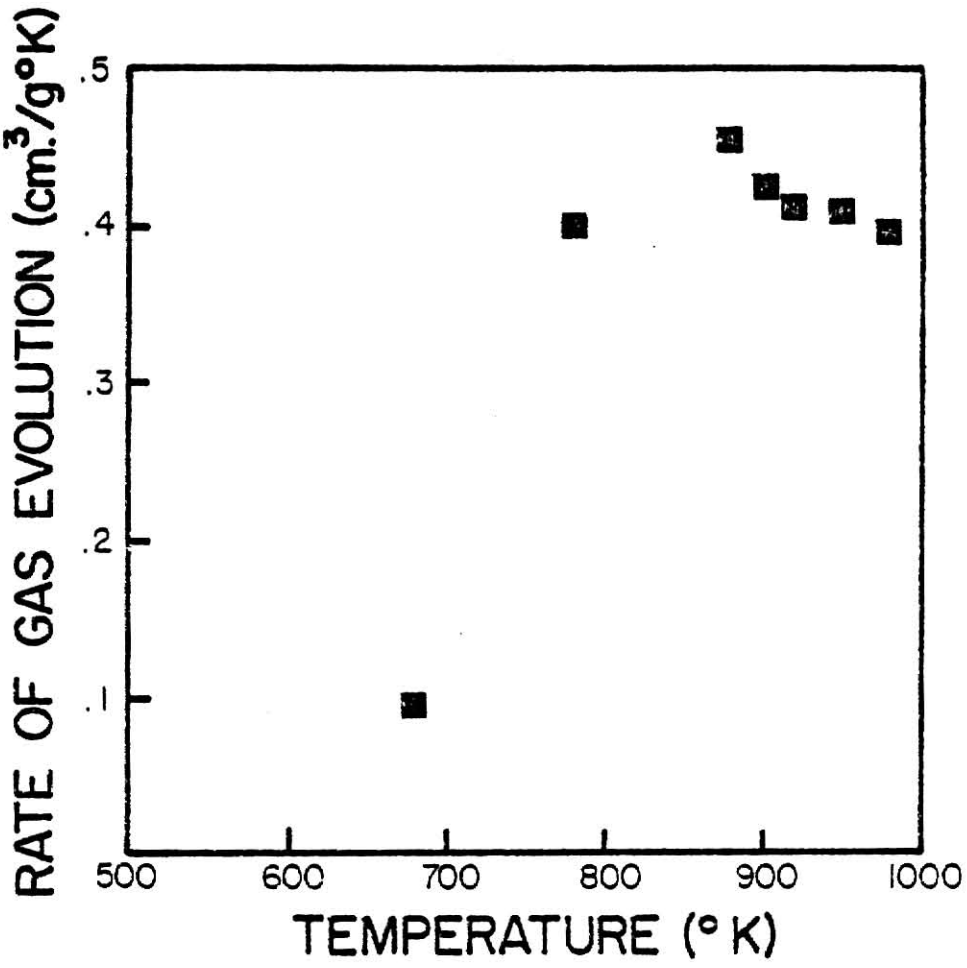

Fig. 3. Combined evolution of CO_2, CO and CH_4 versus temperature for a subbituminous coal[2] (from 15).

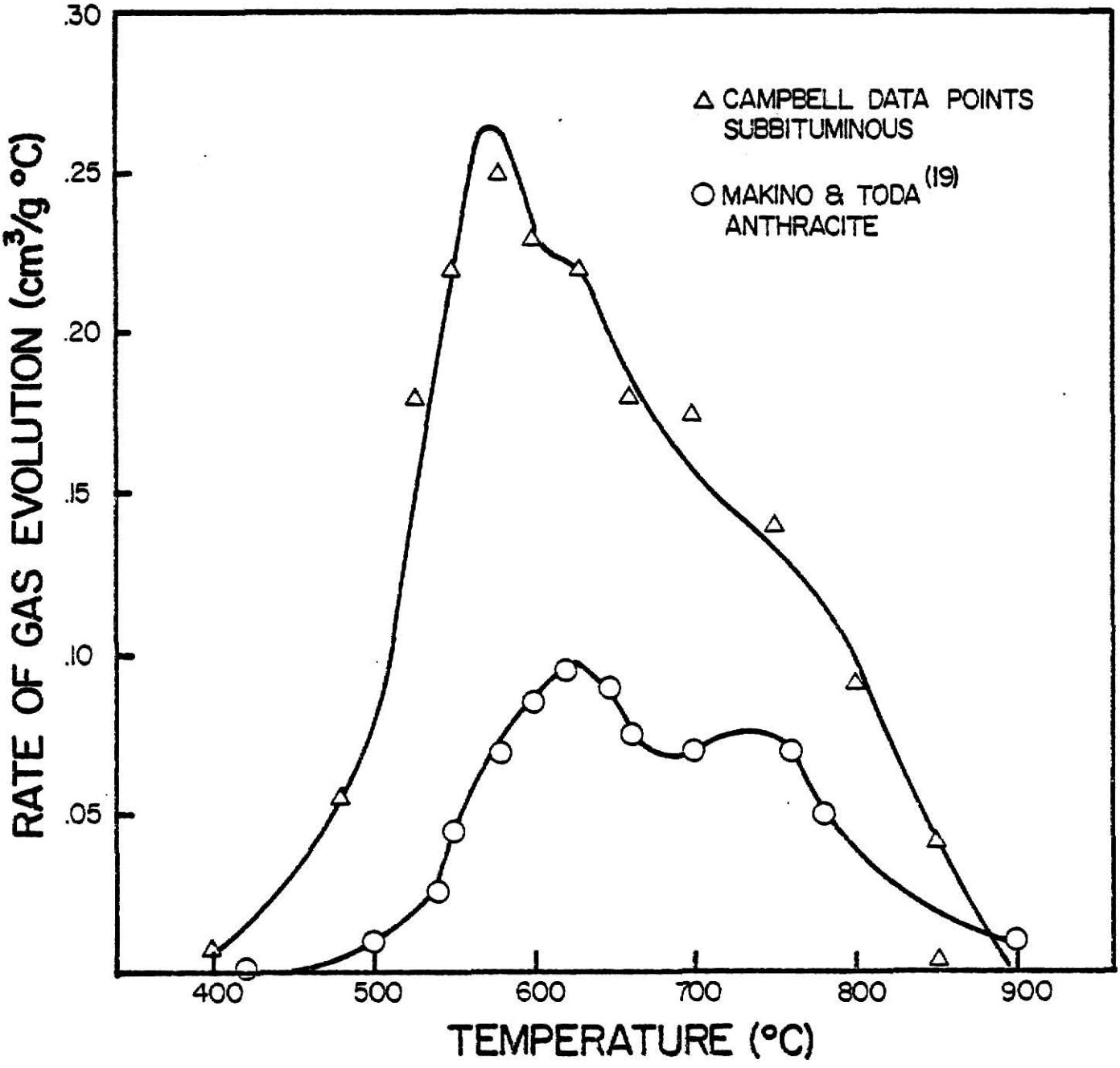

Fig. 4. Evolution of methane during coal pyrolysis as a function of temperature (from 15 and 19). The amount of methane evolved is different for each coal, reflecting the difference in the amount of functional groups possessed by each coal.

and nitrogen between volatiles and char is helpful in understanding the formation of pollutants. A note of caution is warranted, however. The uncertainty with regard to the influence of heating rate on total yield and product distribution makes extrapolation of these results precarious. Transport phenomena, both internal and external to the coal, may have a decisive influence on what products are ultimately realized from pyrolysis.

Tyler[20], at CSIRO (Commonwealth Scientific and Industrial Research Organization), conducted devolatilization experiments on a Victorian brown coal over the temperature range of 400 to 1000 °C at atmospheric pressure. Two size factions, (76-104 μm and 44-53 μm), were subjected to heating rates in excess of 10^4 °C/sec in atmospheres of both nitrogen and hydrogen. The coal particles, entrained in a stream of gas, were heated by direct injection into a heated, fluidized bed of sand. A stream of nitrogen gas at room temperature served as a coolant for the injection probe, and, by issuing from the probe directly over the bed, also served as a quenching medium. The residence time of the coal particles in the bed was estimated to be 300 milliseconds. The residence time of the gas above the hot zone of the bed was estimated to be 400 milliseconds.

The effluent products passed from the pyrolyser into a tar trap cooled with ice or a mixture of CO_2/alcohol. The tar trap was fitted with a Soxhlet[22] thimble which acted as a filter. The Soxhlet thimble was reportedly nearly 100% efficient in removing tar vapors and char

from the effluent stream. After passing the tar trap, samples of the effluent stream were taken and analyzed for C_1-C_6 hydrocarbons by gas chromatography. Tar and char were recovered by solvent washing of the pyrolyser outlet, tar trap, and solvent extraction of the Soxhlet thimble. Tars were defined as the material recovered that was not volatile under conditions of solvent removal.

Tyler reported pyrolysis yields of C_1-C_6 hydrocarbons along with tar and char yields at various temperatures. When pyrolysis was performed in an inert atmosphere (nitrogen), tar yields increased rapidly with increasing temperature, reaching a maximum value of 23% (w/w dry, ash free basis) at 580 °C, and then declined with increasing temperature. Total volatile matter increased continuously with increasing temperature, from 47% at 580 °C to 63% at 900 °C. Gaseous hydrocarbons increased progressively with temperature, with total C_1-C_3 hydrocarbons comprising 8% of the volatile yield at 900 °C. As the pyrolysis temperature increased, the tar atomic H/C ratio decreased from 1.35 to .85 at temperatures of 435 and 900 °C, respectively.

Subsequent research[21] with the same apparatus and methodology investigated the devolatilization behavior of ten bituminous coals in helium and hydrogen atmospheres. Tyler found that all coals studied behaved similarly to the Victorian brown coal used in the preceding study; gaseous hydrocarbons, tars and total volatile yields showed the same temperature dependent behavior (see Figure 5). Tyler correlated tar yields to the H/C ratio of the original coal. Yields were found to increase with increasing H/C ratio. As in the preceding

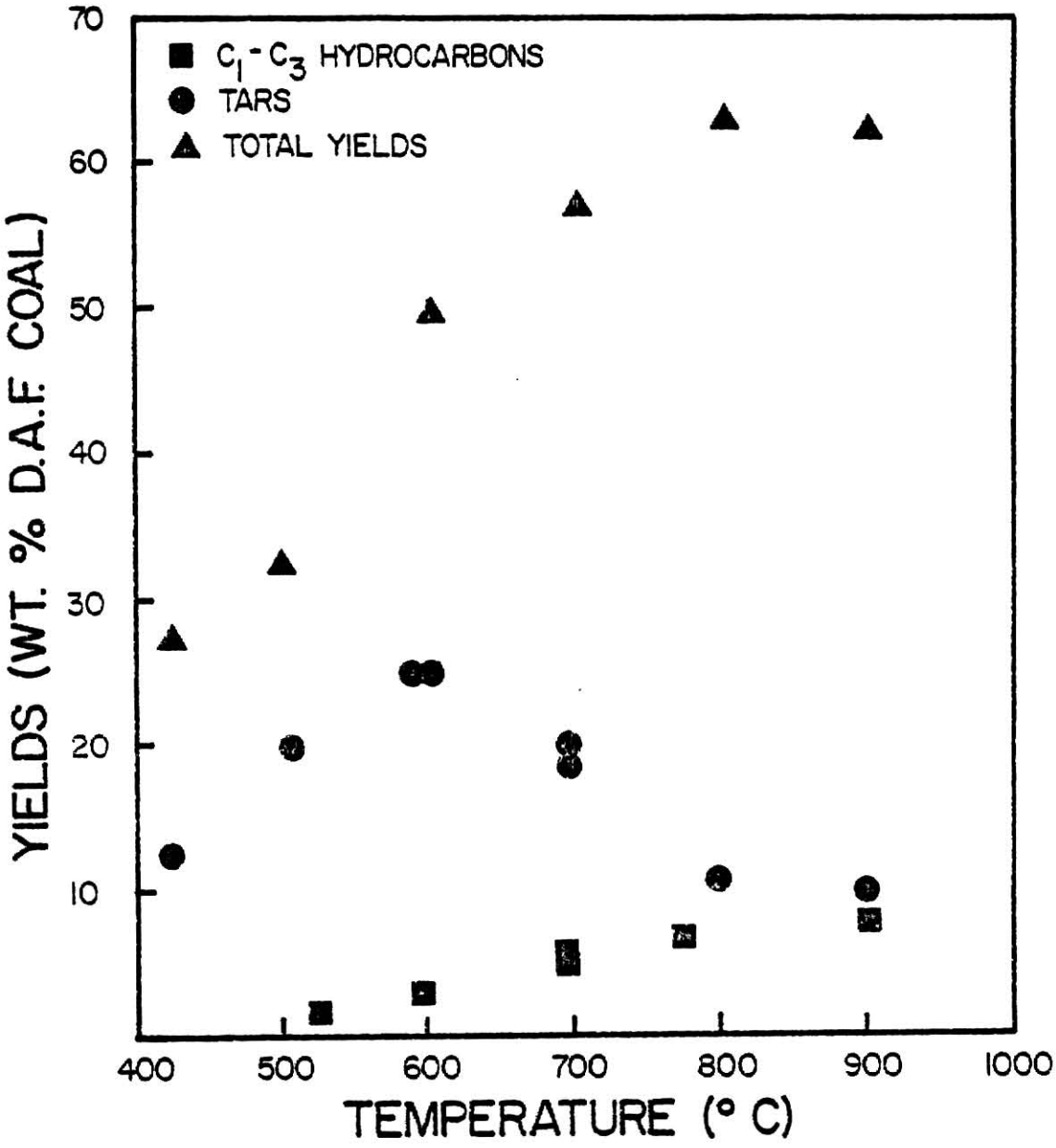

Fig. 5. Pyrolysis product evolution as a function of temperature for a brown coal (from 20).

study, the H/C ratio of the tars was similar to that of the original coal and decreased with increasing temperature.

An interesting aspect of this study is the devolatilization behavior of the Pittsburgh seam coal. This coal, supplied by Jack Howard at M.I.T., had been used in studies discussed later in this text on devolatilization by rapid heating[7,17,18,26,27]. The devolatilization behavior of the coal with respect to temperature is shown in Figure 6; data obtained by researchers at M.I.T. are also plotted. It can be seen that Tyler's total volatile yield exceeds that obtained at M.I.T. This increase in yields was attributed in part to tar recovery techniques employed by Tyler. It should be noted that the heating rates employed in these studies are different; 10^4 °C/sec used by Tyler, 750 °C/sec used in the M.I.T. studies. Also of interest is the evolution of methane, shown in Figure 7, and the evolution of tar, shown in Figure 8. Both species display different evolution behavior with respect to the studies at M.I.T.; however the evolution behavior observed by Tyler is similar to that observed by Menster[12] for bituminous coals. The reader should note that the M.I.T. work was performed in an atmosphere at 23 °C while the CSIRO work was conducted in a hot gas environment. More will be said about this later.

An example of pyrolysis experiments under moderate heating rates in which complete product distributions were determined is the recent work of Solomon and Colket.[23] Pyrolysis was carried out, (according to the authors under isothermal conditions after a heat up at 600 °C/sec), in an electrically heated grid apparatus at times varying from 3 to

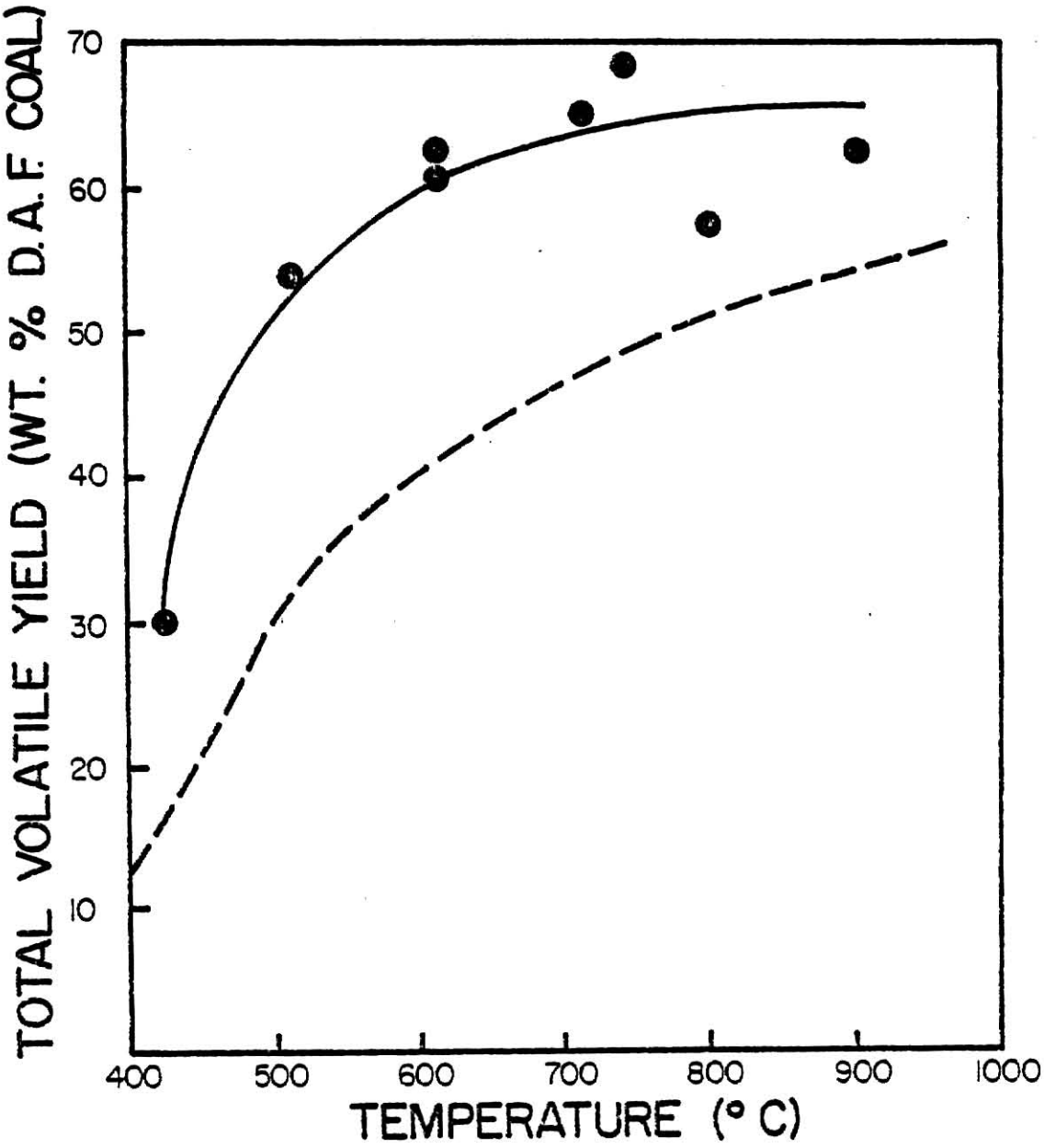

Fig. 6. Total volatile yield as a function of temperature from the pyrolysis of Pittsburgh seam coal in helium. Solid line and circles from Tyler[21], dashed line from Anthony[7].

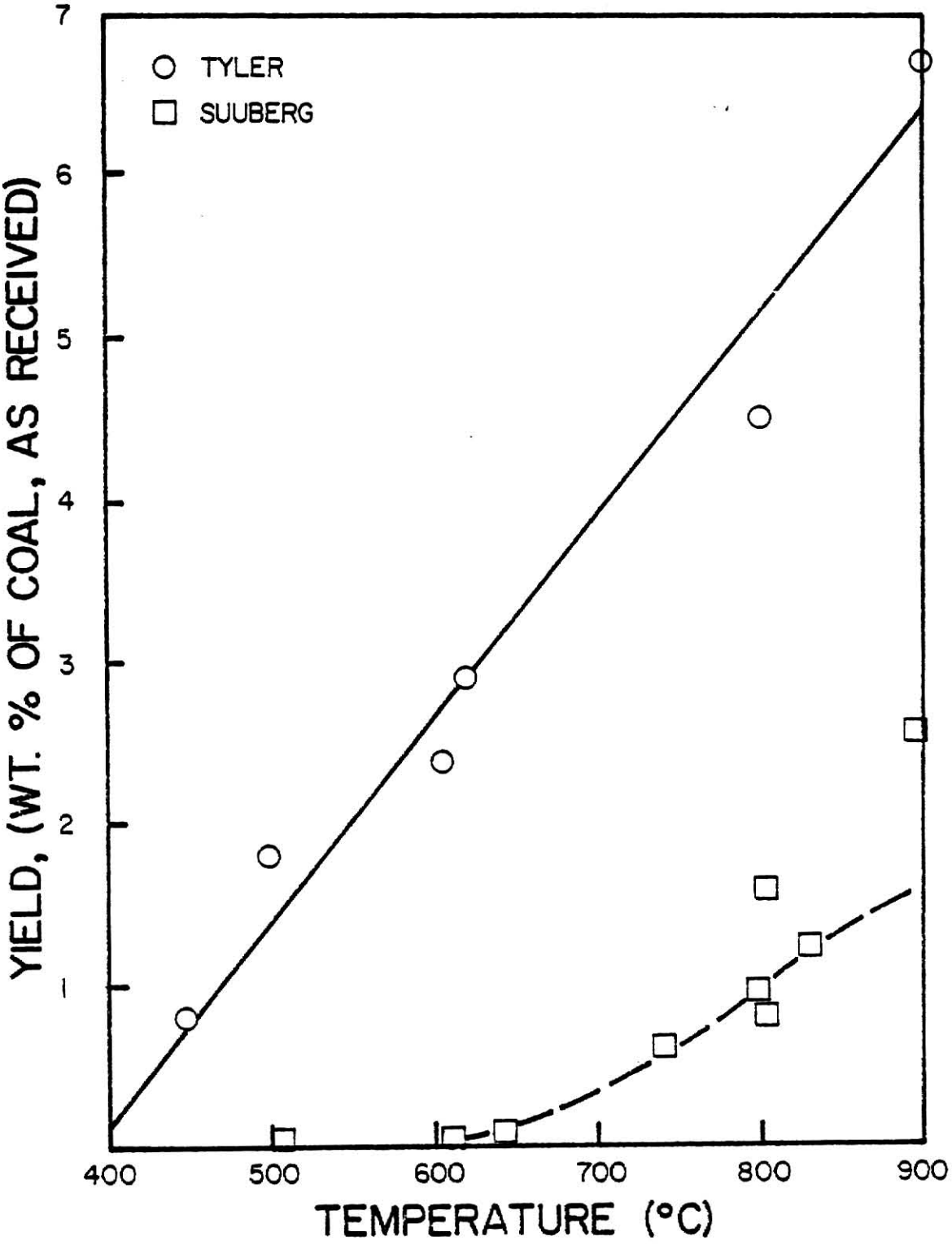

Fig. 7. Evolution of methane from the pyrolysis of Pittsburgh Seam coal as a function of temperature (from 21 and 18).

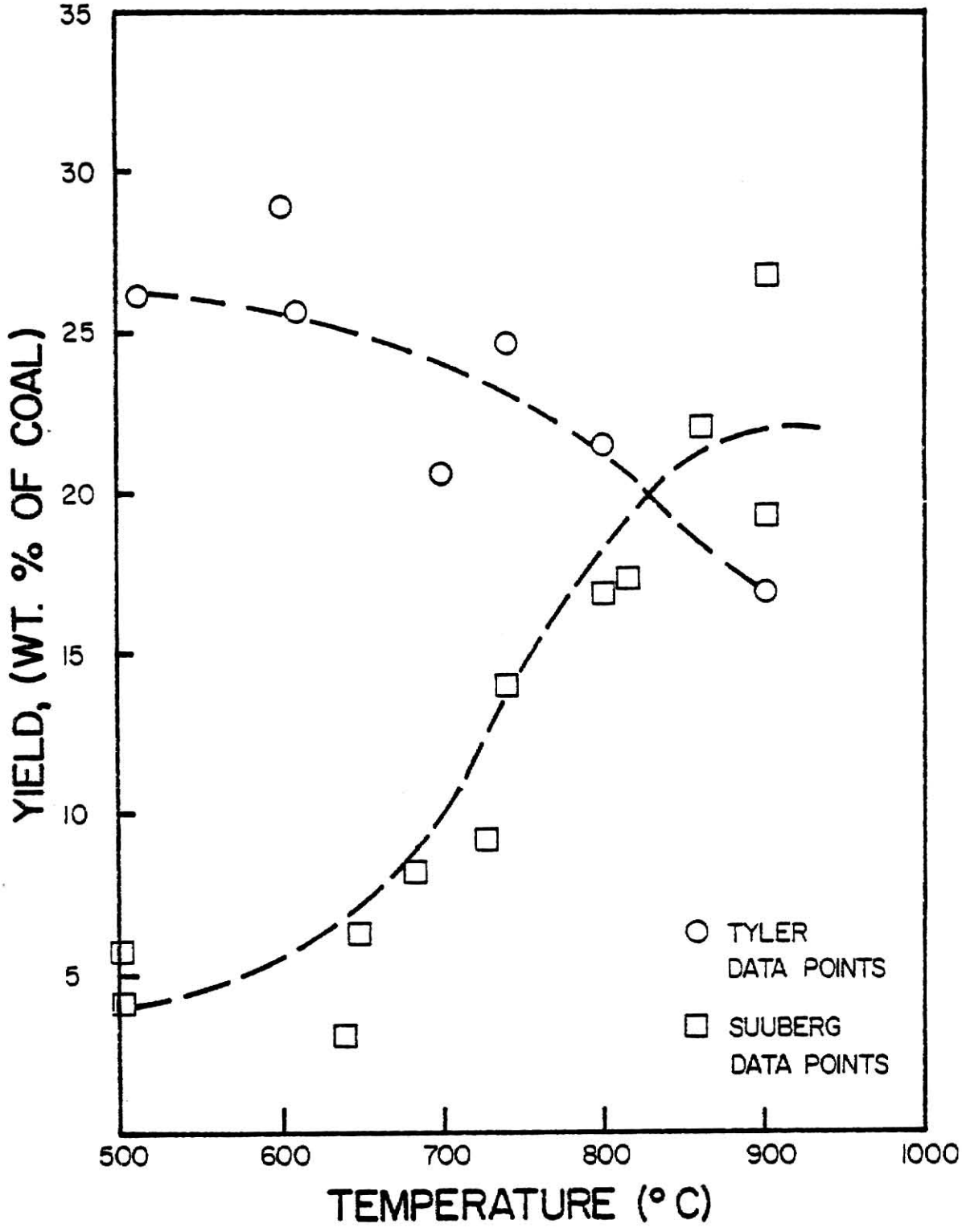

Fig. 8. Evolution of tar from the pyrolysis of Pittsburgh Seam coal as a function of temperature (from 21 and 18).

78 sec. Twelve bituminous coals and one lignite were subjected to vacuum devolatilization over a temperature range of 300 to 1250 °C. The striking result of this research as shown in Figure 9 is that the temperature dependent evolution (at a specific heating rate) of a particular species is similar for all coals, even though the amount of species may vary substantially from one coal to another. The reader is reminded of the weight loss data of Menster[12] (Figure 1), and of the data obtained by Tyler[20,21] (Figure 5) which also displayed this temperature dependent behavior. The authors modeled the evolution of each species by a decomposition reaction, first order in the remaining amount of species to be formed. The Arrhenius pre-exponential factor and activation energy for each species did not change for coals of different ranks. The difference in amount of the species formed from each coal is attributed to the various mix of functional groups possessed by that coal. Hence a coal with a higher aliphatic hydrogen content is predicted to produce more hydrocarbons than a coal with a lower aliphatic hydrogen content. In modeling devolatilization, the authors considered tar evolution and parallel evolution of smaller molecular species. The modeling efforts of the authors are similar to Campbell[15] in their consideration of species evolution as a function of the functional groups possessed by the parent coal. The kinetic parameters, shown in Table 1, are lower than those normally found in the literature. There is considerable doubt as to the validity of the kinetic parameters when extrapolating to temperatures outside the range of this study, or when using heating

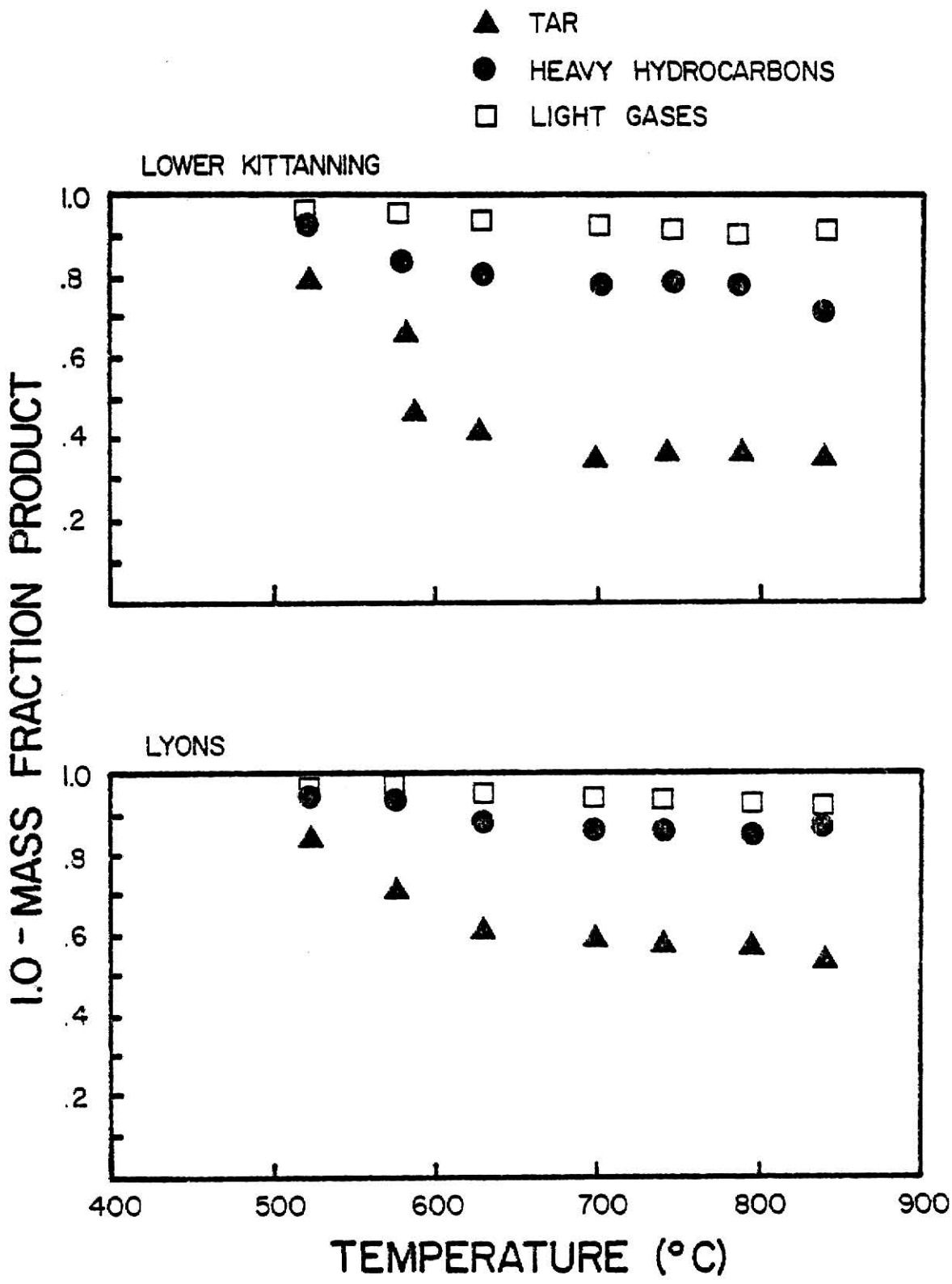

Fig. 9. Evolution of pyrolysis products for two bituminous coals as a function of temperature (from 23).

rates not employed in this study, as brought out by Suuberg and Howard at the Seventeenth Combustion Symposium.

No stepwise behavior of product evolution was noted in this study; except for CO, product evolution monotonically increased with increasing temperature to a maximum value where it remained constant with further increases in temperature.

Infrared analysis of the tar formed showed it to have a molecular structure similar to that of the parent coal; the major difference was that the hydrogen content of the tar was approximately 20% greater than that of the parent coal. Analysis of low temperature char showed it to possess a structure similar to that of the parent coal. Tar is formed, presumably, by the breakage of weak linkages between aromatic clusters in the coal molecule. This produces free radical sites which can recombine for stabilization, or can be stabilized by the addition of hydrogen. From analysis of the tar, it appears that stabilization by hydrogen is the preferred kinetic route.

Concurrent research[24] by the authors on the evolution of nitrogen from coal during devolatilization found volatile nitrogen to be distributed between the tar fraction and the gaseous fraction. The nitrogen content of the tar fraction was identical to that of the parent coal and remained constant at all temperatures. Initially nitrogen evolves from the coal in heavy tar molecules, and at higher temperatures it evolves as a gas from the char. These processes occur by different kinetic mechanisms and hence have different kinetic rates. Beer,[25] in recent work, shows that there are distinctive differences in nitrogen evolution

between ranks of coal. This lends support to Solomon and Colket's hypothesis that species formation is most dependent on the functional groups possessed by the coal.

A similar apparatus, but a different experimental technique, was employed by Anthony[7] and Anthony et al,[26,27] in an investigation of devolatilization under rapid heating conditions. Anthony varied five different parameters to study the influence of each on the weight loss. Specifically of interest were heating rate, particle size, temperature, residence time, and total pressure of inert gas and partial pressures of hydrogen gas. Two different coals were used in this study, a Pittsburgh seam bituminous coal and a North Dakota lignite. Weight loss of the coal was measured, but product composition was left for a follow-up study by Suuberg[17,18].

For the lignite, Anthony found no difference in ultimate yields under different heating rates or total inert gas pressure. Increasing hydrogen pressure did cause an increase in volatile yields from the lignite, and volatile yields increased with increasing temperature. Anthony used several different residence times in his study, and found maximum weight loss could be achieved in 100 ms when the lignite was subjected to a heating rate of 10,000 °C/sec. Coal devolatilization occurred very fast, virtually ceasing within a second in both inert and hydrogen atmospheres.

The bituminous coal behavior under rapid heating was different than that observed with the lignite. Increasing inert gas pressure resulted in decreasing volatile yields at 69 atm pressure (see Figure

10). Heating rate had a moderate effect on yields, insofar as increasing the rate from 6.5×10^2 to 10^4 increased the yields by only two percentage points. As with the lignite, increasing hydrogen partial pressure and increasing temperatures resulted in increased yields.

In attempts to model devolatilization, Anthony also employed a decomposition mechanism, first order with respect to the amount of product yet to be formed. Believing multiple reactions to be occurring, Anthony postulated the use of multiple activation energies, which for mathematical simplicity, were assumed to have a Gaussian distribution. This model is somewhat satisfying as it provides a plausible explanation for the low activation energies found by a single step, first order model.[8] As demonstrated by Juntgen and Van Heek[28], a set of overlapping, independent, parallel first order reactions can be approximated by a single first order model having both lower activation energy and pre-exponential factor than any of the reactions in the set.

Suuberg, et al.[17,18] in their follow-up study to Anthony measured the product evolution for both lignite and biutminous coals. Five different phases of lignite pyrolysis were identified:

1) low temperature moisture removal (~100 °C);
2) evolution of CO_2 and tar (450 °C);
3) evolution of pyrolytically formed water (500-700 °C);
4) evolution of hydrocarbons, carbon oxides, and hydrogen (700-900 °C);
5) high temperature formation of carbon oxides (1100 °C).

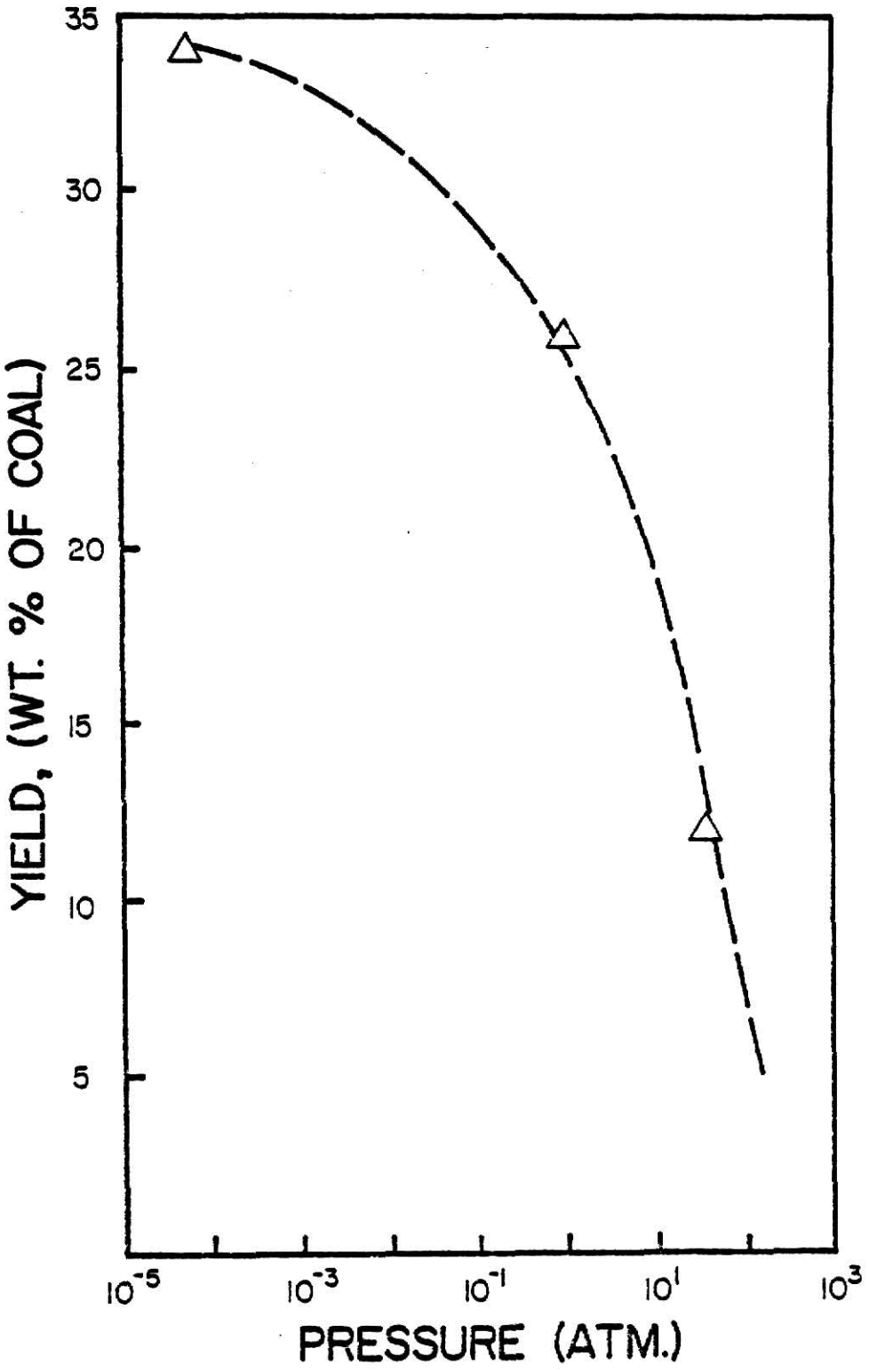

Fig. 10. Effect of pressure on yields obtained from the pyrolysis of a bituminous coal (from 7).

These observations were made in a baseline study with 1 atm helium pressure and heating rate of 1000 °C/sec. Bituminous coal pyrolysis, although not having distinct regions, was broken down into four general stages:

1) low temperature moisture removal (~100 °C);
2) evolution of pyrolytically formed water (300-400 °C);
3) tar and hydrocarbon evolution (400-900 °C);
4) evolution of carbon monoxide and hydrogen (>900 °C).

In the case of lignite pyrolysis all gaseous yields (Figure 11) reached their ultimate values around 800 °C, and remained constant with increasing temperature. These trends all are in qualitiative agreement with those reported by Solomon and Colket,[23,24] except for carbon monoxide, which was observed to increase steadily with increasing temperature in the latter work (see Figure 12). However, this could be attributed to the increased oxygen content of the coal with respect to that studied by Suuberg.[17,18] The lignite pyrolysis products are dominated by oxygenated species and show a marked stepwise behavior for most of the products. This behavior has led the authors to postulate that products may be evolved from more than one structure of the coal via different kinetic pathways.

Bituminous coal pyrolysis products were dominated by hydrocarbons and tars. Pyrolytically formed water evolved at lower temperatures than observed with the lignite, a difference the author attributed to the difference in chemical nature of the hydroxyl groups in the coals. The author believes pyrolytically formed water in bituminous coal devolatilization is characterized by a lower activation energy than that observed in lignite devolatilization. Methane and tar yields

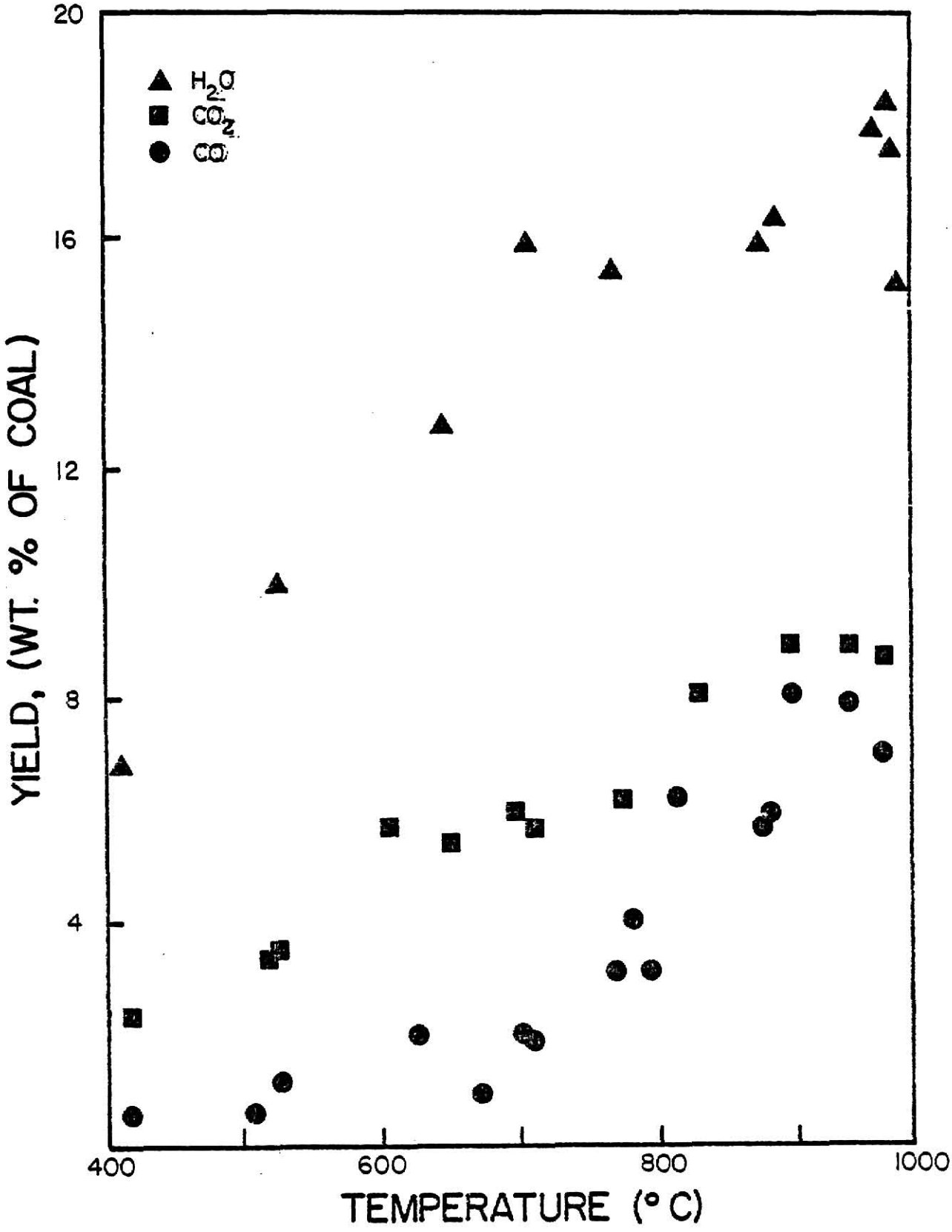

Fig. 11. Yields of H_2O, CO and CO_2 as a function of temperature from the pyrolysis of lignite in helium. (From 18).

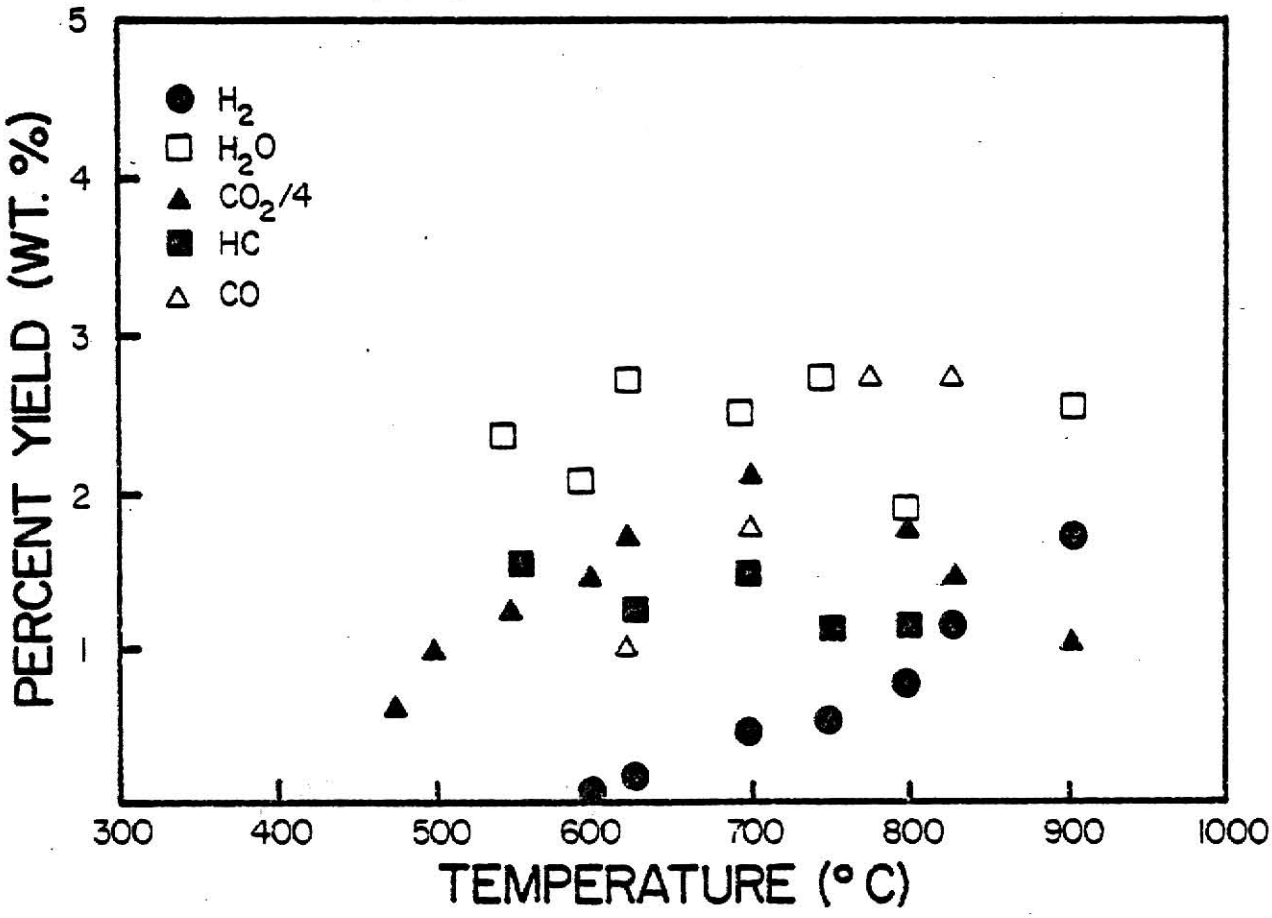

Fig. 12. Gaseous product yields as a function of temperature for the pyrolysis of lignite *in vacuo*. (From 23).

were found to reach a plateau above 800 °C; however, if higher temperatures had been studied, it seems likely that both yields may have decreased.

Sulfur and nitrogen contents of the chars were measured, showing sulfur to be evolved more easily than the nitrogen from both the lignite and bituminous coals. Only 1/4 to 1/3 of the nitrogen was evolved by 1000 °C, whereas 1/2 to 2/3 of the sulfur was converted.

In modeling both the lignite and bituminous coal devolatilization, Suuberg, similarly to Anthony,[26,27] used multiple first order reactions with a distribution of activation energies. The basic difference between the two modeling schemes is the use of different pre-exponential factors and consecutive reactions rather than parallel reactions. Suuberg's analysis uses reactions for each species evolved (i.e., CH_4, CO_2, etc.) and employs a first order approximation in remaining species to be evolved. This is an unrealistic concept in that there is no proof that methane comes only from identifiable methyl groups in the coal. Given the present state of knowledge about coal constitution, this model at present is useless in predicting product yields *a priori* from other coals.

It is interesting to compare Anthony's and Suuberg's bituminous coal weight loss data with that obtained by Menster.[12] As can be discerned in Figure 10, Anthony's data do not display the anomalous decrease in yield with increase in temperature that was observed by Menster for all four bituminous coals he studied. It is noteworthy that this behavior has also been observed by Breipohl[29] in a shock tube study on the de-

volatilization of soybean dust and by Johnson[30] in a study on the gasification of coal with hydrogen and steam. The conflicting results could be a consequence of the experimental technique. In the case of Breipohl[29] and Johnson[30], the primary volatile matter was surrounded by an atmosphere of hot gases after ejection from the particle. The "hot" primary fragments almost certainly undergo secondary reactions; in reducing atmospheres, these primary fragments can combine to form aromatic or heterocyclic structures. Once formed these structures are stable and do not decompose until longer times or higher temperatures are reached. However, upon achieving higher temperatures, these aromatic structures decompose producing mainly light hydrocarbons and soot.[31] The following pathway is proposed:

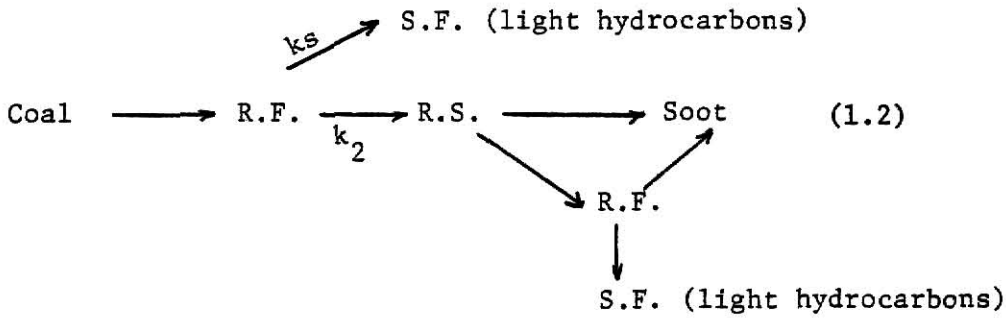

where R.F. stands for radical fragments, S.F. stable fragment, and R.S. recombination species.

When a cold gas surrounds the decomposing coal particle, it can stabilize the radical fragment more effectively, hence, kinetic route 1 dominates. In a hot test gas or vacuum, the radical fragment is not stabilized as effectively by the surrounding test gas, hence

kinetic route 2 dominates. Upon an increase in temperature or time, the recombination species will decompose, yielding light hydrocarbon gases and soot, which then appear in the pyrolysate. In comparing the results of Campbell,[12] Tyler,[20,21] Solomon[23,24] and Suuberg,[17,18] it becomes apparent that the origin of volatile fragments and their subsequent stability plays an integral role in the ultimate yields of pyrolysis products and the product distribution. Aliphatic hydrogen content is believed to play a large role in determining pyrolysis products. For instance, it may be possible to promote the use of internally available aliphatic hydrogen in the stabilization of lower hydrocarbon groups rather than hydroxyl radicals if the heating rate can be increased to such an extent that the production of small hydrocarbon fragments competes effectively with the production of hydroxyl groups. Suuberg and Howard[18] report that at a heating rate of 1000 °C/sec, water forming reactions are about 90% complete before the onset of tar forming reactions while at a heating rate of 2.8×10^5 °C/sec water reactions are only 35% complete before the onset of tar formation, based on their kinetic parameters. Thus control of heating rate and pyrolysis temperature alters product yields. An investigation that does show this effect is that of Wegener.[11]

Wegener studied the pyrolysis of two bituminous coals using a single pulse shock tube. The single pulse shock tube enabled heating rates in excess of 10^6 °C/sec to be obtained. Reaction times were extremely short, normally 1200 μsec ± 150 μsec and cooling rates exceeded -1×10^5 °C/sec. Lower (C_1-C_2) hydrocarbons evolved from the

coal in an inert atmosphere were measured. Methane, ethylene, and ethane yields displayed similar behavior; increasing yields were obtained with increasing temperature. Unlike the results of previous investigators,[15,17,18] yields reached a maximum value, and then declined with increasing temperature. At the onset of the decline in ethane yields (~ 1000 °C) detectable amounts of acetylene were measured. Above 1300 °C acetylene production increased dramatically, never showing a decline over the range of temperatures investigated in this study. Methane and ethylene yields started to decline around 1300 °C. The yields, as reported by Wegener are shown in Figure 13.

Wegener concluded light hydrocarbon formation was primarily the result of C-C bond cleavage in the parent molecules with stabilization by hydrogen. The increase in acetylene production was attributed to increased C-C bond cleavage and fragmentation reactions of higher molecular weight hydrocarbons. A decomposition model, first order in maximum yield to be obtained, predicts an activation energy of 20.7 kcal/mole. Insofar as this value is substantially less than would be expected from a chemical process, either the process at these heating rates becomes limited by transport phenomena or a number of reactions are occurring concurrently.

Polavarapu[33], using the same technique as Wegener,[11] measured the evolution of H_2S and SO_2 from bituminous coals. Polavarapu found H_2S evolution from pyrolysis of coal to increase with increasing temperature to 1250 °C whereupon it suddenly decreased to nearly undetectable amounts. Kinetic analysis yielded an activation energy of 52 $\pm$ 2 kcal/mole

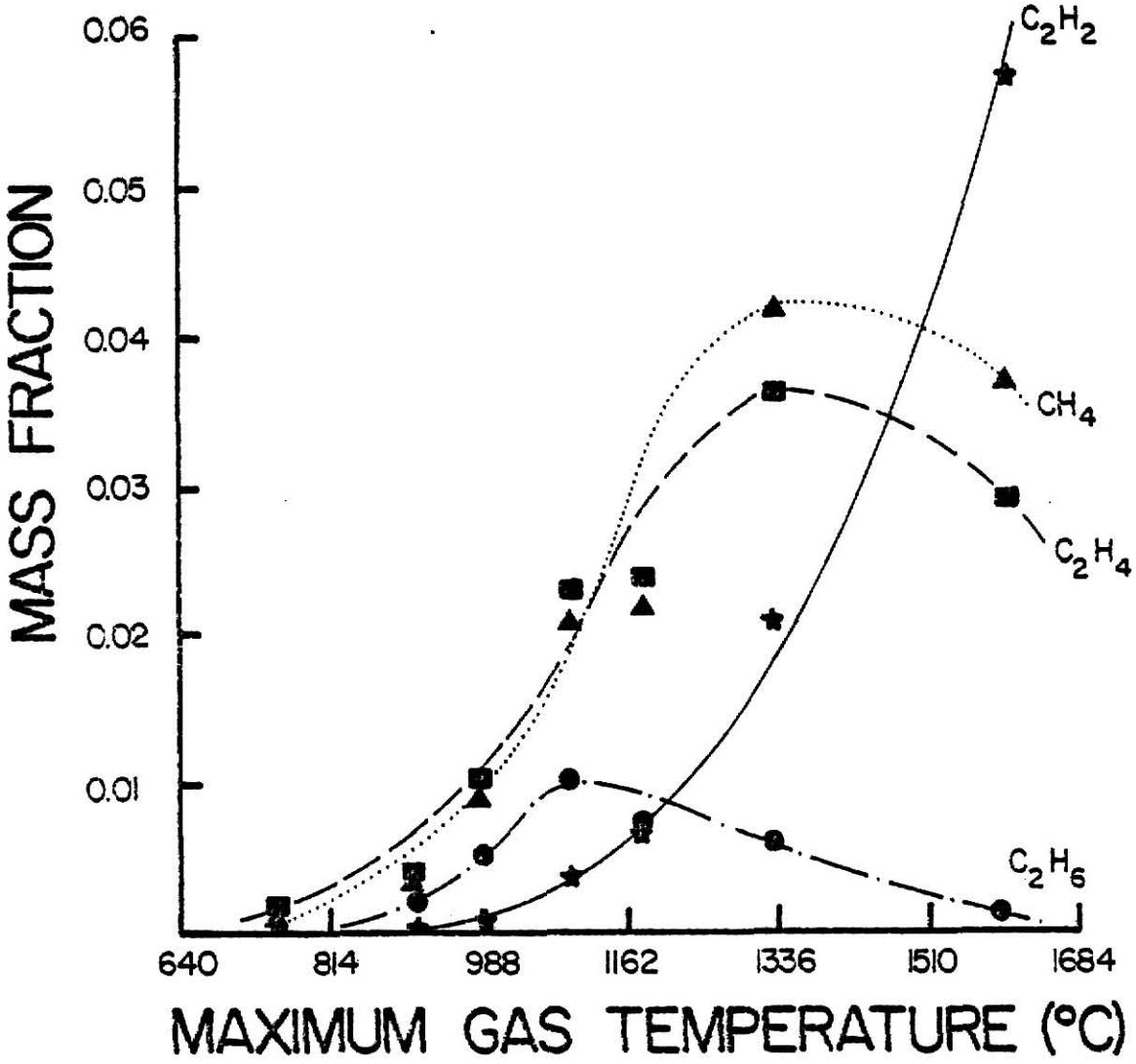

Fig. 13. C_1-C_4 hydrocarbons from the pyrolysis of a Pittsburgh seam coal as a function of temperature (from 11).

for the formation of H_2S from coal. This value is in good agreement with those obtained from the study of model compounds (52 $\pm$ 3 kcal/mole), and implies that H_2S formation is from the rupture of C-S bonds.

The activation energy reported by Polavarapu,[33] coupled with Jungten and Van Heek's[28] theory on parallel reactions, provides a plausible reason or the low activation energy found by Wegener.[11] That is that pyrolysis of coal proceeds by many independent, parallel reactions, each possessing a different activation energy and Arrhenius rate constant.

Another factor that may contribute to the anomalous weight loss behavior is particle size. Seeker, et al.[32] studied pyrolysis of pulverized coal particles to ascertain physical, chemical, and thermal behavior. Using holography as a diagnostic tool, Seeker was able to monitor physical effects occurring to the coal particle during pyrolysis. One of the major findings of this investigation was that physical effects occurring during devolatilization were dependent upon coal type and particle size. Larger bituminous coal particles ($\geq$ 80 μm) ejected a significant portion of volatile matter from the coal in a single jet. This volatile jet then reacts close to the particle producing a trail of small solid particles. Scanning electron micrographs showed particles to be relatively spherical with one large blowhole. Smaller bituminous coal particles, (~40 μm) did not display this behavior; volatile matter tended to diffuse uniformly from the surface. Seeker suggests that the absence of volatile trails in the smaller particles implies that a critical mass of volatile com-

ponent is necessary to build up an internal pressure within the coal particle and escape as a jet. Thus, the evolution of volatiles from the surface of the coal particle may play a significant role in stabilization versus recombination reactions of volatile fragments.

This concludes the review of pyrolysis kinetics and mechanisms. Further discussion is delayed until the end of the chapter.

1.2 Liquefaction and Hydrogasification

A prime objective of coal conversion technologies is to convert as much of the carbon and hydrogen in the coal to the synthetic fuels as possible. Lower C_1-C_2 hydrocarbons, benzene, and toluene are desirable products for their heating value and their commercial use. To obtain the maximum production of these products from coal, the atomic hydrogen to carbon ratio of coal must be upgraded by some means. The atomic hydrogen to carbon ratio (H/C) in coal varies from .3 to 1.0, and generally increases as coal decreases in rank.[5] This ratio is significantly less than the 1.3-1.9 H/C ratio of common fuel oils and substantially less than the 3.5-4.0 H/C ratio of natural gas. Thus, a primary requirement of any conversion scheme is to upgrade the hydrogen/carbon content of the stable products. This can be accomplished directly by pyrolysis of coal which produces a hydrogen-rich volatile fraction along with a carbon rich char. However, one serious drawback to pyrolysis is the attendant production of H_2O, H_2S, and NH_3. These species deplete the hydrogen available for bonding with carbon. To improve the H/C ratio, it is preferred that nearly all of the

hydrogen bound in coal reacts with the carbon in coal. To accomplish this, a more complete knowledge of functional groups found in coal and the mechanism and kinetics of their conversion to stable products is required.

Other methods of increasing the H/C ratio are hydropyrolysis and hydrogasification. For a basis of discussion, hydropyrolysis will be defined as the pyrolysis of coal in an hydrogen atmosphere, hydrogasification as the subsequent gasification of char with hydrogen containing gases. This discussion will be concerned primarily with those results obtained under rapid heating conditions.

Allowing coal to react in an hydrogen atmosphere generally alters the product composition and total volatile yield, but it is difficult to assess the influence of hydrogen. In their review article, Anthony and Howard[5] report that high temperatures and high hydrogen partial pressures give rise to the highest total yields (liquids and gases). The production of heavier hydrocarbons (those not in the gaseous state at 25 °C), is higher with respect to gases at lower temperatures. Similary, the yields at lower hydrogen partial pressures generally have lower H/C ratios than do those observed under higher hydrogen pressures.

Research performed in the 1930's and 1940's, mainly in Germany, showed coal could be converted to methane when subjected to high temperatures and high pressures of hydrogen.[34] However, the methods used to obtain these conditions cause severe agglomeration of most American coals.[35] To prevent agglomeration, researchers tried pretreating coal by drying it in warm air. This effectively prevented

agglomeration, but a consequence of pretreatment, as the researchers discovered, was a severely inhibited coal-hydrogen reaction. Yields obtained from pretreated coal were not as high as those obtained from raw coal.[36,37]

During the 1950's coal research ignored gasification and liquefaction effects; the main emphasis was placed on low temperature pyrolysis of coal to produce char to be used as a boiler fuel. Tar and liquids were by-products of the pyrolysis schemes; but the optimization of their production was not investigated. More recent investigators[38-42] are making use of much of the results of this earlier research in more directed study aimed at the increase of the hydrocarbon gas and liquid yield obtained from the reaction of coal and hydrogen.

1.2.1 Liquefaction

Although both gasification and liquefaction can convert coal to nonpolluting fuels, liquefaction has a higher thermal efficiency, uses less process water, and its environmental impact is less severe.[45] Liquid fuels have a higher specific energy content than gaseous fuels, and hence storage and transportation are less expensive. Production of liquid fuels from coal can be accomplished via reactions with hydrogen or a hydrogen donor solvent. The latter process is referred to as solvent refined coal and is not included in the scope of this review.

Two different emphases can be placed on coal liquefaction; the production of synthetic crude oil to be upgraded by a refinery, or the production of aromatics for use as petrochemical stocks. This review will attempt to briefly cover both aspects.

The production of aromatics generally occurs at short residence times with high partial pressures of hydrogen. For instance, Graff, et al.[38] conducted experiments on the flash hydrogenation of Illinois #6 bituminous coal. The influence of heating rate, solids-contact time, and vapor-product residence time on products produced and product distribution were investigated using a novel captive technique. To demonstrate the effect of hydrogen on product yields and distribution, the authors performed experiments where the only parameter varied was the type of gaseous environment. The results, given in Table 2, show an increase in both gaseous and liquid products when coal is subjected to flash heating under 100 atmospheres of hydrogen. The authors, however, did not vary the pressure of hydrogen to determine what effect, if any, this parameter had on the product yields and distribution. From the results shown in Table 2 the authors concluded that both liquid and gaseous yields were increased by hydrogen. A consequence of the hydrogen is an increase in saturated gas yields along with a corresponding decrease in unsaturated gas yields.

The effects of heating rate, solids-contact time, and vapor-product residence time are also given in Table 2. The researchers concluded that at a heating rate of 650 °C/sec, a solids-contact time of 10 sec, and a vapor-product residence time of .6 sec were optimal values for the production of liquid products.

Subsequent research[39] concentrated on the influence of the reaction temperature on liquid yields. Benzene, toluene, and xylene yields increased with increasing temperature, and reached a maximum

Table 2. Product yields for flash pyrolysis and hydropyrolysis of Ill. #6 coal.[38,39]

Run number	46	52	22	66	69	54	37	70	55	67
Atmosphere	N_2	H_2	N_2	H_2	H_2	H_2	H_2	H_2	H_2	H_2
Temperature (°C)	741	731	850	798	790	789	781	819	808	817
Heating rate (°C/s^{-1})	650	650	650	650	20	650	1400	650	650	650
Solids-contact time (sec)	11	10	28	10	65	10	10	2	10	30
Vapor-residence time (sec)	0.6	0.6	0.6	0.18	0.6	0.6	0.6	0.6	0.6	0.18
Products										
wt% CH_4	6.2	12.9	8.0	18.1	12.6	19.2	21.1	18.2	21.3	27.7
wt% C_2H_4	0.73	6.4	0.43	6.4	5.1	5.8	6.2	6.2	5.7	7.3
wt% $C_3H_8 + C_4H_{10}$	--	0.41	--	0.27	0.98	--	--	0.32	--	0.14
wt% C_6H_6	1.0	5.8	1.6	7.8	3.3	11.4	12.0	9.9	11.6	11.4
wt% Toluene and Xylene	0.68	2.0	0.28	0.95	0.93	0.15	0.15	0.68	--	0.32
wt% Char	96	63	89	57	43	60	63 m	65	55	57
Total Carbon recovered	106	90	--	91	66	97	102	100	94	104

value of 12% (wt %, product/carbon in coal) at 800 °C. Above 800 °C liquids declined, and accounted for only 3% of the total products at 1000 °C. On the other hand, methane yields increased with increasing temperature from 5% at 620 °C to 38% at 980 °C. Ethane production reached a maximum value of 6.8% at 760 °C, then began an abrupt decrease to less than .5% at 940 °C. The authors found little, if any, tars produced. Although substantially all liquids were formed within 2 sec at 800 °C and 100 atm hydrogen pressure, gas yields continued to climb with longer vapor-product residence times. From Table 2, it appears the increased gas yields at longer vapor-product residence times are at the expense of the liquid yields, not due to additional hydrogasification of the char. This indicates a progressive conversion of liquid fragments to gaseous fragments that are subsequently stabilized by hydrogen.

Cities Service Co.,[40] following the lead of Graff, et al., initiated a research program to develop a commercially attractive process to convert coal to valuable hydrocarbons. The process is based on the premise that the following three conditions optimize the product yields:

1) rapid heating of pulverized coal particles by conduction from hot hydrogen gas;
2) hydrogenation reactions at 50-900 milliseconds residence time and at commercially feasible reactor pressures; and
3) rapid quenching of the volatilized products to prevent unwanted decomposition reactions.

The experimental program employed a free fall reactor surrounded

by an electric furnace. Dried pulverized lignite particles (50-450 μm diameter) were fed into the reactor where they contacted hot hydrogen gas. The temperature-time history of the coal was controlled by the introduction of cryogenically cooled hydrogen via a variable length probe. The residence time of the coal particles was varied from 100-3000 msec by use of this probe. Heating rates varied from about 3×10^4 to 10^5°C, reactor pressures were maintained between 500 and 3000 psi, and the vapor residence time was varied from .8 to 14 sec. Liquid and gaseous yields were determined for the temperature range 620-860 °C.

No tar formation was detected, and the principal products were benzene, methane and ethane. Liquid yields were approximately 94% benzene, with smaller amounts of napthalene and anthracene. Gas yields were composed of methane and ethane. At short residence times (500 msec), carbon conversion to liquids and gases became independent of temperature above 800 °C. Carbon conversion was also found to increase as heating rate increased; however, as the residence time was increased the benzene fraction was cracked, ultimately leading to coke and hydrogen rather than showing increases in methane.

The researchers were able to correlate liquid production to carbon conversion. Above a carbon conversion of 45%, hydrogasification of the lignite takes place with methane the principal product. Although several different hydrogen pressures were employed, the authors did not comment what effect, if any, this had on conversion to liquids and gases in this study. The reader is reminded that Anthony[26,27] found no

pressure influence on yields in the pyrolysis of lignite. No comment was made on the role of the quench temperature which also was varied during the experimentation.

Further studies[41] centered on the hydrogasification of subbituminous coal. Increases in temperature and time were reflected in increases in overall conversion and a change in product distribution. At short residence times C_2-C_4 hydrocarbons and light oils are prominent products; at longer times these products undergo decomposition to form principally methane and benzene. The researchers found light oil production and ethane production to be independent of the reactor temperature; their production was found to be a function of residence time. At 855°C, essentially all light oil formed has undergone nearly complete decomposition by 3 seconds while at 880 °C nearly complete decomposition is accomplished in 1 second. The maximum amount of benzene formed was also independent of temperature; however, its production was a function of residence time. Maximum benzene production was obtained at residence times between 1 and 3 seconds. At higher temperatures, less time was needed to achieve maximum benzene yields. The researchers concluded that their process displayed a two stage mechanism; rapid devolatilization followed by hydrogenation of the coal/char. The authors state that rapid devolatilization is inhibited by high pressure and that hydrogenation reactions are controlled by the hydrogen partial pressure.

Tyler,[20,21] whose pyrolysis work was reported earlier, also investigated pyrolysis in an hydrogen atmosphere. The main influence of hydro-

gen was an increase in methane yields. Tyler found no change in the quantities of tar or total volatile matter evolved. There was no difference in yields between pyrolysis and hydropyrolysis carried out at temperatures up to 700 °C. Above 700 °C, pyrolysis in hydrogen produced greater quantities of C_1-C_2 hydrocarbons, with CH_4 reaching 8.0%. In both hydrogen and nitrogen atmospheres, Tyler[20,21] found ethylene production to remain essentially constant up to 600 °C, and then dramatically increase with increasing temperature. Ethylene production in an hydrogen atmosphere was slightly higher than that observed in a nitrogen atmosphere.

Research dealing with the effects of hydrogen on liquefaction for the production of aromatics is difficult to find, as this topic is only now being investigated in depth. At Brookhaven National Laboratories, research is being conducted on the short residence time hydropyrolysis of coal.[42] During residence times from ~0 to 9 seconds, it is reported that maximum liquid yields of 20% (wt %/carbon in coal) are obtained at 750 °C and a heating rate of 5×10^4 °C/sec. At this temperature nearly 50% of the liquid product is benzene.

Rockwell International[43] reports the operation of a coal liquefaction pilot plant based on short residence time technology. Yields and product distributions have not been reported.

Production of synthetic crude oil from coal generally is conducted at low temperatures (500-600 °C) and normally at longer residence times. Only the Garrett process (discussed below) makes use of short residence times. The major goal of the processes described

in this section is to produce a liquid faction that can be upgraded by current technology and converted into useful fuel oils.

Garrett Research Corporation[44] has devised a method of obtaining high liquid yields by employing entrained-bed, low temperature pyrolysis with short residence times. Operating at atmospheric pressure with solids-residence times less than 2 seconds, researchers have been able to produce liquid yields of nearly 33% of the original coal. This process does not produce a substantial amount of hydrocarbon gases; the major by-product is a low sulfur content char, suitable for use as a boiler fuel.

The Union Carbide Coalcon Process is another process aimed at producing liquid fuels.[45] The Coalcon process produces liquid yields of up to 29% of the original coal at residence times between 5 to 11 min at a temperature of 560 °C and hydrogen pressure of 2000 psi. The liquid yield from the Coalcon process is approximately a function of the square root of the hydrogen pressure. It is of interest to note that the Coalcon process under an inert atmosphere produces nearly 11% liquid yields at 560 °C. As both temperature and partial pressure of hydrogen are increased, char yields decrease due to hydrogasification of the char. At an operating temperature of 550 °C, the Coalcon process will produce hydrogen as a byproduct if the total hydrogen partial pressure is below 225 psia. Above 225 psia this process begins to consume hydrogen.

The COED process upgrades the liquid fraction obtained from pyrolysis to synthetic crude oil by hydrotreatment.[46] Using a staged reactor

system, coal is subjected to pyrolysis at temperatures ranging from 288 to 816 °C at pressures varying from 6 to 10 psia. After a residence time between 1 to 4 hours, liquid yields of 20% and gaseous yields of 15% are obtained. Liquid yields are then upgraded to synthetic crude oil by treatment with hydrogen.

All of these carbonization and hydrocarbonization processes are well into the pilot plant stage; however, no kinetics or mechanistic routes have been proposed. The main feature of these processes is the utilization of all products obtained from the conversion scheme, not the emphasis on one particular product.

1.2.2 Hydrogasification

Coal conversion schemes can also be geared to the production of hydrocarbon gases. Reacting coal with hydrogen or hydrogen containing gases can, in principle, produce gases suitable for use in electrical power generation or as a substitute natural gas. Research into the effects of hydrogen containing gases on gasification is more extensive than that on liquefaction.

Coates, et al.[47] investigated devolatilization of coal in an entrained flow reactor. Finely ground coal (less than 200 mesh) was entrained in either nitrogen or hydrogen gas streams and subjected to heating rates varying from 4.5×10^3 to 1.3×10^5 °C/sec. Hydrogen partial pressures varied from .194 to .553 atm. in 1 atm. total pressure. The main devolatilization products were methane, ethylene, and acetylene. Methane yield was found to increase to a maximum at 927 °C and then decrease with increasing temperature. Acetylene production increased

with increasing temperature while ethylene production decreased. The main effect of hydrogen partial pressure was to decrease the amount of carbon dioxide produced, and increase the amount of methane produced. It is interesting that the presence of hydrogen causes the available carbon to be used more effectively. Although the increase of hydrogen partial pressure has little, if any, effect on the production of acetylene and ethylene, overall the influence of hydrogen is to increase hydrocarbon yields, a finding at variance with Anthony and Howard's[5] model. (Discussed elsewhere in the text). The effect of hydrogen partial pressure on conversion to light hydrocarbons is given in Figure 14.

Coates also varied the residence time of the coal particles from 12 to 343 milliseconds at reaction temperatures between 827 and 1027 °C. Methane and ethylene yields increased to a constant value after 100 milliseconds; however, acetylene yields decreased with increasing residence time. The authors did not record weight loss data, but the increase in methane and ethylene at longer residence times is not accounted for by the decrease in acetylene. Since acetylene production from coal pyrolysis is normally not seen at these temperatures, acetylene fragments could be reacting further to yield aromatics or other recombination products. Coates determined that optimal yields of hydrocarbons would be obtained at residence times less than 50 milliseconds, since at this residence time nearly all of the methane and ethylene is produced and acetylene production has not decreased substantially. The authors made no attempt to model their results or postulate possible mechanisms.

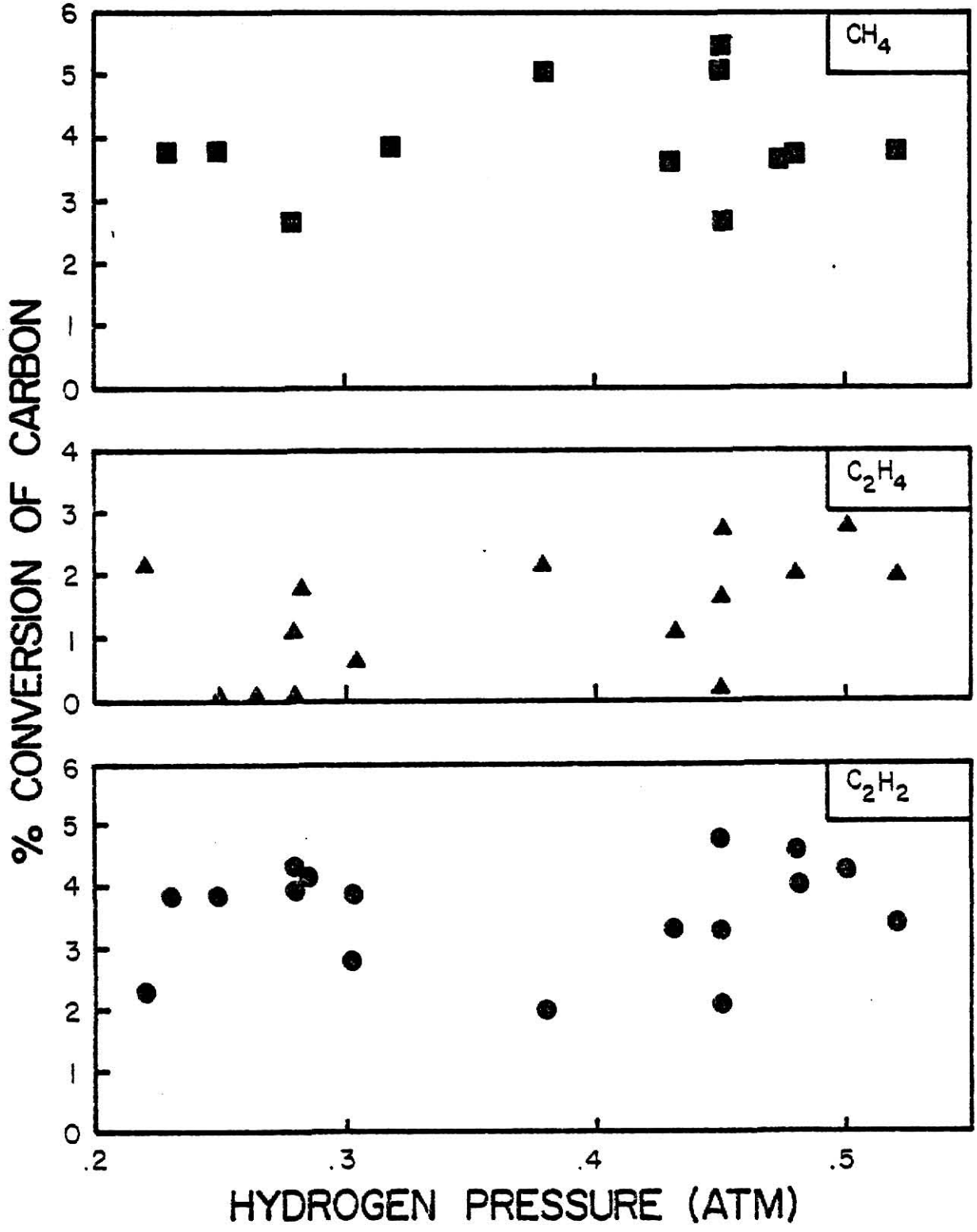

Fig. 14. C_1-C_2 hydrocarbon yields as a function of hydrogen partial pressure for pyrolysis of coal over the temperature range 1200-1400 °K. (From 47).

Zahradnik and Glenn,[48] reported on the direct methanation of coal with steam and synthesis gas. Using data obtained by Mosely and Patterson,[49], Lewis et al.[50] and, Glenn and Grace,[51] they developed a model to predict the methane formation in the presence of hydrogen gas. The model equation is

$$\Delta\omega_c = \Delta\omega_i + \frac{f(1-\Delta\omega_i)(k_1 P_{H2}/k_2)}{1 + k_1 P_{H2}/k_2} \quad , \tag{1.3}$$

where $\Delta\omega_c$ = methane yield appearing per gram of carbon in coal,

$\Delta\omega_i$ = weight of carbon lost by initial devolatilization per gram of carbon in coal,

k_1, k_2 = Arrhenius rate constants for methane formation and deactivation by active intermediates,

P_{H_2} = partial pressure of hydrogen,

$f(1-\Delta\omega_i)$ = weight of active intermediate per gram carbon in coal at time zero.

This model is based on the premise that carbon forms an active intermediate that both the methanation reaction and inactive-char forming reactions compete for. Although temperature dependence of active carbon formation as a variable parameter is not included in equation (1.3), the authors have not neglected this parameter in their analysis. The authors state that the value of $\Delta\omega_i$ is dependent on temperature, and the value corresponding to the specific temperature of interest must be employed when evaluating equation (1.3). Temperature dependence of active site formation is also included with a value chosen for f ranging from 0 to 1.0.

When the value of $k_1 P_{H_2}/k_2$ is much less than one, methane formation is proportional to hydrogen partial pressure. If $k_1 P_{H_2}/k_2$ is much larger than 1, methane formation becomes independent of hydrogen partial pressure. Since k_1 should have an appreciable activation energy compared to k_2, the rate constant for radical-radical recombination or radical-molecule reaction, the model predicts that methane production will be first order at higher temperatures and under lower hydrogen pressures, but will tend to zero order at higher hydrogen pressures. Anthony and Howard[5], in their review, questioned the validity of this model because they believed that the authors had ignored the temperature dependence of the formation of the active intermediate. As was pointed out earlier in this discussion, that was not the case.

In place of models like that given in Eq. (1.3), Anthony and Howard[5] propose the following correlation based on a material balance of reactive volatile species in a coal particle:

$$V^{o} = V_{nr}^{**} + V_{r}^{**} \frac{[1 + k_2/k_c \; P_{H_2} \; P_T]}{[1 + k_1/k_c \; P_T + k_2/k_c \; P_{H_2} \; P_T]} + k_3 \; P_{H_2} \qquad (1.4)$$

where P_{H_2} = partial pressure of hydrogen (atm),

P_T = total system pressure (atm),

V_{nr}^{**} = nonreactive volatiles lost from particle up to t=∞,

V_r^{**} = amount of reactive volatiles formed up to t=∞,

k_2 = overall rate constant for hydrogenation of reactive volatiles (sec^{-1} atm^{-1}),

k_1 = overall rate constant for deposition reactions (sec^{-1}),

k_3 = rate constant for rapid rate methane formation (sec^{-1} atm^{-1}),

k_c = pressure independent overall mass transfer coefficient $(atm^{+1} sec^{-1})$.

Equation (1.4) predicts a minimum yield in volatiles between 1 and 10 atm. hydrogen pressure, and the authors use the results shown in Fig. 15 as a basis for justifying the acceptability of the model. Nonetheless, close examination of the data reveals that only the most tenuous conclusions can be drawn regarding whether in fact the weight loss follows the model predictions. The authors contend that the minimum predicted by the model results from the opposing influence on yields by decomposition and hydrogenation reactions. The authors then state that both decomposition and hydrogenation are favored at increased hydrogen partial pressures, which would then imply that the increase in yields at higher pressures is due solely to hydrogenation of the remaining char. This model is not very satisfying conceptually, especially the predicted minimum behavior. Although this model predicts an increase in yields as hydrogen pressure is decreased from 1 atm to 10. atm, the reader is reminded that Coates[47] saw an increase in yields with an increase in hydrogen pressure at these levels. It is possible in the case of Anthony's[26,27] research, that the hydrogen may not have had a chance to react with the radical fragments before they stabilized in the cold bath gas.

One severe omission in this model is the contribution of what the authors term non-reactive volatiles, those species evolved from the coal which are stable. When subjected to a sufficiently long residence at elevated temperatures or hotter conditions at shorter residence times, these species can decompose to yield reactive fragments that also can be

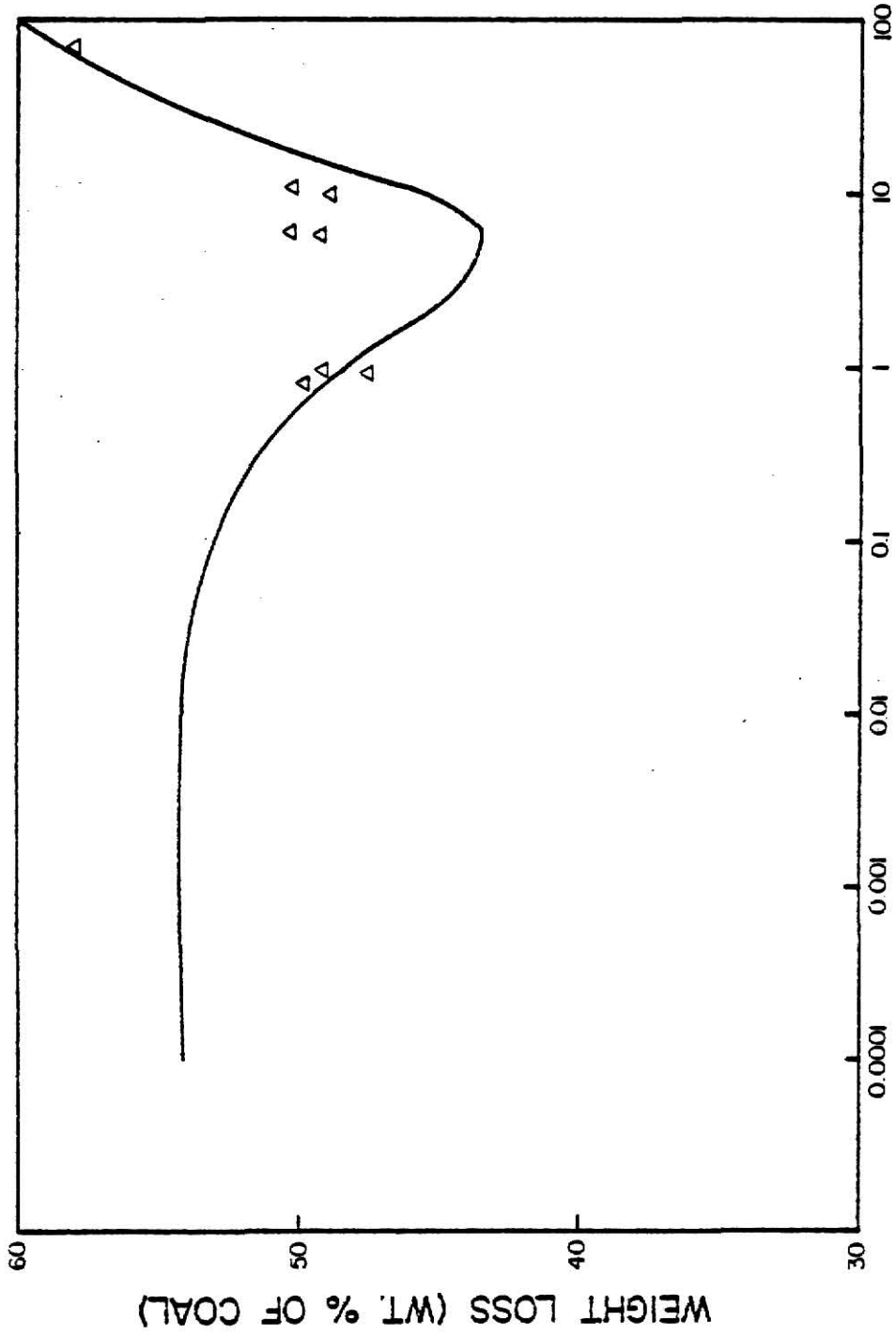

Fig. 15. Total weight loss as a function of hydrogen pressure. Δ experimental points, solid line prediction of model. (From 5).

stabilized by hydrogen. The reader is reminded that the thermal degradation of coal produces a variety of organic products. Depending on the time frame and temperature of the experiment, these organic products can also undergo decomposition producing lighter molecular weight hydrocarbons or soot.

Hydrogasification of coal is a rapid process, usually described by two steps, hydrogenation of volatiles followed by hydrogasification of the char. Data of Anthony et al.[5,26,27] indicate that rapid hydrogenation of volatiles occurs in a time frame comparable to pyrolysis. The rate of char gasification by hydrogen is much slower than the hydrogenation reactions. Anthony and Howard,[5] contend that heating rate does not significantly alter the path of secondary reactions or affect the reactivity of the residual char; thus conversions at a given partial pressure of hydrogen will converge in time for different heating rates.

In concluding this review, the two general mechanistic theories on coal pyrolysis and the influence of hydrogen on these theories will be discussed. Anthony and Howard[5,26,27] postulate that tars and liquids evolve first from the coal particle, followed by evolution of gaseous products. The tars and liquids evolving contain radical sites that can be stabilized by radical-radical recombinations to form repolymerization products. At higher temperatures, the tars and liquids undergo secondary reactions to form coke and hydrogen. Thus, the effect of an hydrogen atmosphere would be to inhibit repolymerization at lower temperatures and thus increase the tar and liquid yields. At higher temperatures

the hydrogen would have no effect on the secondary reactions of the tar and liquids, but would react with the highly active coke or char to produce light hydrocarbon gases. At the same time the hydrogen would stabilize the radical sites of the gaseous products evolved from the coal particle.

Solomon and Colket[23,24], however, believe that heavier molecular weight hydrocarbons and gases evolve independently of each other; each is dependent upon the relative distribution of certain functional groups found in coal. Primarily, they speculate that tar and liquid production are dependent on the aliphatic hydrogen content of the coal. Thus, in an inert atmosphere there is competition between the tar and liquid free radical fragments with the gaseous free radicals for stabilization by the available aliphatic hydrogen. It is their view[48] that hydrogen external to the coal should have little influence on the yields under modest hydrogen pressures. Only if the hydrogen can be made to penetrate into the pores of the coal particles will it have an effect.

In summary, the effect of hydrogen is to increase the amount of gaseous hydrocarbons, but this may be due solely to hydrogasification of the char. There is not enough evidence to conclusively decide if there is an effect on liquid yields. The exact mechanism of coal devolatilization is not known; however, there is some evidence to support a functional group theory. The following observations can be discerned from this review:

1) Heating rate may or may not have an effect on total volatiles realized; however, at higher heating rates hydrocarbon yields may increase at the expense of H_2O if aliphatic hydrogen can be utilized effectively.

2) Anomalous weight loss behavior over limited temperature ranges most likely is a function of experimental technique coupled with secondary reactions of primary volatile fragments, and the composition of the solid material.

3) First order models based on functional groups may be more accurate in predicting yields from all types of coals than those models based on consecutive reactions.

4) The similarity of behavior at many different heating rates and residence times suggests that if even shorter residence times were employed, comparable yields could be achieved under higher heating rates. Additionally, shorter residence times will be necessary to avoid repolymerization to char and soot.

5) Even at the highest heating rates heretofore studied, yields of H_2S suggest that results are not limited by transport phenomena, but are kinetically controlled. In concert with this observation is that lower activation energies obtained by first order decomposition models are indicative of parallel reactions.

1.3 Objectives

The objective of this study is to determine what effects temperature, residence time, and partial pressure of hydrogen have on pyrolysis product yields and product distributions. Experiments at various temperatures and residence times will be conducted in an inert (argon) atmosphere to establish baseline product yields and product distributions.

Use of the single pulse shock tube for these experiments will provide ultra rapid heatup, thereby promoting very quick volatile evolution with a minimum of deposition. Experiments will be conducted in the free stream eliminating packed bed problems. Lower C_1-C_2 hydro-

carbons, benzene, and toluene will be measured by gas chromatography; solid residue will be recovered and sent to an independent laboratory for analysis.

2.0 EXPERIMENTAL

2.1 The Single Pulse Shock Tube

The single pulse shock tube (SPST) is ideal for use in combustion studies requiring temporal resolution of short duration (3 msec or less) phenomena. The SPST provides a means by which test gases or solid suspensions can be elevated to high temperatures and pressures very rapidly; furthermore, use of the region behind the reflected shock wave provides an experimental zone essentially free of temperature, velocity and concentration gradients.

The SPST, as designed and constructed by Seeker,[52] differs from a conventional shock tube by the addition of a dump tank at an oblique angle. The SPST, whose schematic is given in Fig. 16, is a device in which a plane shock wave is generated by the sudden rupturing of a diaphragm separating high pressure gas from sub-atmospheric gas. The addition of the dump tank allows for the test gas and/or solid suspension to be processed by only one reflected shock wave. Upon rupture of the diaphragm, a number of accoustic waves are successively formed in the low pressure gas. Each accoustic wave travels at the speed of sound of the gas into which it propagates. With its passage, each of these isentropic waves increase infinitesimally the temperature, pressure and, density of the gas. Therefore, succeeding waves travel through test gases that have been heated by the passage of previous waves. Insofar as each wave travels with the local speed of sound, the waves coalasce to form, ultimately, a non-isentropic shock wave,

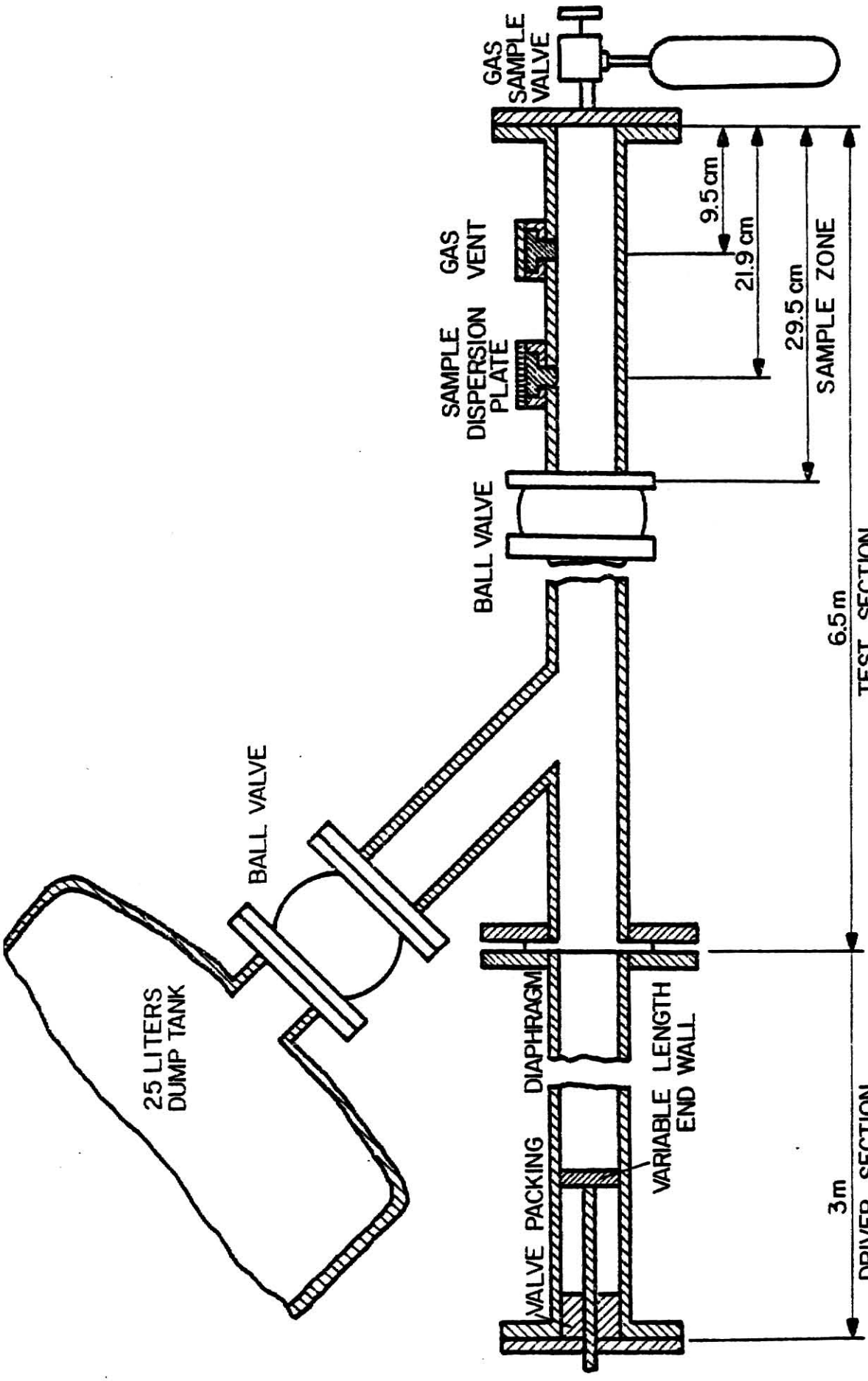

Fig. 16. Schematic of the single pulse shock tube.

travelling at several times the speed of sound in the still undisturbed test gas. At the same time, an isentropic rarefaction or expansion wave, travelling at the speed of sound of the undisturbed high pressure gas, is generated by the diaphragm rupture. A time-distance or x-t diagram, showing the displacement of various waves within the shock tube as a function of time, is given in Fig. 17.

The incident shock wave raises the temperature of the test gas within several nanoseconds and accelerates the gases to speeds that can be greater than the sonic speed with respect to laboratory coordinates. The bulk gas motion disperses the coal particles into the test gas. Kaufmann,[53] in a recent study on grain dust, showed that grain dust particles with diameters ranging from several microns to nearly 100 microns rapidly accelerate to the bulk gas velocity. In the wave diagram, (Fig. 17) this velocity is identical to that identified with the contact surface, the idealized interface between test gas and driver gases. The incident shock wave reflects from the end wall, and because it is proceeding now into a column of gas with a bulk velocity of perhaps 900 m/sec, the reflected shock velocity with respect to laboratory coordinates is much less than that of the incident shock wave which propagated into a stagnant gas. The reflected shock wave further increases the temperature, the pressure, and the density of the test gas. Additionally, both test gas and particles are brought nearly to rest with respect to laboratory coordinates; hence, behind the reflected shock wave forms an ever lengthening column of stagnant, high temperature, high pressure test gas in which the coal particles are suspended.

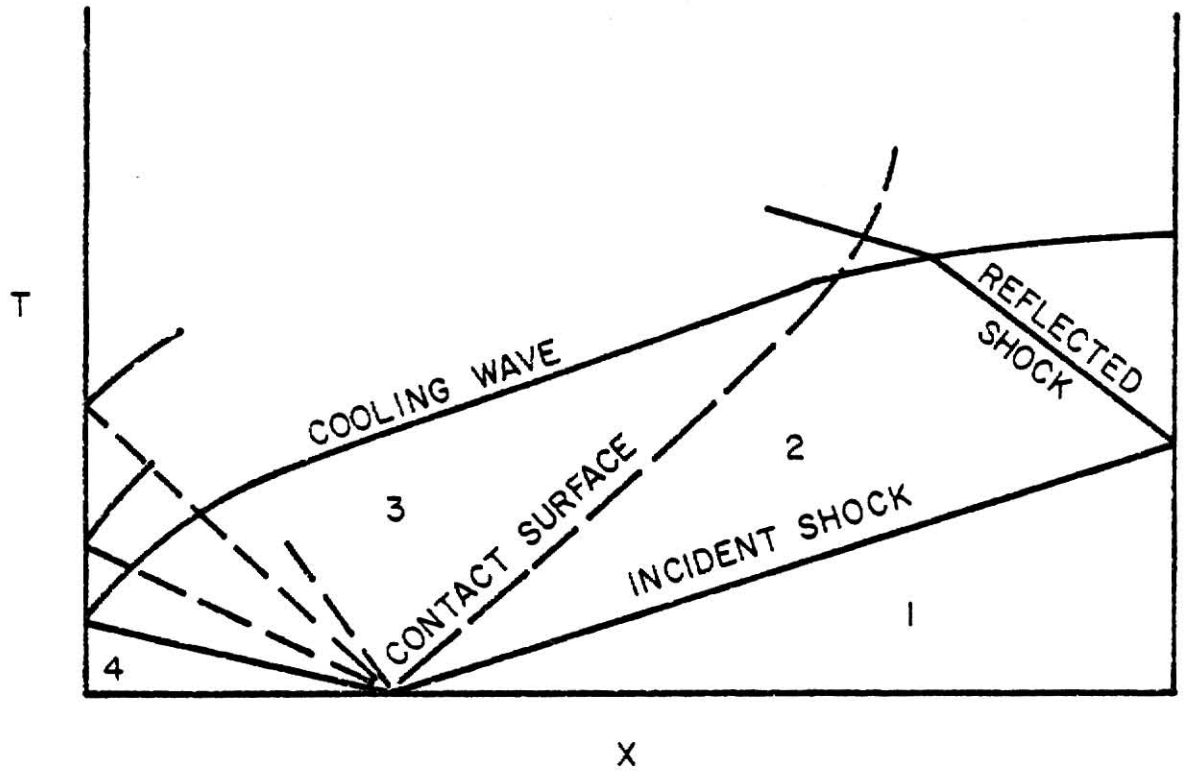

Fig. 17. A time versus distance wave diagram for a conventional shock tube.

The suspended coal particles are heated by conduction from the hot test gas. Assuming the thermal conductivity, k, of the coal particle is sufficiently large so that the particle remains at a uniform temperature throughout the heatup period, the net rate of energy transfer to the particle assumes the form

$$\rho_p \, c_p \, v_p \frac{dT_p}{dt} = hA_p \, (T_p - T_g) \, , \tag{2.1}$$

where

v_p = particle volume ($= \pi dp^3/6$),

A_p = external particle surface area ($= \pi d_p^2$),

ρ_p = particle density,

c_p = particle heat capacity,

T_g = gas temperature,

T_p = particle temperature,

h = convective heat transfer coefficient,

d_p = particle diameter.

Using the definition of the Nusselt number and assuming spherical particles, Eq. (2.1) becomes

$$\frac{dT_p}{dt} = \frac{6 \, Nu \, k_g}{c_p \rho_p d_p^2} \, (T_g - T_p) \, , \tag{2.2}$$

where

$$Nu = \frac{hd_p}{k_g} \, , \tag{2.3}$$

Integration of Eq. (2.2) yields

$$\frac{T_g - T_p}{(T_g - T_p)_o} = \exp \left(- \frac{6 \, Nu \, k_g \, t}{c_p \rho_p d_p^2} \right) . \tag{2.4}$$

To evaluate the Nusselt number the form for Stokes flow[54] is used,

$$Nu = 2 + \beta(Re)^{1/2} (Pr)^{1/3} , \qquad (2.5)$$

where β is a constant determined experimentally to be about .69, Re is the particle Reynolds number with respect to the gas, Pr is the gas Prandtl number. If there is no relative motion between the particle and the test gas, (i.e., both the gas and particles are stationary behind the reflected shock wave (Re=0)), the Nusselt number then becomes two. Additional information on this topic can be found in Appendix K of Reference 54. The temporal response of particle temperature as a function of diameter, calculated by Eq. (2.4) using a Nusselt number of 2 is given in Fig. 18 for a gas temperature of 1285°K. The temperature response for particles of 25 μm diameter is also shown for Nu = 4 that corresponds to a particle Re = 192 and a velocity relative to the test gas of 89.0 m/s. This calculation assumed an initial particle temperature of 600 K, the temperature to which the particles are elevated by passage of the incident shock wave. As can be seen in Fig. 18, this analysis predicts that it takes over one millisecond for 25 μm diameter particles to reach the gas temperature. Insofar as the velocity relaxation is slower for larger particles,[54] the larger particles may be expected to heat faster than predicted by the foregoing analysis. Evidence of this has been accumulated during previous experimentation in this laboratory.[52] Temperatures deduced from pyrometry measurements of radiation from Illinois #6 coal (number means diameter of 4.1 μm) dispersed in nitrogen at three different temperatures are shown in Fig. 19. The measurements indicate

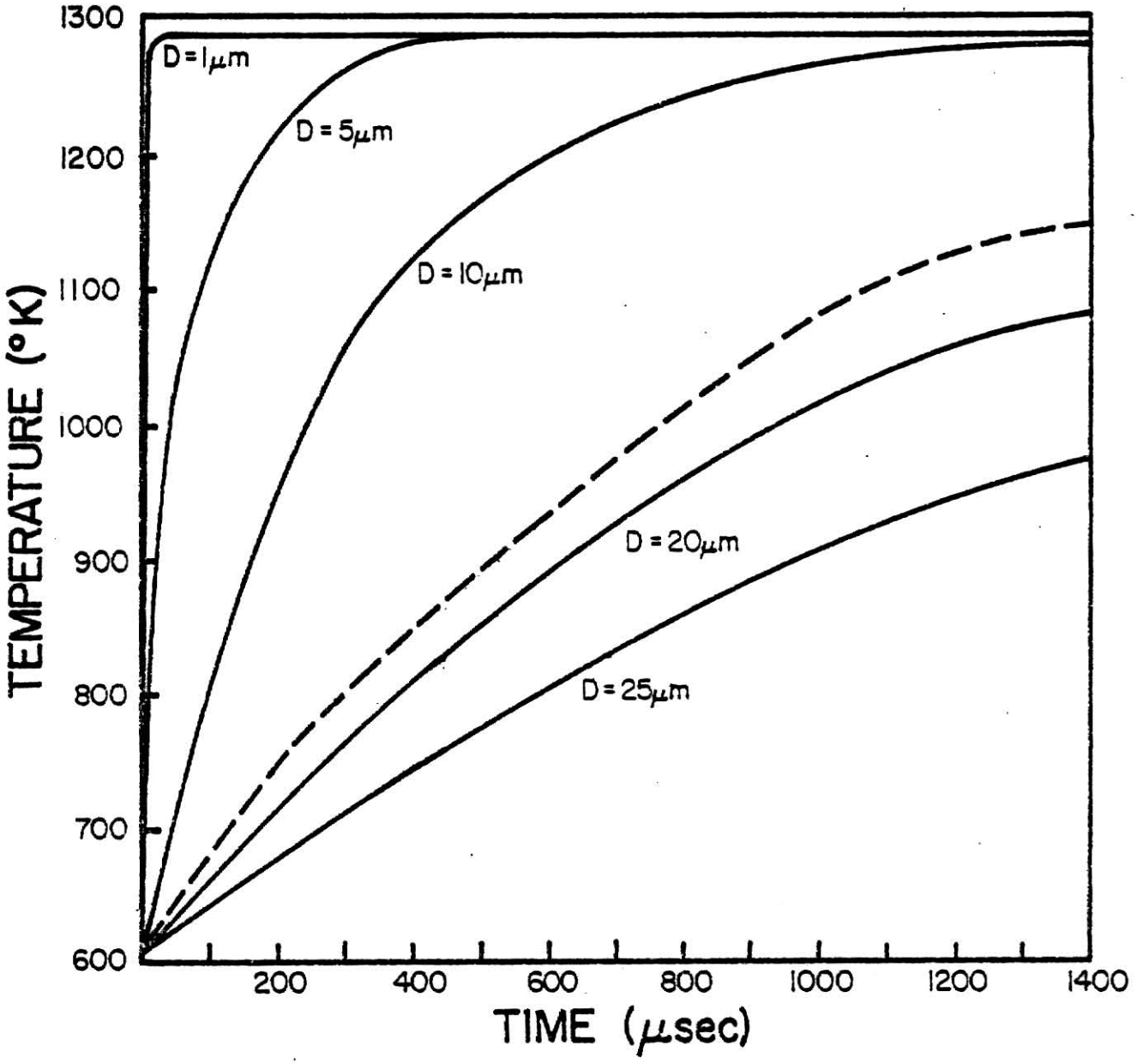

Fig. 18. Temporal response of particle temperature for various particle diameters. Solid lines calculated by Eq. (2.4) for Nu=2, reflected shock temperature of 1285 K, and initial particle temperature of 600 °K. Dashed line calculated by Eq. (2.4) for Nu=4, reflected shock temperature of 1285 K, and initial particle temperature of 600 K.

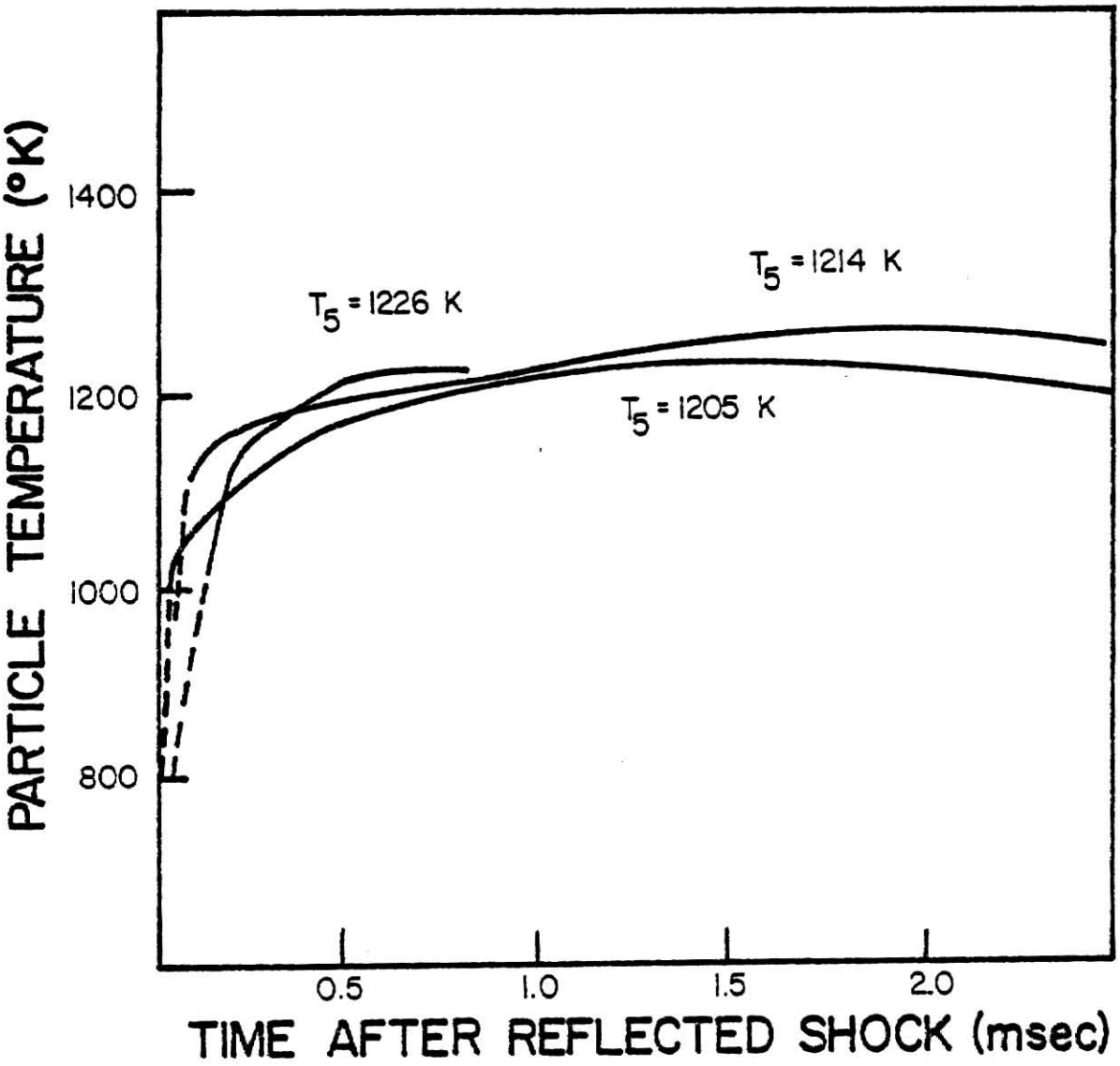

Fig. 19. Pyrolysis temperature histories of shock heated Ill. #6 coal in nitrogen.

that the polysuspension relaxes to the final reflected shock temperature in approximately 200 μsec.

Depending on the configuration of the shock tube, the reflected shock wave will first interact with the contact surface following several meters behind the incident shock wave or with the rarefaction fan. Comprehensive examination of the resulting wave behavior is beyond the scope of this thesis, and the interested reader is referred to specific treatment of shock wave mechanics by Seeker[6,52] and Gaydon and Hurle,[55] or to more general discussions of wave interactions by Shapiro.[56]

It may be briefly stated, however, that if the relative lengths of the shock tube sections are appropriate, the oncoming contact surface will be brought nearly to rest by the reflected shock wave. If not, serious mixing of the reacting gases behind the reflected shock wave with colder gases in the contact layer will ensue. Ideally, the reacting mixture is cooled quickly by the rarefaction fan at rates approaching -5×10^5°K/sec. The SPST used in this study was designed so that the rarefaction fan overtakes the contact surface before the latter enters the test section, although for certain combinations of conditions some mixing undoubtedly occurred. The approximate axial dispersion of the particles with respect to time is shown in Fig. 20.

In this study, it is the time between the passage of the reflected shock wave and the rarefaction fan at a specific axial location that is defined as the dwell period. Near the end of the test section, (see Fig. 21), where the experiments in this study were conducted, this

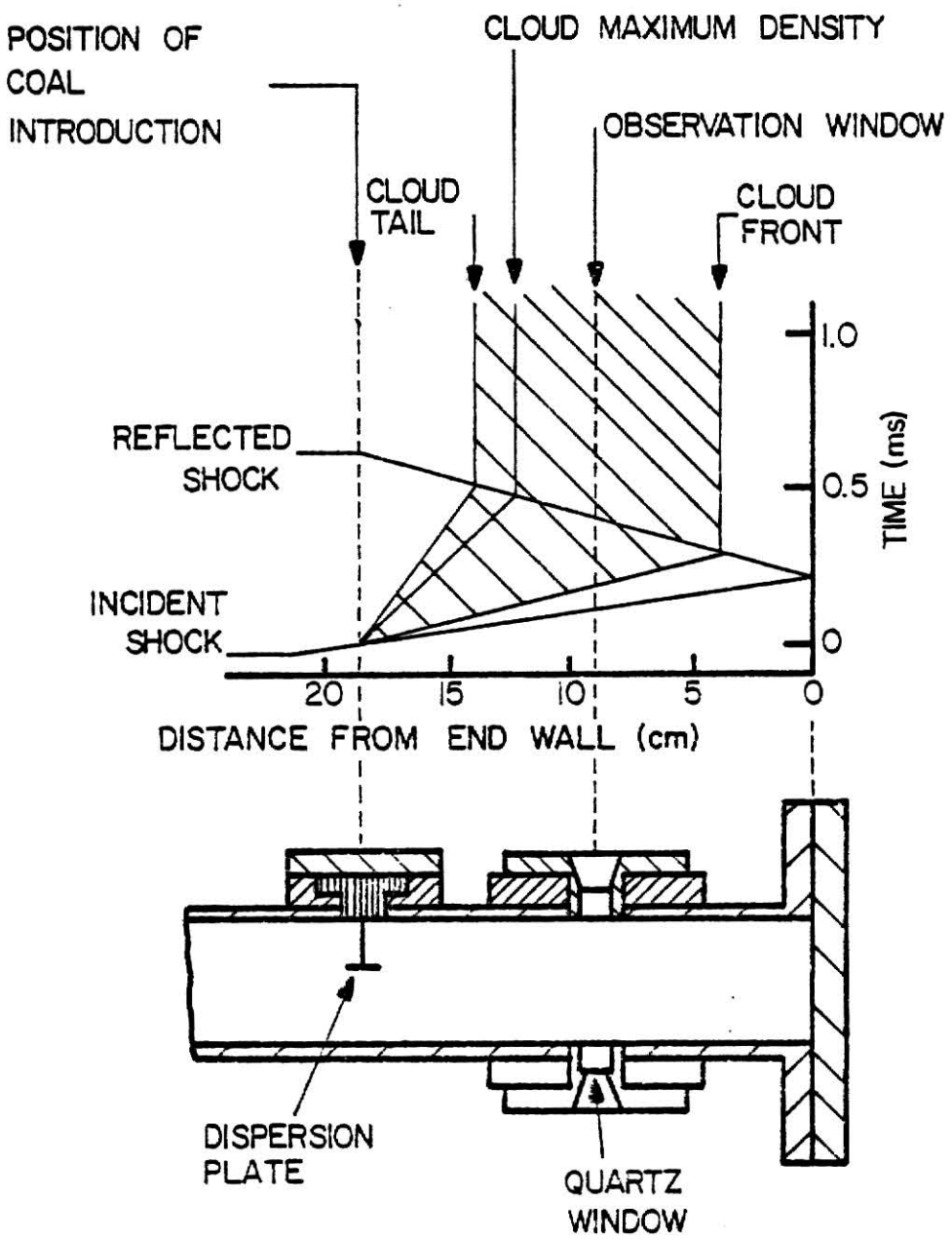

Fig. 20. Axial particle dispersion as a function of time. (From 52).

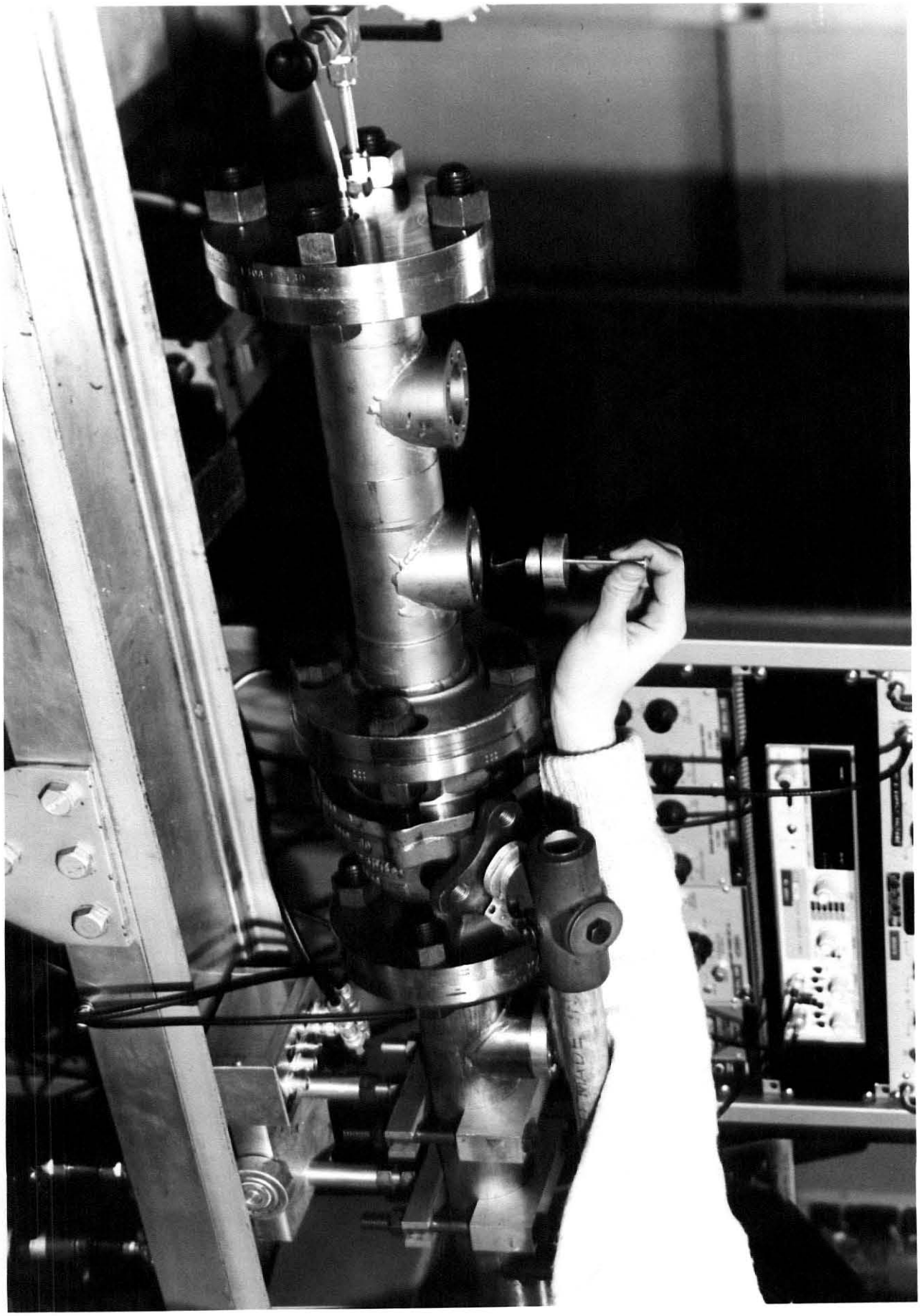

Fig. 21. View of solid sampling test section showing dispersion plate and coal loading technique.

dwell period can vary between less than 100 μsec to more than 2.5 msec, depending on the relative lengths of the driver and driven sections.

2.2 Shock Tube Operation

The SPST employed in this study was modified to allow for the collection of solid and liquid residues. A new test section, shown in Figs. 21 and 22 was constructed of type 304 stainless steel. Twenty-seven cm. in length and 5.7 cm in inside diameter, the test section allows for the insertion of aluminum liners. The aluminum liners, 5.08 cm inside diameter, can be removed after completion of an experiment. The test section contains two radial access ports. The first port, located 7.66 cm downstream from the isolation ball valve, is used to introduce the coal sample. The second port, 20.3 cm downstream from the ball valve, is used for venting of the gaseous products.

The individual steps followed to prepare the SPST for an experiment are given in Appendix A. Helium, (Airco, 99.995% purity) was used as the driver gas in all experiments. The length of the driver section was varied from 1 to 3 m to produce different shock dwell periods. A variety of gases, listed in Table 3, were used as test gases. Inasmuch as the original shock tube was designed with air, nitrogen or argon as test gases, some modification to the driven section of the shock tube had to be undertaken when using test gases with hydrogen contents of 40% (by volume) or more. The driven section was shortened to 5.5 m to enable temporal experiments of 1 msec or less to be performed with high hydrogen content test gases. The observation time, or dwell period available, depends upon the reflected shock wave and

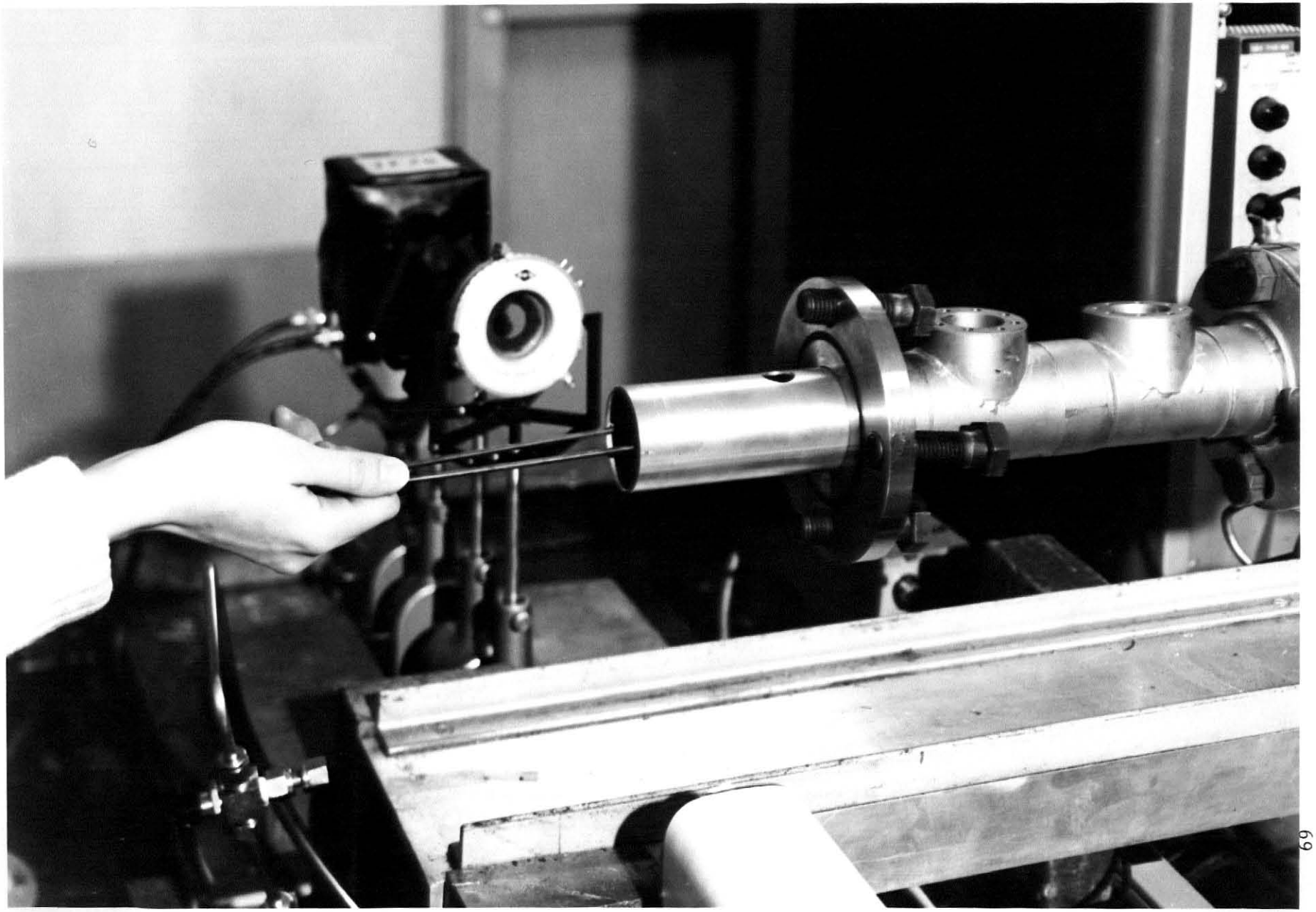

Fig. 22. View of solid sampling test section showing removal of aluminum liner.

Table 3. Gas parameters.

Test Gas Composition	Ratio of Specific Heats* $\gamma(298)$	Speed of Sound** a (298) $\frac{km}{sec}$	Ratio of Specific Heats $\gamma(1300)$	Ratio of Specific Heats $\gamma(avg)$
Argon	1.667	.321	1.667	1.667
94% Argon, 6% H_2	1.642	.329	1.634	1.638
90% Argon, 10% H_2	1.626	.334	1.614	1.620
80% Argon, 20% H_2	1.590	.349	1.569	1.579
60% Argon, 40% H_2	1.530	.391	1.496	1.513
36% Argon, 64% H_2	1.472	.482	1.430	1.451

*Specific heats are calculated from:

$$c_p = [a + bT + cT^2 + dT^3 + eT^4]\ R_i$$

$$c_v = c_p - R_i$$

$$\gamma = \frac{\Sigma x_i cp_i}{\Sigma x_i cv_i}$$

where R_i is the unverisal gas constant divided by the molecular weight of species i (Joules/kg °K) and correlation coefficients for H_2 are from Zuchrow and Hoffman[58] (1000-5000 °K).

$a = 3.10019$ $\quad b = .511195 * 10^{-3}$ $\quad c = .052644 * 10^{-6}$

$d = -.03491 * 10^{-9}$ $\quad e = .003694 * 10^{-12}$

**Speed of sound values calculated from:

$$a = [\gamma_{298}\ T(\Sigma\ x_i R_i)]^{1/2}.$$

its interaction with the contact surface or rarefaction fan. If, at the observation location the rarefaction fan has not overtaken the contact surface, the reflected shock wave will then first interact with the contact surface. The reflected shock wave can produce three different wave systems upon its interaction with the contact surface; abruptly bringing the contact surface to rest, slowing down the contact surface, or reversing the direction of the contact surface.[55] If the direction of the contact surface is reversed, the dwell period will increase over that obtained with a stationary contact surface because the rarefaction fan is now propagating into a column of gases travelling towards the driver. Due to momentum considerations, the velocity of the rarefaction fan will then decrease. Reducing the length of the driven section reduces the amount of time between the interaction of the reflected shock wave and rarefaction fan.

To minimize contamination of the solids recovered, 0.0406 mm aluminum diaphragms were used in place of mylar diaphragms. Upon rupturing, mylar diaphragms tend to shatter, allowing minute particles to be carried downstream into the test section. Tests determined that the mylar particles, even in low concentrations, caused significant interference in the infra-red absorption spectra of the coal residue. The aluminum diaphragms, when properly scored, petal back and do not fragment upon rupturing. The only difficulty encountered with aluminum diaphragms was the inability to consistently reproduce shocks.

To further minimize contamination, filters were installed on all incoming gas lines. The filters, containing activated charcoal and

molecular sieve 5A, absorbed any moisture or hydrocarbons present in the gases. A molecular sieve foreline trap (Veeco) was installed on the vacuum line to absorb any oil vapors formed by the operation of the pumps.

To determine the speed of the incident shock wave and the resulting pressure history of the test gas, two diagnostics were employed. A piezoelectric pressure transducer, (Kistler, Model 603A), is mounted into the end flange of the test section. The output of the transducer is displayed on a Tektronix Type 7623A storage oscilloscope and photographed with a Tektronix C-5B oscilloscope camera. From the oscillogram, (Fig. 23), any non-uniformities in the pressure history of the shock wave can be discerned, along with a good estimate of the dwell period. Two platinum thin film gauges are used to record the speed of the incident shock wave. The voltage pulses from the thin film guages are fed into an amplifier, which then transmits the signals to a digital counter (Fluke, Model 1952B). The signal from the first thin film gauge starts the counter, the signal from the second thin film gauge stops the counter and triggers the oscilloscope.

All runs were conducted with 40 $\pm$ 0.8 mg Illinois #6 coal. The coal, the analysis of which is given in Table 4, had been sieved to -400 mesh. A size distribution of the coal, as supplied by Dutcher,[57] is given in Fig. 24. To avoid absorption of gases and water vapor the coal was stored in a dessicator. The coal sample was introduced into the shock tube by means of a dispersion plate suspended from a saddle block. (See Fig. 21.) The saddle block was

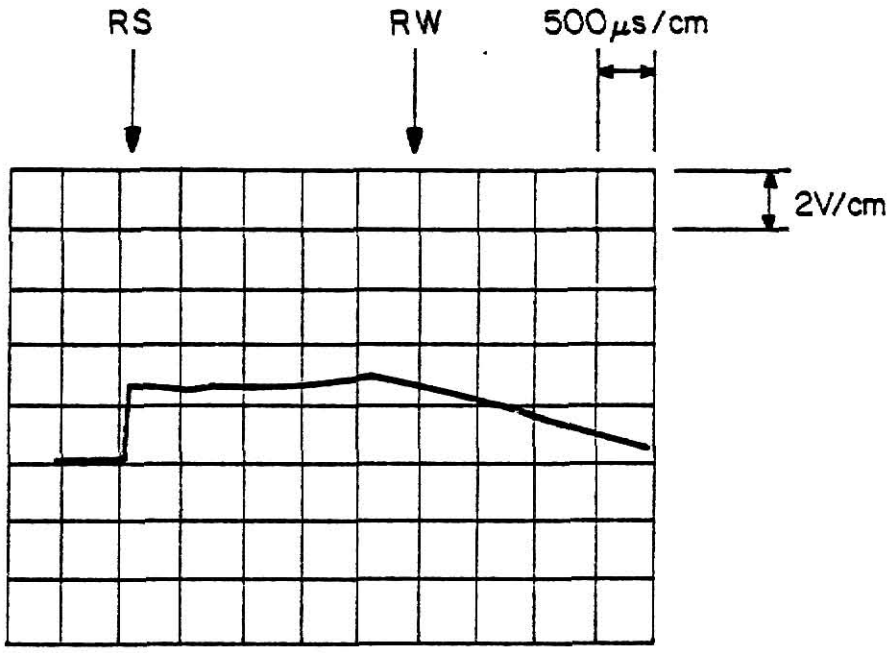

Fig. 23. Typical oscillogram showing pressure trace and a dwell period of approximately 2.3 ms between the reflected shock (RS) and rarefaction wave (RW).

Table 4. Analysis of Illinois #6 Coal.[57]

Proximate Analysis	
Volatile Matter	37.77 %
Fixed Carbon	49.82 %
Moisture	2.07 %
Ash	10.34 %
Ultimate Analysis	
Carbon	66.95 %
Hydrogen	4.49 %
Oxygen	10.64 %
Nitrogen	1.23 %
Sulfur	3.27 %
Ash	10.52 %
Water	2.90 %

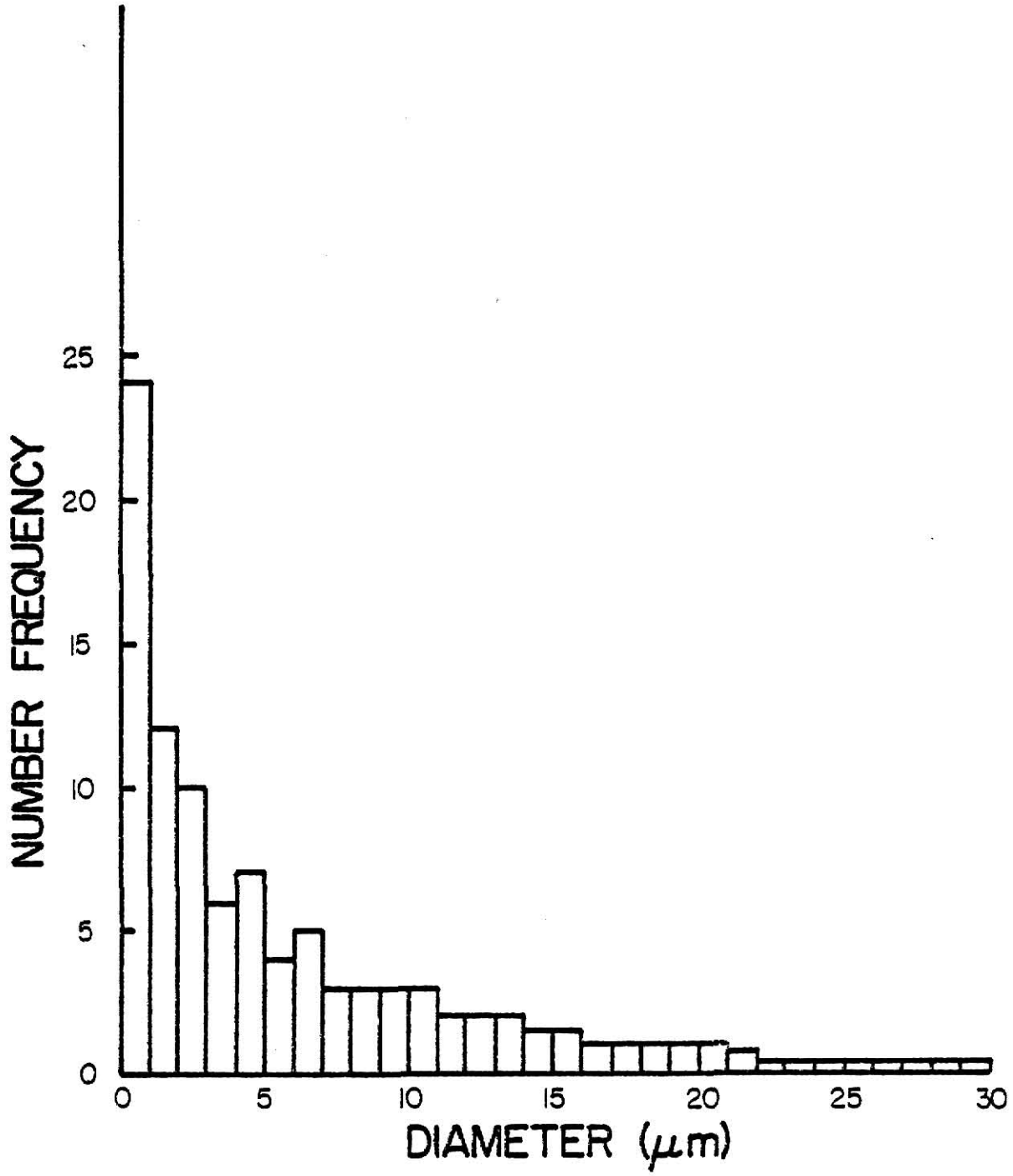

Fig. 24. Size histogram of Illinois #6 coal. (From 57).

designed to meet flush with the inner surface of the shock tube.

An experiment was initiated by the mechanical rupturing of the diaphragm. Immediately after rupture, the ball valve (see Fig. 21) was closed, isolating the test section from the rest of the shock tube. The test section was isolated for one hour to allow gaseous products to achieve an uniform composition axially. The final pressure in the shock tube and time on the digital timer were recorded. The Mach number of the incident shock wave was calculated from

$$M_1 = \frac{V_1}{a_1}, \tag{2.6}$$

where V_1 was calculated from the time required for the shock wave to traverse the distance between the thin film gauges, 0.2032 mm and a_1, the local speed of sound of the undisturbed test gas mixture, was determined for each mixture as listed in Table 3.

The temperature and pressure behind the reflected shock wave are determined from ideal shock relations:[55]

$$\frac{T_5}{T_1} = \frac{[2M_1^2(\gamma-1) + 3 - \gamma)]\ [(3\gamma-1)\ M_1^2 - 2(\gamma-1)]}{(\gamma+1)^2\ M_1^2}, \tag{2.7}$$

$$\frac{P_5}{P_1} = \frac{[2\gamma M_1^2 - (\gamma-1)]}{(\gamma+1)}\ \frac{[(3\gamma-1)\ M_1^2 - 2(\gamma-1)]}{[(\gamma-1)\ M_1^2 + 2]}, \tag{2.8}$$

where subscript one refers to initial conditions, subscript five refers to reflected shock conditions, and γ is the specific heat ratio, the determination of which is covered shortly.

Equation (2.7) was derived on the assumption of constant specific heats, an assumption clearly violated by the use of diatomic gases. While the specific heat ratio of argon is constant because there are no rotational or vibrational degrees of freedom, the specific heats and the specific heat ratio of molecular hydrogen are strong functions of temperature. To determine this dependence, a fourth order polynomial fit to specific heat data was used.[58] The form of the equation and the coefficients specific to hydrogen are shown in Table 3.[†]

To account for the variable specific heats, an iterative procedure is required wherein the reflected shock temperature is predicted first using the specific heat ratio at 298 °K. Following Wittig,[59] the average of the specific heat ratio from 298 °K to T_5 is then used in subsequent iterations until the degree of convergence desired is reached. It has been observed, however, that very little error is introduced if the average specific heat ratio between 298 and 1300 °K is used. This is because the vibrational and rotational levels are nearly completely excited above 1000 °K. Thus,

$$\gamma_{avg} = \frac{\gamma_{(298)} + \gamma_{(1300)}}{2} \qquad (2.9)$$

was used in the determination of the reflected shock temperatures in

---

[†]It should be noted that the pressure and temperature behind the reflected shock waves can, of course, be calculated without recourse to specific heats if the enthalpies are used with the three conservation equations and the perfect gas law. However, both the incident and the reflected shock velocities must be measured insofar as the non-ideal reflection of the shock wave from the end wall cannot be accounted for from first principles.

this study. The specific heat ratios calculated by Eq. (2.9) are given in Table 3. A study by Vaughn[60] on the decomposition of n-butane, showed temperatures calculated in this manner to be within $\pm$ 50 °K of the temperature determined from the kinetic rate data for n-butane decomposition. Measurements were also made by Vaughn of the incident and reflected shock velocities, from which the reflected shock temperatures may be computed directly from the conservation equations. Vaughn also determined that the introduction of the dispersion plate, used to load the coal, did not significantly affect the temperatures.

Although the products of reaction and particles were cooled at rates greater than -10^5 °K/sec, this is still not fast enough to quench reactions with Arrhenius activation energies of approximately 30 kcal/mole or less. Some contribution to the product distribution will occur during the quench for these type reactions. Vaughn,[60] in his study on n-butane decomposition, provides the following scheme to account for the increase from the cooling down period. An effective reaction dwell time is defined,

$$t_r \equiv t_o \left(1 + \frac{\Delta t'}{t_o}\right) \tag{2.10}$$

where

t_r is the effective reaction time,

t_o is the measured dwell period, and

$$\Delta t' \equiv \frac{\int_{t_o} \ell^{-E/RT(t)}\, dt}{\ell^{-E/RT_5}} . \tag{2.11}$$

The corrected rate constant at any temperature, k_c can then be determined from:

$$\frac{k_c}{k_o} = \left(1 + \frac{\Delta t'}{t_o}\right)^{-1}, \qquad (2.12)$$

where k_o is the rate constant found using the measured dwell period. This correction factor ($\Delta t'$) would be 1.8 msec for a reaction at 1700 °K with an activation energy of 55 kcal/mole (from 18). Thus, the corrected rate constant for a 1.0 msec measured dwell time would be

$$k_c = k_o\ (2.8)^{-1} \qquad (2.13)$$

or

$$k_c = .36\ k_o. \qquad (2.14)$$

Figure 25 shows the dwell time correction versus temperature for various activation energies.

After the gaseous products reached a uniform composition, heating tape, wrapped around the test section, was used to heat the test section to an internal wall temperature of approximately 66 °C to drive off any products volatile at this temperature at a total pressure of 3.5 atm or less. A 75 cm^3 gas sample was extracted through a 2 μm stainless steel filter into a previously evacuated stainless steel bottle. The rest of the gaseous products were vented first through a 2 μm stainless steel filter, and then through an activated charcoal filter at a flow rate of 1 liter per minute. A schematic of the sampling system is given in Fig. 26. Stainless steel filters were used to trap any unreacted coal or particle fragments greater than

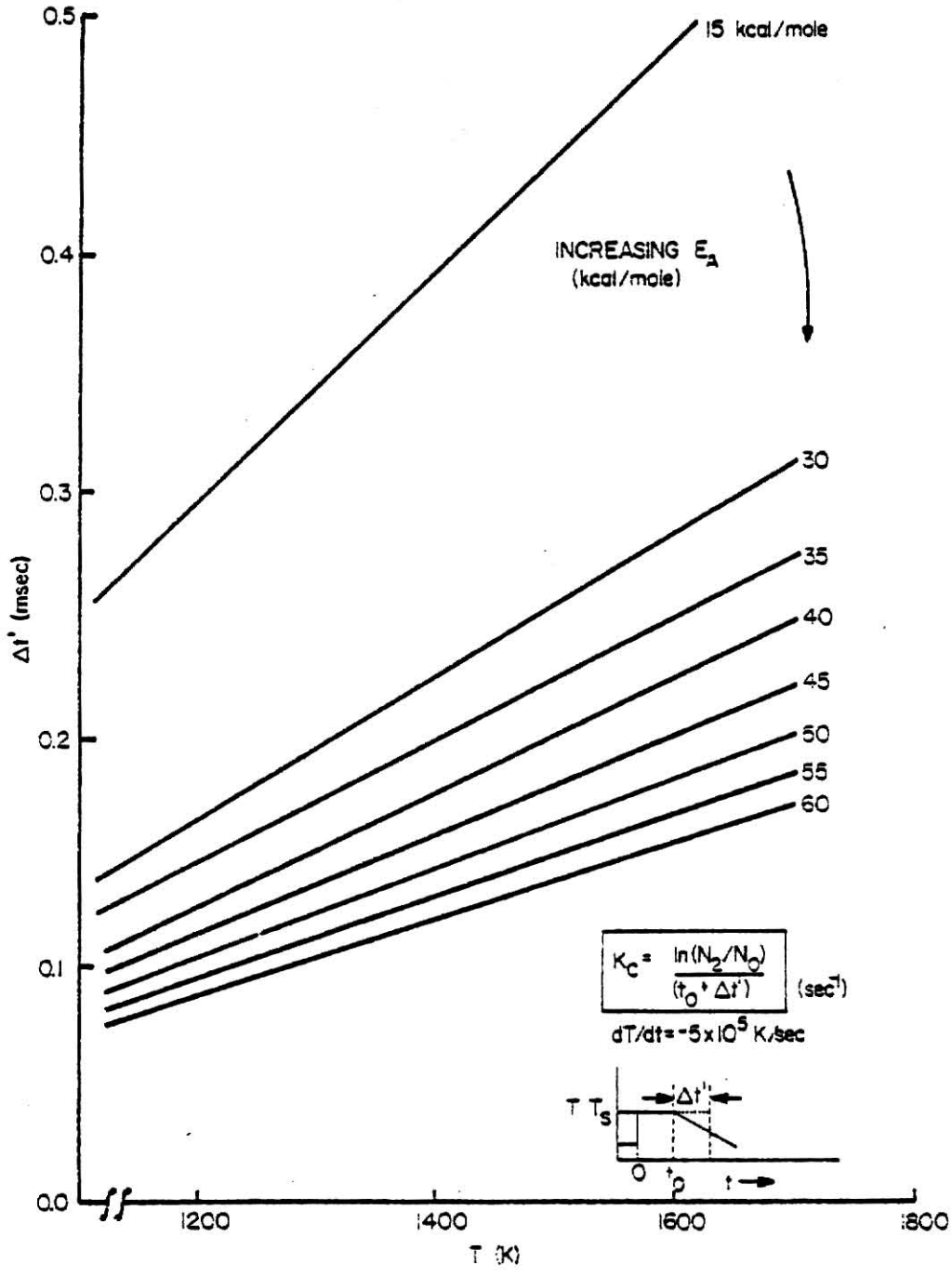

Fig. 25. Dwell time correction for finite rate cooling in argon. (From 31).

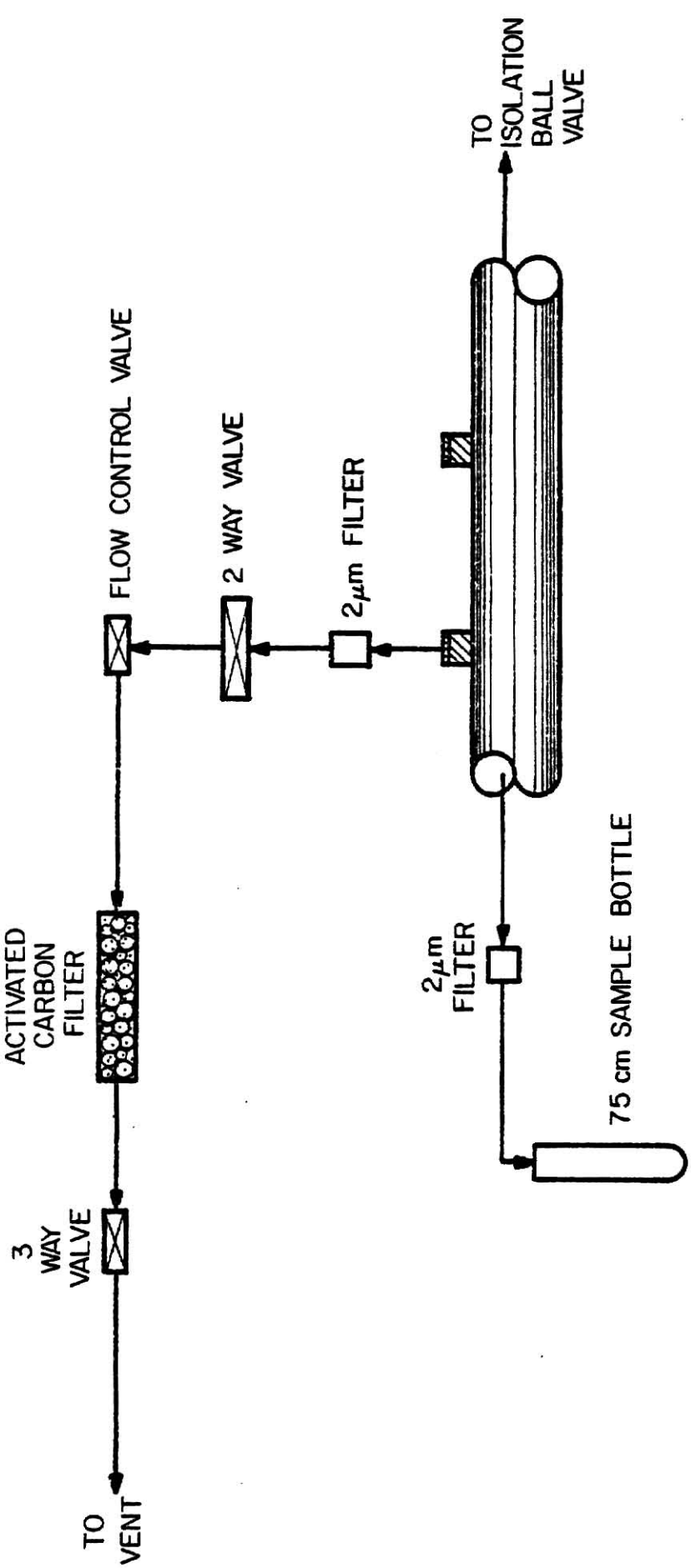

Fig. 26. Schematic of gas sampling system.

2 μm diameter. The activated charcoal filters served as lipophylic traps, absorbing all hydrocarbons greater than C_4 that were present in the effluent stream. Gas chromatographic analysis of the effluent stream after passing through the activated charcoal filters showed no hydrocarbons greater than C_2 present. When complete venting was accomplished, the end flange was removed. Any solids deposited on the flange were recovered and weighed. The inline filters were dismantled and filter elements were weighed. Surfaces of the gas venting block and dispersion plate block were wiped clean of residue and the residue weight was recorded. The aluminum liner was then removed, the ends capped, and placed in a shipping canister. The aluminum liners were refluxed by an independent laboratory, where the amounts of solid and liquid products present were determined.

2.3 Gas Chromatograph Analysis

Lower (C_1-C_2) hydrocarbons, benzene and toluene were analyzed by a Tracor 550 gas chromatograph equipped with dual flame ionization detectors. Operating parameters are given in Table 5. The gas chromatograph was calibrated with a known standard each time samples were analyzed. The calibration standard yielded a factor of grams/count as determined by the integrator. Thus, determining the number of grams of component i in the gas sample was easily accomplished via,

$$m_i = CF \times c_i \qquad (2.15)$$

where m_i is the number of grams of component i, c_i is the number of counts of i, and CF is the calibration factor.

Table 5. Gas Chromatograph Operating Conditions.

Species	C_1-C_2	Aromatics
Column	Carbosieve B	OV-101
Column Temp.	150 °C	70 °C
Inlet Temp.	175 °C	175 °C
FID Temp.	175 °C	175 °C
Carrier Gas Flowrate	45 ml/min	35 ml/min
Hydrogen Flowrate	35 ml/min	35 ml/min
Air Flowrate	400 ml/min	400 ml/min
Calibration Gas	C_2H_2 in N_2	C_6H_6

To relate the number of grams in the sample to the initial amount of coal loaded, the perfect gas law was employed. First, the number of moles of product gas contained in the test section was determined from the final equilibrium pressure of the shock tube as

$$n_p = \frac{P_p V_p}{RT} , \qquad (2.16)$$

where

n_p = number of moles,

P_p = final pressure of the shock tube,

V_p = volume of the test section,

R = universal gas constant,

T = ambient temperature.

Since V_p, R, and T are constant for all experiments this simplifies to:

$$n_p = P_p \ (2.446 \times 10^{-2}) \text{ moles} \qquad (2.17)$$

when P_p is given in atm.

The number of moles contained in the sample injected is found in the same manner. For all samples injected this value is 8.179×10^{-6} moles. Since the concentration of species i in the sample is the same as the concentration of species i in the test section, the following relation holds

$$\frac{n_s}{m_s} = \frac{n_p}{m_p} . \qquad (2.18)$$

Thus, the mass of component i in the test volume can be determined by

$$m_p = \frac{(2.4462 \times 10^{-2})(P_p)(m_s)}{(8.17 \times 10^{-6})} . \qquad (2.19)$$

To convert this to weight percent of initial coal loaded, the mass of product was divided by the initial charge of coal, and multiplied by 100.

3.0 EXPERIMENTAL RESULTS

In order to assess the influence of an hydrogen atmosphere on pyrolysis of pulverized coals, a baseline investigation of coal pyrolysis in an inert (argon) atmosphere was undertaken to establish maximum product yields and product distributions as a function of time and temperature. The technique of response surface methodology[61] was employed in the experimental design. The experimental conditions that were desired are listed in Table 6.

3.1 Coal Pyrolysis in an Argon Atmosphere

A series of experiments were performed at various temperatures and residence times at a total reaction pressure of 10 $\pm$ 1 atm. (Total reaction pressure is defined as the pressure to which the test gas is elevated by passage of the reflected shock wave.) Temperatures were varied from 1000 to 1900 K and residence times from .3 to 3.0 milliseconds. Temperatures listed in all tables and figures are those temperatures to which the test gas is elevated by passage of the reflected shock wave. Residence times cited refer to the length of time between passage of the reflected shock wave and arrival of the rarefaction wave at the end wall of the test section.

Initial experiments concentrated on establishing the new solids recovery technique. During this phase of the experimentation, it was determined that the method employed operated satisfactory; however, use of mylar diaphragms caused interference in the absorption spectra obtained by infrared spectrometry of the liquid products. To eliminate

Table 6. Experimental Design Based on Response Surface Methodology.

Run Number	Hydrogen Pressure (atm)	Temperature (°K)	Residence Time (Milliseconds)
1	0	1550	.52
2	0	1100	.52
3	0	1550	1.92
4	0	1100	1.92
5	0	1285	1.00
6	0	1285	1.00
7	0	1285	1.00
8	0	1285	1.00
9	0	1000	1.00
10	0	1800	1.00
11	0	1285	.30
12	0	1285	3.00
13	1	1550	.52
14	1	1100	.52
15	1	1550	1.92
16	1	1100	1.92
17	2	1285	1.00
18	2	1285	1.00
19	2	1285	1.00
20	2	1285	1.00
21	2	1000	1.00
22	2	1800	1.00
23	2	1285	.30
24	2	1285	3.00
25	2	1285	1.00
26	2	1285	1.00
27	6.4	1285	1.00
28	.624	1285	1.00
29	4	1550	.52
30	4	1100	.52
31	4	1550	1.92
32	4	1100	1.92
33*	2	1285	1.00
34	2	1800	2.00
35	2	1800	2.00
36	2	1800	2.00
37	1	1550	3.00
38	1	1550	3.00
39	1	1550	3.00
40	4	1550	3.00
41	4	1550	3.00
42	4	1550	3.00

*Deseret coal in place of Ill. #6.

this interference, aluminum diaphragms were substituted for the mylar diaphragms. Due to partial adsorption of C_2 hydrocarbons on the activated charcoal filters, the gas sampling technique was modified. Stainless steel gas sample bottles were connected to the test section by a three way ball valve. Sample bottles were evacuated during evacuation of the test section. Upon completion of an experimental run the pressure in the shock tube and volume of the sample bottle were recorded. Gaseous products were then directed to the sample bottle; sufficient time was allowed for the sample bottle and test section to reach an equilibrium pressure. The remaining gaseous products were then vented through the activated charcoal filter at flow rates of 1 liter/minute. The number of moles of product gas contained in the sample bottle was determined using Boyle's law and the perfect gas law. For an ideal gas at constant temperature Boyle's law is:

$$P_f = \frac{V_p}{V_f} P_p \qquad (3.1)$$

where

P_f = final pressure (absolute),

P_p = the pressure in the test section upon completion of a run (absolute),

V_p = volume of test section,

V_f = final volume ($= V_p + V_b$),

V_b = the volume of the sample bottle.

Table 7. Effect of post-shock heating on gas analysis.

T (k)	P (atm)	t (msec)	Moles $CH_4 \times 10^6$	Moles $C_2H_2 \times 10^6$	Moles $C_2H_4 \times 10^6$	Hold time at 128 °C
1452	9.11	1.0	7.40	1.10	5.19	No heat
1452	9.11	1.0	7.21	1.08	5.15	1 Sec
1596	10.5	1.0	13.8	5.41	8.31	1 Sec
1596	10.5	1.0	13.5	5.34	8.14	10 min.
1601	10.6	1.0	12.2	4.09	6.55	10 min.
1601	10.6	1.0	11.9	4.03	6.43	20 min.

Thus the final pressure of the gas sample bottle is found by

$$P_f = \frac{V_p P_p}{V_p + V_b} \quad . \tag{3.2}$$

The number of moles of product gas contained in the sample bottle is then found from the perfect gas law:

$$n_s = \frac{P_f V_b}{RT} \tag{3.3}$$

where

R is the universal gas constant,

T is the ambient temperature.

A test was undertaken to establish what effect, if any, heating of the test section to drive off volatile products had on subsequent gas analysis.[†] Three consecutive experiments were performed under identical experimental conditions. Two gas samples were taken from each experimental run after a known period of heating and analyzed by gas chromatography. As can be seen in Table 7, heating of the test section did not induce secondary reactions, or change the distribution of the pyrolysate.

Upon establishing gaseous, liquid, and solid recovery techniques, a series of pyrolysis runs in an argon atmosphere was undertaken. Lower C_1-C_2 hydrocarbon gases, benzene, and toluene present in the pyrolysate were measured by gas chromatography. Table 8 lists the

---

[†]Volatile products are those species in the gaseous phase at temperatures just above 298 °K and at pressures up to 3.5 atmospheres.

Table 8. Hydrocarbon yields for the pyrolysis of Illinois #6 in argon.

Temperature (°K)	Pressure (Atm)	Time (msec)	CH_4 Moles$\times 10^5$	C_2H_2 Moles$\times 10^5$	C_2H_4 Moles$\times 10^5$	C_6H_6 Moles$\times 10^6$	Total Moles $\times 10^5$
1097	8.2	1.0	.124	.00	.00	NM*	1.24
1118	8.5	2.0	.124	.00	.00	.00	.124
1129	9.8	2.0	.524	.00	.00	.00	.524
1159	11.2	2.0	2.04	.00	.271	NM	2.31
1217	9.8	3.0	1.22	.00	.00	1.20	1.34
1251	11.0	1.0	.532	.00	.00	.00	.532
1255	11.1	1.0	.332	.180	.00	.00	.512
1281	10.6	.3	.00	.00	.00	.00	.00
1294	10.8	3.0	3.09	.00	.120	.00	4.29
1303	10.9	1.0	2.10	.00	.512	NM	2.61
1305	10.9	1.0	.472	.00	.472	NM	.944
1306	9.4	1.5	1.47	.00	.00	NM	1.47
1307	10.9	1.0	.472	.00	.444	NM	.916
1314	11.1	1.0	1.22	.00	.412	NM	1.63
1337	7.7	1.0	1.23	.00	.00	NM	1.23
1357	7.9	1.5	2.51	.00	.00	NM	2.51
1377	11.6	3.0	5.36	.460	2.26	.00	8.08
1381	9.1	.3	.200	.00	.00	.333	.233
1386	10.4	.3	.476	.00	.00	.774	.553
1414	10.4	2.0	3.22	.508	1.76	NM	5.49
1418	11.2	.3	.524	.00	.00	.784	.602
1433	8.9	2.0	2.64	.524	1.51	NM	4.67
1452	9.1	1.0	.728	.108	.512	NM	1.35
1478	7.5	1.0	2.27	.369	.912	.220	3.57
1526	9.84	1.0	3.64	.740	1.43	NM	5.81
1573	9.9	2.0	3.99	1.89	1.63	.00	7.51

*Not measured.

Table 8 - Continued

Temperature (°K)	Pressure (Atm)	Time (msec)	CH_4 Moles$\times 10^5$	C_2H_2 Moles$\times 10^5$	C_2H_4 Moles$\times 10^5$	C_6H_6 Moles$\times 10^6$	Total Moles $\times 10^5$
1581	10.8	2.5	5.96	1.95	2.04	.00	9.95
1593	11.3	2.0	5.76	2.64	2.44	2.44	11.1
1596	10.5	1.0	1.35	.524	.812	NM*	2.69
1601	10.6	1.0	1.20	.396	.656	NM	2.25
1618	10.35	1.0	2.35	.391	.00	NM	2.74
1639	11.4	2.4	4.24	2.48	1.74	1.58	8.62
1671	10.9	1.5	2.83	.606	.00	NM	3.44
1732	8.7	2.0	2.24	3.12	.472	.00	5.83
1775	9.5	1.0	1.75	1.54	.237	.461	3.57
1848	9.1	1.0	5.12	4.32	1.00	.354	10.5
1878	10.3	1.0	1.92	2.06	.444	.277	4.45

*Not measured.

pyrolysate products obtained for 37 runs in order of ascending temperature. Methane was the dominant pyrolysis product at temperatures up to 1600 K, thereafter methane and acetylene were in approximately equal abundance.

Analysis of the gaseous products obtained is divided into two regimes; the first regime up to 1550 K assumes all light hydrocarbon gases are a result of coal pyrolysis only, the second regime, above 1550 K assumes decomposition of heavy hydrocarbons (benzene, toluene, and light oils) takes place enhancing the yield of light hydrocarbon gases obtained. For the sake of kinetic analysis, the quantity V* is defined as the maximum amount of methane that could be formed if all of the volatile carbon in the coal was converted to methane. For experimental runs with 40 mg. of Illinois #6 coal, (see Table 4), this value is 5.71×10^{-4} moles CH_4. Thus, a decomposition model, first order in amount of light hydrocarbons to be formed for regime one takes the form:[†]

$$\frac{dV_g}{dt} = k_1 (V^* - V_g) \quad . \qquad (3.4)$$

[†]First order decomposition models do not reflect the actual varied processes occurring during coal devolatilization. Jungten and Van Heek[28], however, have reported that multiple parallel reactions can be expressed by a single reaction with an activation energy and pre-exponential factor that are lower than those of the parallel reactions. Since coal pyrolysis involves the simultaneous cleavage of various bonds, identifying the multiple parallel reactions and determining their kinetic parameters would be a herculean task. The main goal of this model is to predict the extent of devolatilization for Illinois #6 coal at the conditions of this experimentation. Extrapolation to higher or lower temperatures, or use of different heating rates may result in erroneous predictions.

Assuming Arrhenius behavior, the substitution $k_1 = A \exp(-E_1/RT)$ can be made yielding

$$\frac{dV_g}{dt} = [A \exp(-E_1/RT)] [V^*-V_g] \qquad (3.5)$$

where

$\frac{dV_g}{dt}$ = instantaneous rate of production of light hydrocarbon gases, (moles/sec) at temperature T,

E_1 = global activation energy for regime one, (kcal/mole),

R = universal gas constant (kcal/mole K)

T = temperature (K),

A = Arrhenius pre-exponential factor (sec^{-1}).

Integration of Eq. (3.5) yields

$$-\ln(V^*-V_g)\Big|_t + \ln(V^*-V_g)\Big|_{t=0} = A \exp(-(E_1/RT))\ t. \qquad (3.6)$$

At t=0, V_g=0 and Eq. (3.6) simplifies to

$$-\ln\left(\frac{V^*-V_g}{V^*}\right) = A \exp(-(E_1/RT))\ t. \qquad (3.7)$$

Values for A and E_1 can be obtained from a plot of $\ln\left\{\frac{1}{t}\left(\ln\left(\frac{V^*-V_g}{V^*}\right)\right)\right\}$ versus $\frac{1}{T}$. This is plotted in Fig. 27 for experiments up to 1550 K, along with data obtained by Wegener for Pittsburgh seam coal and Illinois #6 coal. A least squares fit of the data yields a global activation energy of 24.7 kcal/mole with a pre-exponential factor of 2.93×10^5 sec^{-1} for this study. Values obtained for Wegener's data are an activation energy of 22.6 kcal/mole and 20.7 kcal/mole for Pittsburgh seam and Illinois #6 respectively, with pre-exponential factors of 2.73×10^5 sec^{-1} and 1.25×10^5 sec^{-1}.

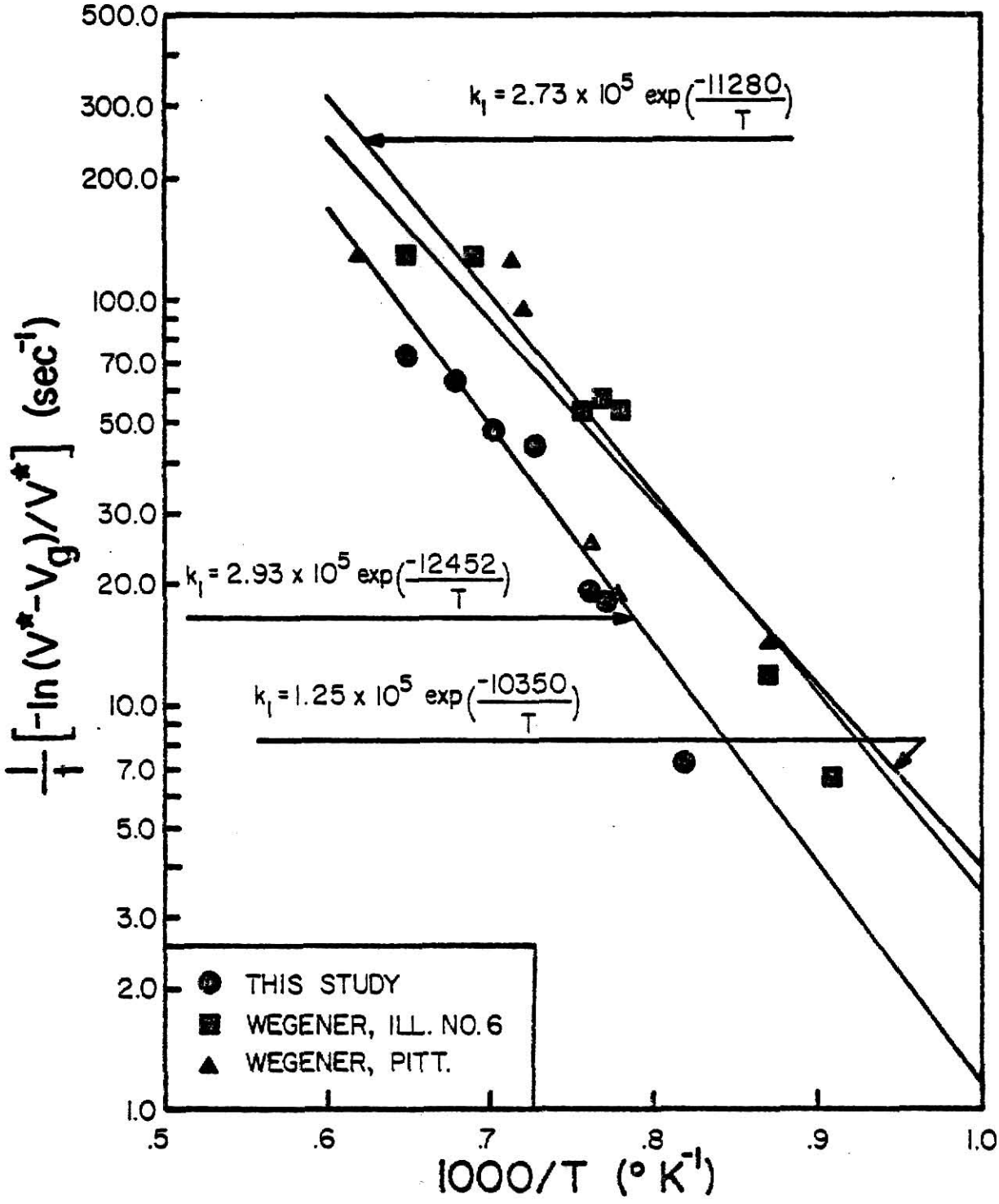

Fig. 27. First order rate constants for the evolution of gaseous hydrocarbons during pyrolysis of bituminous coals. ●, ▲, ■ denote experimental data, solid lines are from a least squares fit of the experimental data.

Pyrolysis gas yields obtained at different residence times and temperatures are shown in Fig. 28 along with projected yields predicted by the model for various residence times. Based on the model, approximately complete conversion of volatile carbon to methane could be achieved in 45 milliseconds at 1600 K, and nearly 50% conversion could be obtained at 1500 K, and 6.4 milliseconds. Hence high conversions to gaseous products can be achieved at much shorter residence times than heretofore believed.

To distinguish between temperature effects and time effects on pyrolysis products and product distribution, the rate of gaseous products evolved with respect to temperature is displayed in Fig. 29 for methane, ethylene, and acetylene. Rates were obtained subject to the assumption that the increase in product yield was directly proportional to time. Upon examination of Fig. 29 it can be seen that methane and ethylene show similar temperature dependent behavior. Both gases display an increase in yield with increasing temperature up to 1500 K. Maximum yields of both gases occur between 1500 and 1600 K. Above 1600 K yields of both gases begin to decline. Acetylene yields display a different behavior than that of methane and ethylene; acetylene yields steadily increase with increasing temperature over the temperature range employed in this study. Regime one methane evolution (up to 1550 K) is thought to be primarily a result of recombination of methyl radicals and hydrogen produced during devolatilization. Initial ethylene production is thought to be due to recombination of radical fragments from larger molecules decomposing and from the decomposition of ethane via

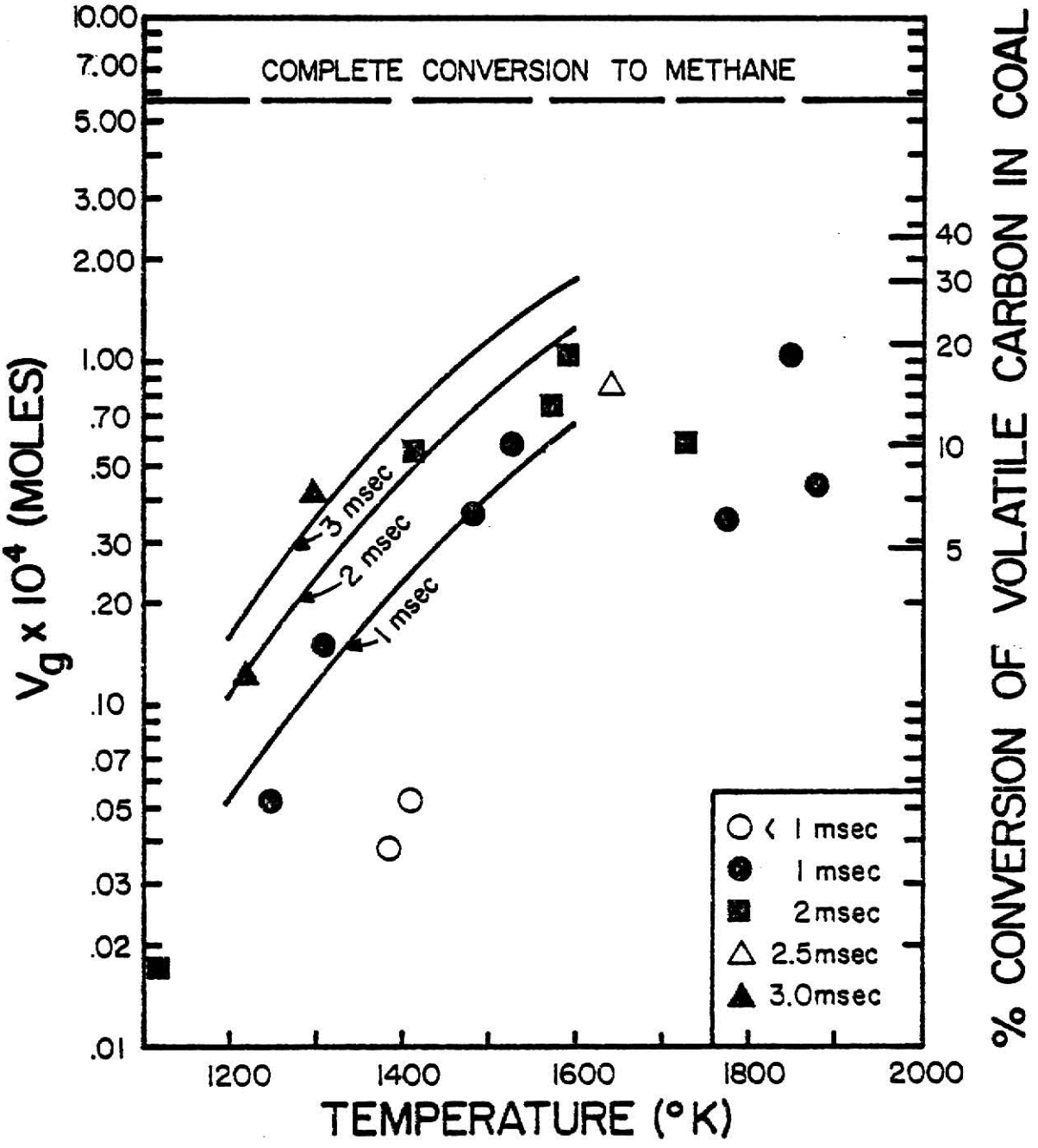

Fig. 28. C_1-C_2 hydrocarbon yields from pyrolysis of Ill. #6 coal. Solid lines denote predictions from the model at various residence times.

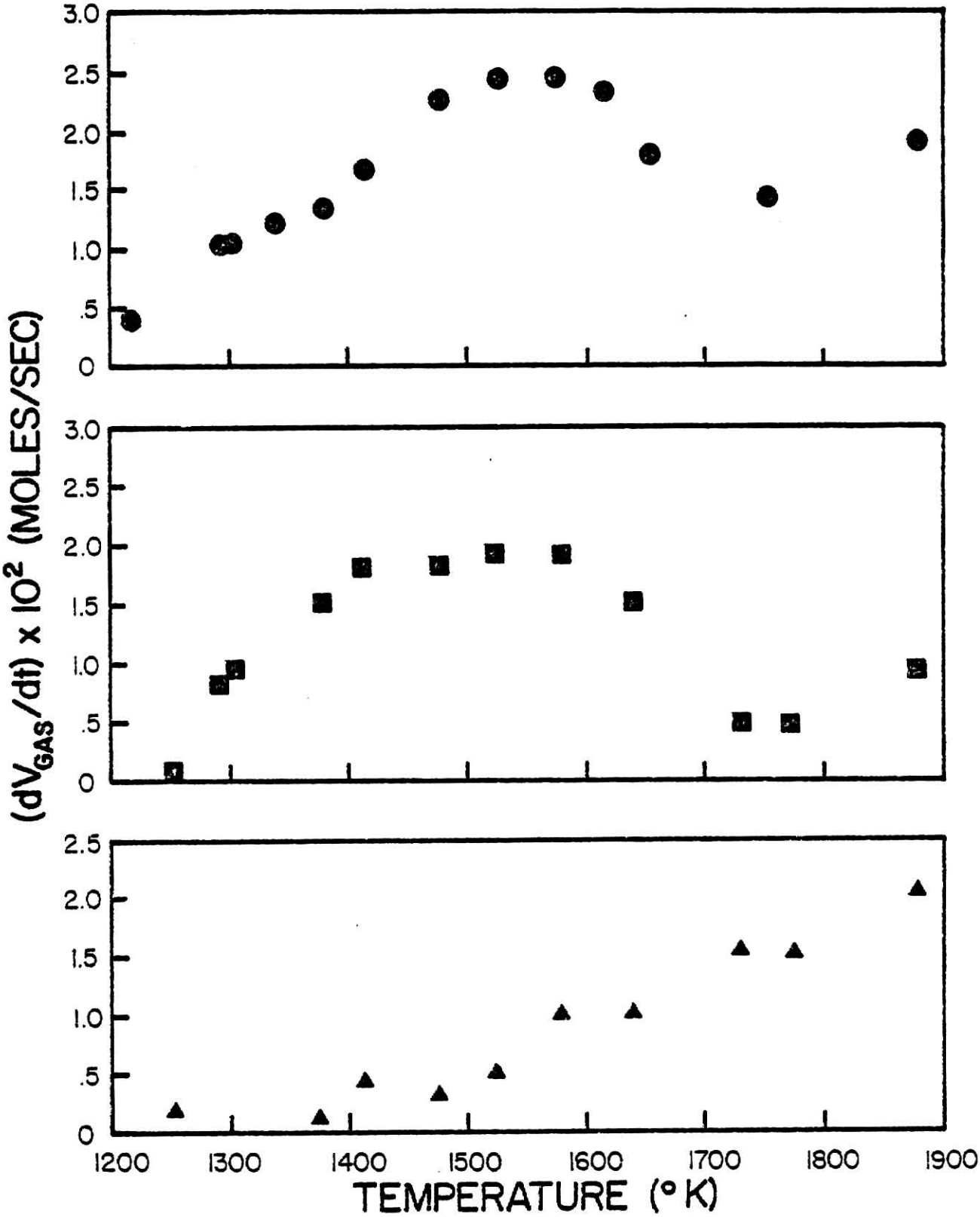

Fig. 29. Rate of hydrocarbon evolution versus temperature for the pyrolysis of Ill. #6 in argon. ● evolution of CH_4, ■ evolution of C_2H_4, ▲ evolution of C_2H_2.

$$C_2H_6 \rightleftarrows C_2H_4 + H_2. \qquad (3.8)$$

Acetylene production in regime one most likely is also due to radical stabilization. Regime two methane and acetylene production is attributed to decomposition of heavier hydrocarbons (benzene, toluene, and light oils). Acetylene production in this regime also is due in part to ethylene decomposition via

$$C_2H_4 \rightleftarrows C_2H_2 + H_2. \qquad (3.9)$$

The main effect of residence time on gaseous pyrolysis yields was to increase product yields as residence times were increased. At extremely short residence times methane was the principal pyrolysis gas present; as residence times increased methane yields increased and ethylene and acetylene appeared in the pyrolysate.

Liquid yields behaved differently than gaseous products. Benzene yields began appearing in the pyrolysate when temperatures above 1350 K were attained. Although benzene yields do show a dependence on temperature, they display a much stronger dependence with time. Shorter residence times generally produced increased benzene yields. Maximum benzene production occurred at 1593 K and 2.0 milliseconds residence time. Above this temperature benzene yields decrease, reaching nearly zero at 1732 K and 2.0 milliseconds. Benzene yields at 1878 K and 1.0 millisecond are approximately one order of magnitude less than the maximum value obtained. A study by Vaughn[63] on the decomposition of benzene shows nearly 70% of benzene undergoes decomposition at 1700 K and 2.4 $\pm$ .4 milliseconds residence time. Thus, the decrease in benzene above 1600 K is attributed to decomposition, not to the

primary kinetic pathways of coal devolatilization. Benzene yields obtained during pyrolysis of coal with respect to temperature are included in Fig. 30.

3.2 Coal Pyrolysis in an Hydrogen Atmosphere

A series of 42 experiments involving various hydrogen partial pressures, temperatures, and residence times were conducted. Total reaction pressure was maintained at 10 $\pm$ 1 atm when possible. Use of test gas mixtures containing 40% or more hydrogen by volume resulted in slightly lower total reaction pressures. Table 9 lists the product yields obtained from hydropyrolysis in order of ascending temperature.

The main feature of the hydropyrolysis experiments is a slight overall increase in product yields obtained over that obtained during pyrolysis. Figure 31 displays the total gaseous hydropyrolysis yields obtained at different temperatures; no distinction is made between various partial pressures of hydrogen for reasons to be explained shortly. Gaseous yields begin to exceed those obtained under pyrolysis at temperatures above 1400 K. More information can be obtained from an examination of the individual gaseous products, the mole fractions of which are tabulated in Table 10 for nine experiments. As can be discerned from Table 10, the various proportions of the gaseous products are changing with variations in hydrogen partial pressures. This variation is most evident at temperatures of approximately 1700 K, where methane fractions in hydrogen are twice that of pyrolysis while acetylene ratios are half that of pyrolysis.

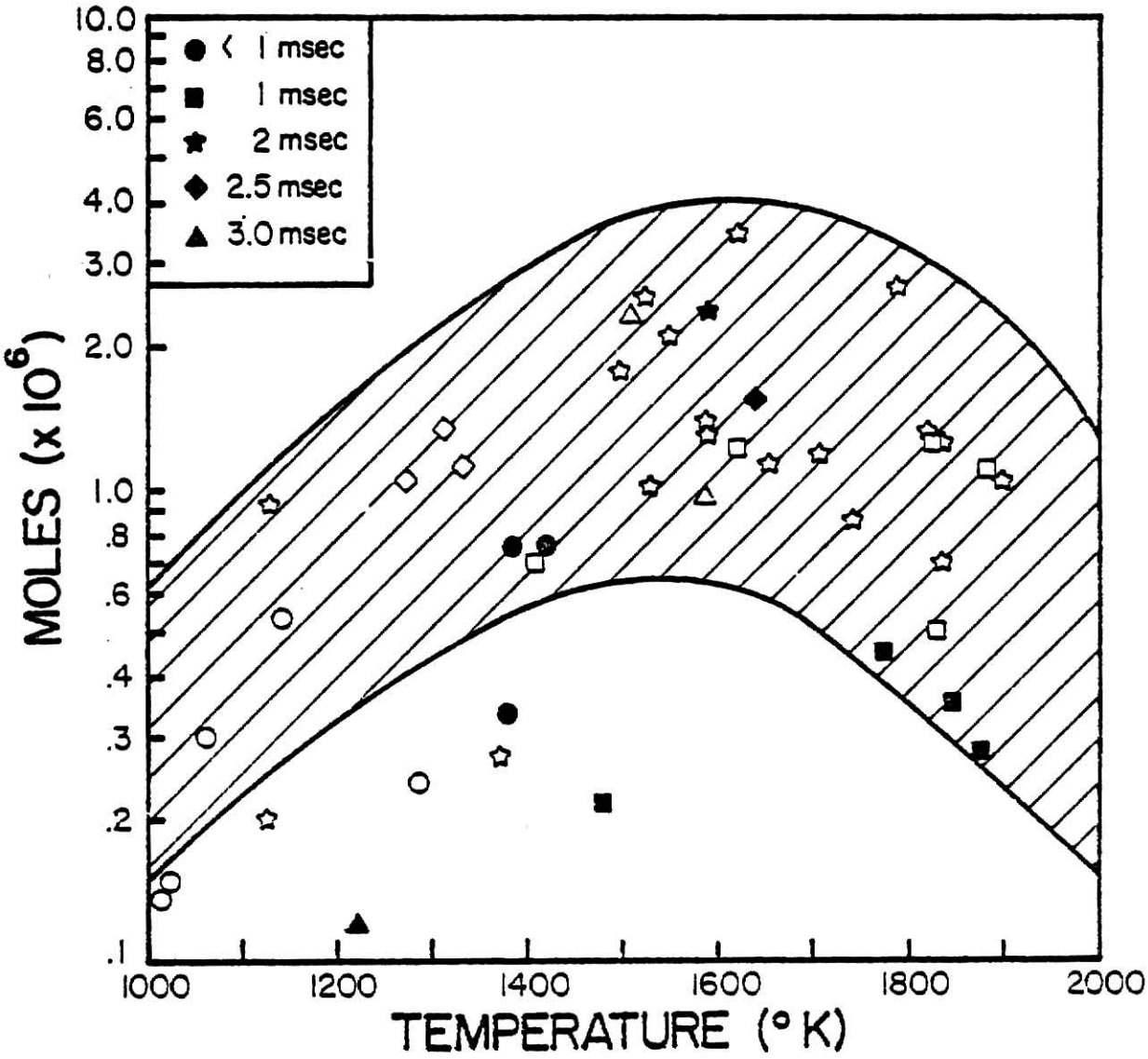

Fig. 30. Benzene yields as a function of temperature from the pyrolysis of Ill. #6 in argon and hydrogen/argon mixtures. Filled symbols denote an argon atmosphere, open symbols denote an hydrogen/argon atmosphere. Cross hatched area is to aid the reader in discerning trends.

Table 9. Hydrocarbon yields for the pyrolysis of Illinois #6 in Hydrogen/Argon mixtures.

Temp. (°K)	Total Pressure (atm)	Hydrogen Partial (atm)	Time (milli-seconds)	CH_4 Molesx10^5	C_2H_2 Molesx10^5	C_2H_4 Molesx10^5	C_6H_6 Molesx10^6	Total molesx10^5
988	8.0	.80	.4	.00	.00	.00	.138	.014
1015	10.1	2.01	1.0	.224	.00	.00	.103	.234
1017	8.2	.82	.3	.00	.00	.00	.138	.014
1022	8.1	.81	.5	.00	.00	.00	.149	.015
1062	8.5	.85	.5	.00	.00	.00	.297	.029
1127	9.7	3.9	2.0	2.096	.00	.599	.251	2.72
1133	10.2	1.02	2.0	.748	.00	.00	.928	.841
1139	10.2	4.08	.5	.700	.00	.128	.533	.881
1170	9.98	.99	2.0	.500	.00	.00	.027	.500
1259	10.3	.62	1.0	1.27	.00	.400	.00	1.67
1275	10.4	4.6	2.5	4.88	.215	1.33	1.01	6.53
1291	10.4	2.08	.3	.500	.00	.057	.241	.581
1315	8.4	3.36	2.5	8.80	.308	2.82	1.34	12.0
1316	6.0	3.87	2.0	1.80	.031	.484	.00	2.31
1327	9.4	3.76	2.5	4.88	.338	1.28	1.16	6.61
1335	10.3	2.05	3.0	5.08	.154	1.43	.00	6.66
1371	9.1	.912	2.0	8.40	2.55	1.61	.277	12.6
1414	6.8	4.35	1.0	6.32	.444	1.96	.697	8.79
1499	8.3	3.33	2.0	6.00	.984	1.40	1.81	8.57
1509	9.8	.98	3.0	11.1	3.43	2.98	2.27	17.7
1523	9.94	.99	2.0	8.36	4.84	1.86	2.65	15.3
1523	8.73	3.49	2.0	7.00	2.00	1.63	1.01	10.7
1549	8.77	3.51	2.0	7.12	1.38	1.70	2.15	10.4
1572	10.4	1.04	3.0	15.9	7.64	5.60	3.33	29.5
1587	10.6	1.06	3.0	8.24	3.58	1.51	.948	13.4
1590	9.25	3.70	2.0	4.76	1.18	1.06	1.27	7.13
1592	8.58	3.43	2.0	9.36	2.58	2.27	1.36	14.4

Table 9 - continued

Temp. (°K)	Total Pressure (atm)	Hydrogen Partial (atm)	Time (milli-seconds)	CH_4 Molesx10^5	C_2H_2 molesx10^5	C_2H_4 Molesx10^5	C_6H_6 Molesx10^6	Total moles x10^5
1620	10.6	4.24	1.0	8.00	1.77	2.11	1.22	12.0
1623	9.14	.914	2.0	9.96	3.20	1.51	3.00	14.9
1656	8.52	3.41	2.0	8.2	2.4	1.80	1.18	12.5
1704	8.26	3.30	2.0	5.44	1.91	1.03	1.22	8.50
1742	7.78	1.56	2.0	4.04	2.00	.500	.856	6.63
1793	8.12	1.62	2.0	12.8	8.64	2.50	2.74	24.2
1816	8.27	1.65	2.0	2.34	1.52	.00	.00	3.86
1819	8.3	1.66	2.0	6.96	4.44	.928	1.33	12.5
1822	8.3	1.66	1.0	6.16	2.97	1.16	1.27	10.4
1831	8.4	1.68	2.0	6.40	4.48	.928	1.26	11.9
1833	8.51	3.40	1.0	3.52	1.23	.728	.502	5.53
1835	7.81	3.12	2.0	7.20	2.95	1.68	.712	11.9
1884	7.5	1.50	1.0	4.20	3.23	.500	1.11	9.03
1898	7.5	3.00	2.0	4.80	2.37	.964	1.06	8.24
1321*	11.9	2.38	1.0	4.52	.108	2.07	.364	6.73

*Deseret coal.

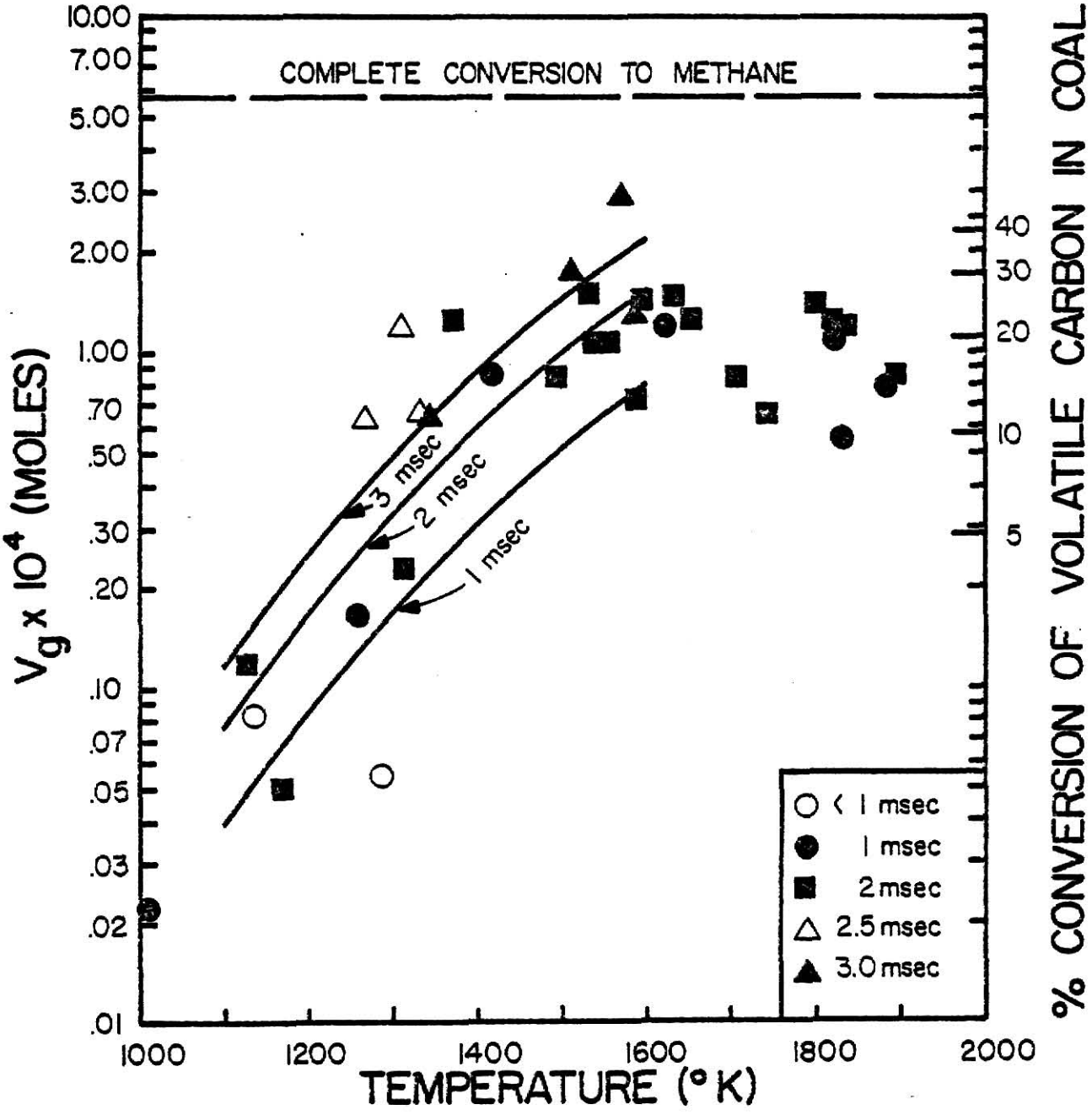

Fig. 31. C_1-C_2 hydrocarbon yields from the pyrolysis of Ill. #6 in hydrogen/argon mixtures. Solid lines denote predicted yields from the model at various residence times.

Table 10. Yields of hydrocarbon gases (mole fractions) from the pyrolysis of Ill. #6 coal in argon and hydrogen/argon mixtures.

Time (milli-seconds)	Temp. (°K)	Hydrogen Partial Pressure (atm)	Mole fraction CH_4	Mole fraction C_2H_2	Mole fraction C_2H_4
2.0	1129	0	1.00	.00	.00
2.0	1133	1.02	1.00	.00	.00
2.0	1127	3.87	.78	.00	.22
2.0	1593	0	.53	.24	.23
2.0	1623	.914	.68	.22	.10
2.0	1592	3.43	.66	.18	.16
2.0	1732	0	.38	.53	.08
2.0	1742	1.56	.62	.31	.08
2.0	1704	3.30	.65	.23	.12

*Numbers do not sum to 1.0 because of rounding.

Another method of discerning the effect of an hydrogen atmosphere is to examine the ratio of unsaturated gases to saturated gases. The logarithm of the ratio of acetylene to ethylene concentrations is plotted in Fig. 32 for both pyrolysis and hydropyrolysis. Examining Fig. 32 reveals that ratios do not deviate significantly from one atmosphere to another atmosphere. To better discern the effect of hydrogen on pyrolysis products and product distribution, the rate of individual gaseous products evolved is plotted in Fig. 33 as a function of temperature. In comparing Fig. 33 with Fig. 29 , it can be seen that the rate of ethylene formation is unaffected by hydrogen until temperatures greater than 1700 K are attained. Likewise the rate of formation of acetylene shows little or no effect due to hydrogen until temperatures greater than 1700 K are reached. Methane is the gaseous constituent that is most affected by the hydrogen atmosphere; yields of CH_4 in hydrogen are approximately 60% greater than those obtained in an argon atmosphere. Liquid yields began appearing at lower temperatures than in pyrolysis experiments, and generally displayed an increase over that obtained during pyrolysis. Although Virk, et al.[63] state pyrolysis of benzene is unaffected by hydrogen atmospheres of up to 100 atm pressure, the presence of hydrogen in these experiments may have had an inhibiting effect on benzene pyrolysis.

In assessing the influence of hydrogen on pyrolysis products and product distributions, two mechanisms were proposed; chemical reaction of hydrogen and radical fragments or stabilization of vibrationally excited radical fragments through recombination reactions using hydrogen

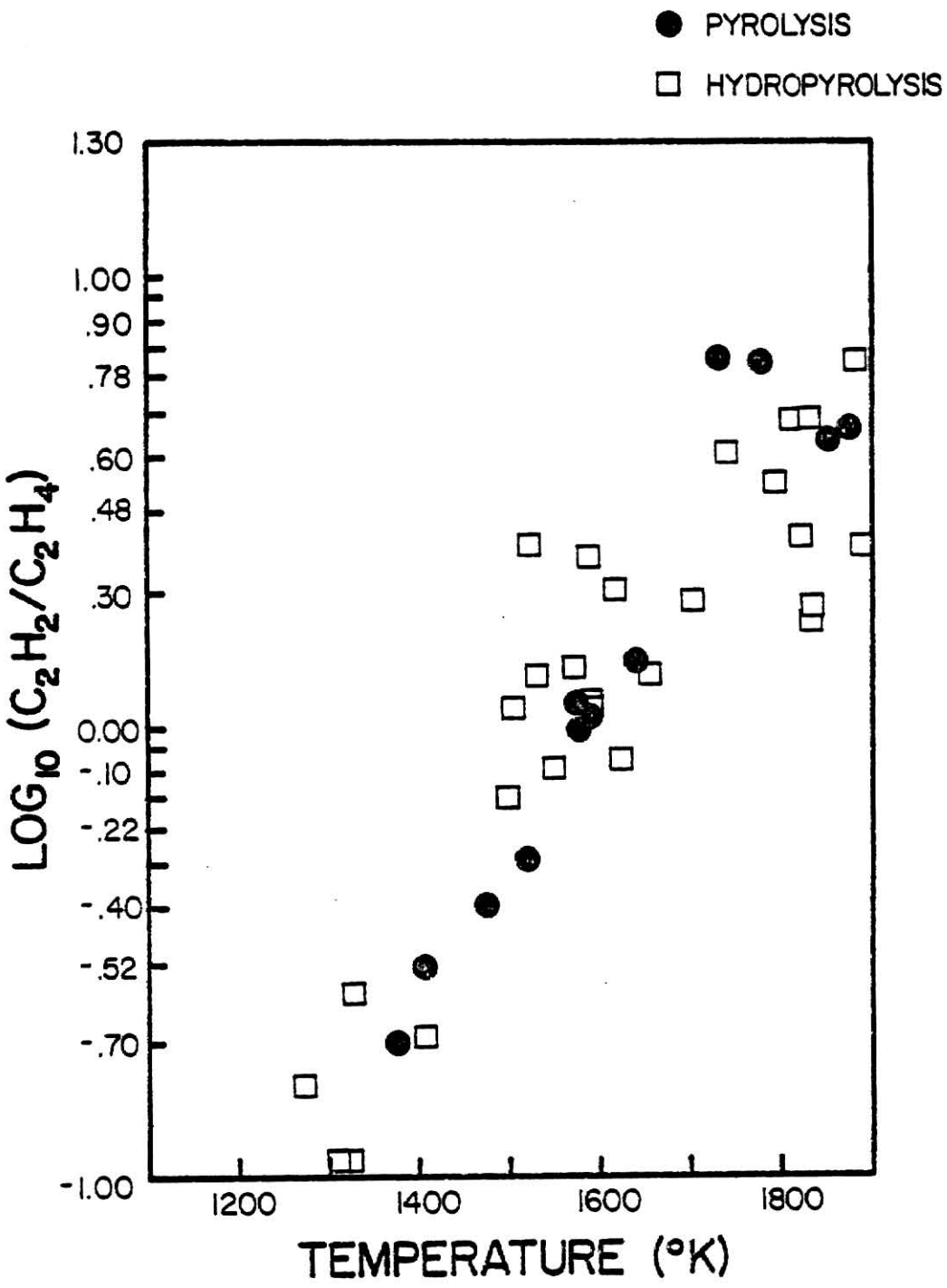

Fig. 32. Logarithmic ratio of C_2H_2/C_2H_4 versus temperature for pyrolysis and hydropyrolysis.

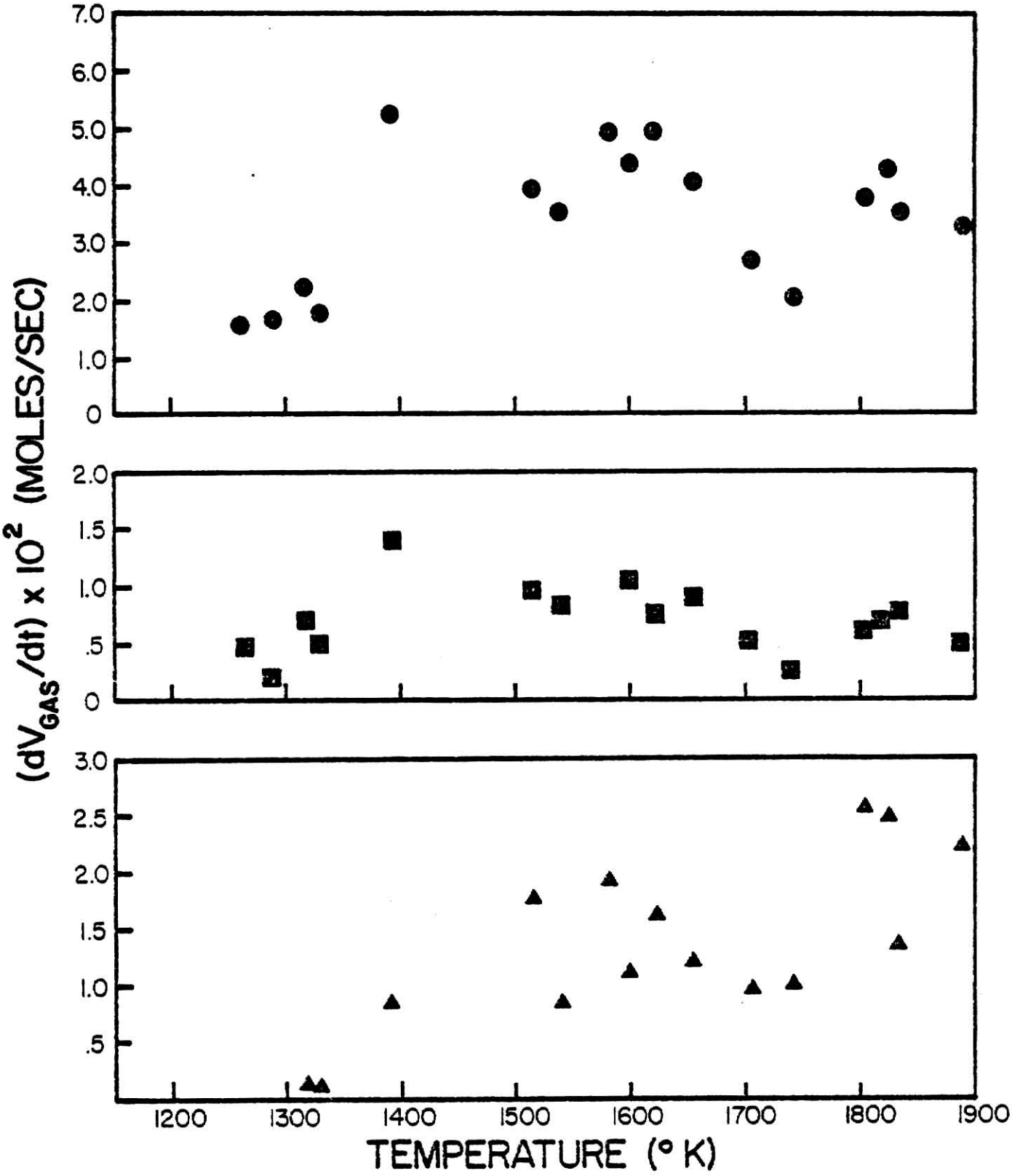

Fig. 33. Rate of gaseous hydrocarbon evolution as a function of temperature for the pyrolysis of Ill. #6 coal in hydrogen argon mixtures. ● CH_4, ■ C_2H_4, ▲ C_2H_2.

as a third body. If hydrogen is participating chemically, the evolution of gaseous hydropyrolysis products can be described by the sum of a reaction n^{th} order in hydrogen partial pressure plus the contribution from the coal decomposition. The resulting equation is

$$\frac{dV_g}{dt} = k_1(V^*-V_g) + k_2(V^*-V_g)\, P_{H_2}^n , \qquad (3.10)$$

where V_g^* is defined in Section 3.1,

$\frac{dV_g}{dt}$ = instantaneous gas phase composition (moles/sec)

k_1 = Arrhenius rate constant for pyrolysis (sec^{-1}),

P_{H_2} = partial pressure of hydrogen (atm),

k_2 = Arrhenius rate constant for the contribution to the gaseous yields by reaction with hydrogen ($sec\text{-}atm^{-1}$),

n = order of model.

Using different values of n, an attempt was made to determine k_2, the rate constant for the contribution due to the influence of hydrogen. Values of 1, 1/2, -1/2, 3/2, 2, .1, .2 and -2 were substituted in Eq. (3.10) for n, but no acceptable correlation for k_2 could be obtained. Thus it was concluded that at the very least the influence of hydrogen could not be discerned by this method, and perhaps that hydrogen was not influencing the gas yields through chemical reaction. However, another explanation is equally as plausible.

It has been shown[64] that in mechanisms of atom and radical combinations, the reaction will appear to be zero order with respect to the third body if the third body concentration is much greater than the reactants.

Furthermore, even if hydrogen were to react chemically with radical fragments through a global reaction such as Eq. (3.10), the reaction will appear to be zero order in hydrogen if its concentration is much in excess of the reaction partner. Any change in product distribution should appear in such instances with the first incremental addition of hydrogen. In Table 10, it appears that this is, in fact, the case since the greatest changes in the methane mole fraction occurs between an argon atmosphere and the first addition of hydrogen at the two higher temperatures where chemical interaction of hydrogen is more likely. The total amount of H_2 in the test section at 1 atm and 1285 °K is 5.7×10^{-3} moles, much greater than the concentration of volatile carbon (5.7×10^{-4} moles), hence it is justified to use a model equation identical to Eq. (3.4) to determine kinetic parameters. Kinetic parameters determined by the model are an activation energy of 21.9 kcal/mole and a pre-exponential factor of 1.50×10^{5} sec^{-1}. The resulting best fit line is shown in Fig. 34, along with experimental data points. The first order rate constant is slightly greater than that obtained under an argon atmosphere, but lower than that obtained by fitting Wegener's data obtained in a nitrogen atmosphere. Table 11 lists first order rate constants obtained by use of the first order model for this study and that of Wegener.[11] If, indeed, stabilization through a third body mechanism is the dominant influence, the rate constants should have the same global activation energies (to within experimental uncertainty) but different pre-exponential factors. Using the method reported by

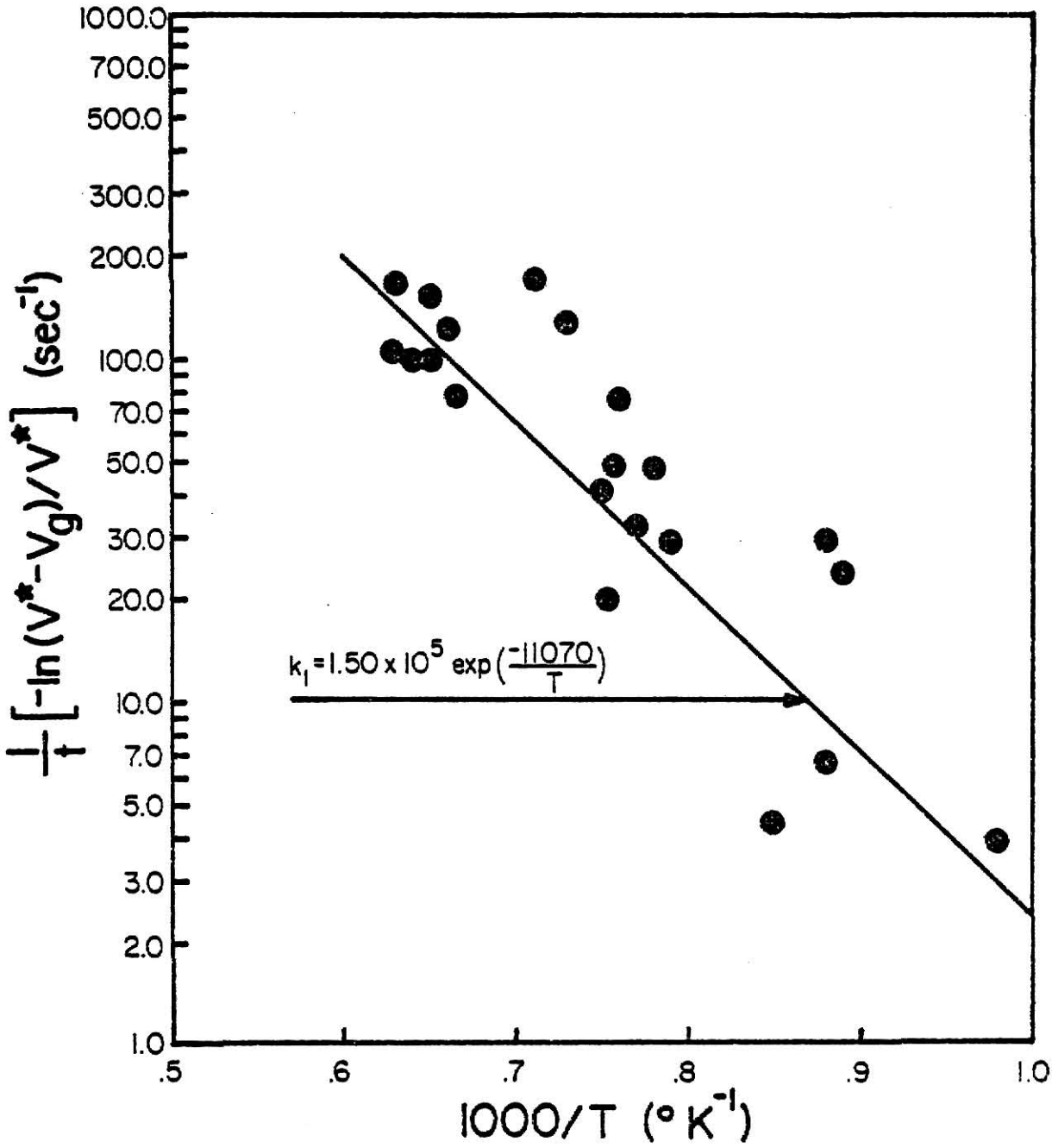

Fig. 34. First order rate constant for the evolution of gaseous hydrocarbons from the pyrolysis of coal in an hydrogen/argon mixture. ● Experimental data, solid line from a least squares fit of the experimental data.

Table 11. First order rate constants (1000-1550 °K).

Investigator	Illinois #6		Pittsburgh Seam	
	Activation Energy (kcal/mol)	Pre-exponential Factor (sec^{-1})	Activation Energy (kcal/mol)	Pre-exponential Factor (sec^{-1})
Szydlowski (in argon)	24.7	2.93×10^5		
Szydlowski (in hydrogen/argon)	22.0	1.50×10^5		
Wegener (in nitrogen)	20.6	1.25×10^5	22.4	2.73×10^5
Wegener (in air)			31.5	8.29×10^6

Breipohl,[29] a standard deviation of 1.09 kcal/mole was determined for the activation energy. A more extensive discussion on stabilization effects and implications is included in the discussion section of this chapter.

Yields of benzene from pyrolysis in an hydrogen atmosphere increased over those from pyrolysis in an argon atmosphere. Detectable amounts of benzene began appearing in the hydropyrolysate at low temperatures (ca. 1000 K) and very short residence times ($\leq$ .5 msec). The relatively low temperature appearance of benzene suggests that chemical reaction with hydrogen is not occurring, but does not preclude this observation. Kershaw and Barrass[65] performed an investigation of coal hydrogenation using deuterium to elucidate the mechanisms involved. In a preliminary report on experiments conducted at 450 °C, they report that the relative increase in various hydrogen types on hydrogenation indicates that hydrogenation of aromatic rings is not the major process occurring. Hence, it is more likely the increase in benzene in an hydrogen atmosphere is due to stabilization effects, not chemical effects.

Above 1700 K, hydrogen does have a chemical influence on the pyrolysate products. In comparing the ethylene and acetylene yields above 1700 K in argon and hydrogen/argon atmospheres, the decomposition of ethylene to acetylene is apparently inhibited by the presence of hydrogen. This influence can be explained by the principal of Le Chatelier which states that a system, when subjected to a perturbation, responds in a way that tends to eliminate its effect. Thus the increase in hydrogen tends to promote an increase in ethylene to maintain an equilibrium position through Eq. (3.9).

3.3 Discussion

The objectives of this investigation were to determine what yields could be achieved in inert and hydrogen atmospheres at short residence times, and under what conditions optimal benzene formation occurs.

Figure 35 displays the yield of light hydrocarbon gases obtained in this investigation in an inert atmosphere along with data from two other investigations conducted in inert atmospheres at longer residence times. As can be seen in Fig. 35, yields from this investigation lie in between those of the other investigations. Hence, comparable yields of gaseous products can be obtained at high heating rates and short residence times. Based on the model described in Sec. 3.1, yields identical to those reported by Tyler could be achieved at 1500 °K and 7.5 msec. The model predicts nearly 94% of the volatile carbon in the coal (corresponds to 16.7 wt. percent of the coal) would be converted to methane at 1000 °C and 300 milliseconds, a yield that exceeds that obtained by Tyler.

An interesting aspect of Fig. 35 is that the yields reported for Tyler and Suuberg are for the same coal. What is the reason for the increased yields observed by Tyler over that of Suuberg? Is it a function of the heating rate, or an artifact of the experimental technique? To answer these questions, the fundamental processes of coal devolatilization must be addressed.

Thermal decomposition of coal involves the cleavage of bonds between molecules to yield radical fragments. Once clear of the char

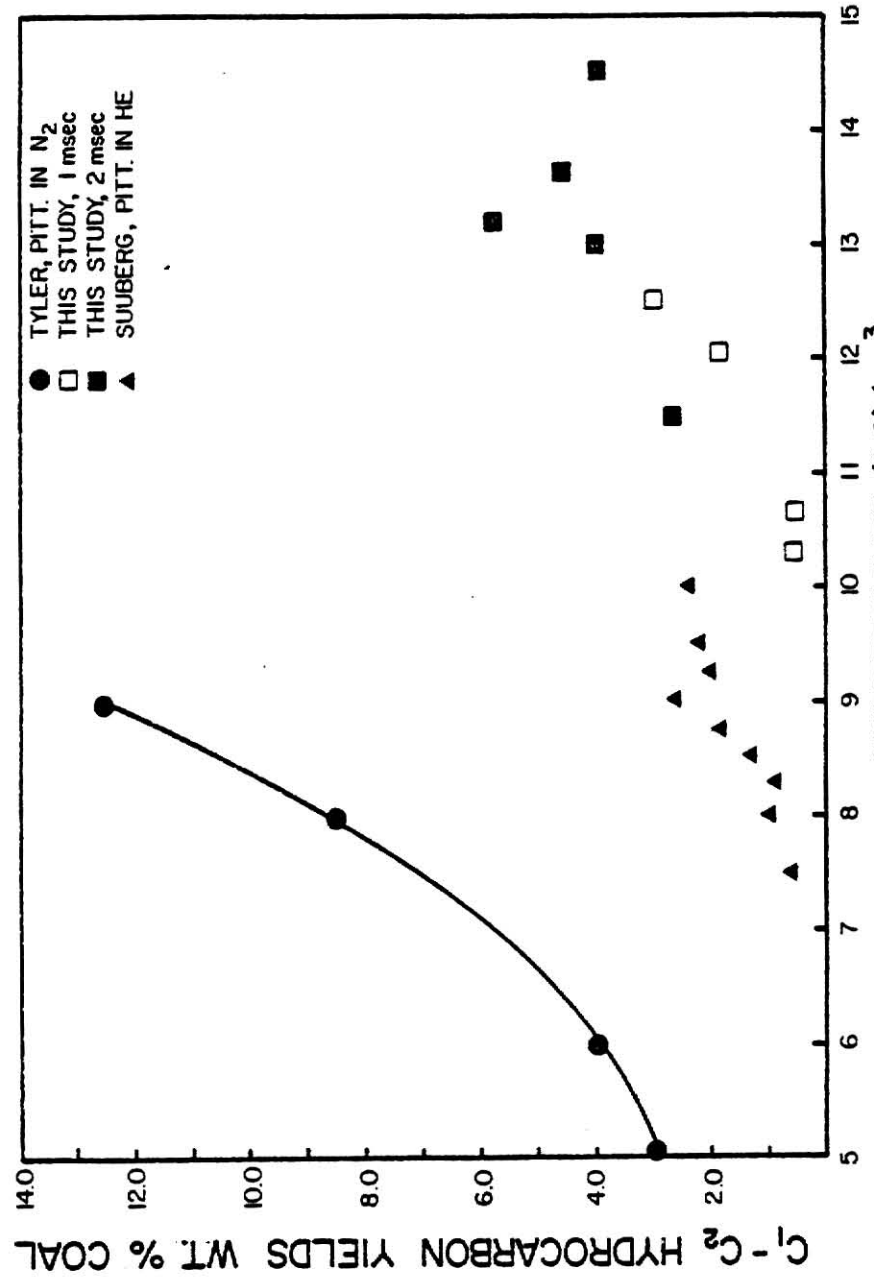

Fig. 35. $C-C_2$ hydrocarbon yields as a function of temperature for pyrolysis in inert atmospheres.

these radical fragments, many of which are vibrationally excited, recombine with similar small radical fragments to form hydrocarbon gases or with larger radical fragments to form heavier fractions or even soot. Figure 36 displays coal particles before shock heating and Fig. 37 after shock heating. The shock heated coal contains many blow holes, indicating that volatile release is most likely a violent, jetting action. Seeker,[32] has reported evidence that volatiles are ejected from the coal particle in a single stream. Thus, for most cases, the volatiles that escape must recombine in the gaseous atmosphere surrounding the coal particle, away from the surface of the coal particle. If, however, as in the case of Anthony, et al.[27], and Suuberg, et al.[18,17] the surrounding atmosphere has penetrated the pores of the coal particle prior to the onset of decomposition, the radical fragments can then be stabilized within the pores of the coal particle, leading, perhaps, to larger volatile species and lesser amounts of light hydrocarbons. An important aspect as discussed in Chapter one, is the rapidity with which the surrounding gas can de-excite energetic recombination species. Anthony and Suuberg both used cold bath gases in which these energetic molecules were quenched effectively before further decomposition could ensue. Figure 8 displaying the tar yields obtained by both Suuberg and Tyler, shows increasing tar yields for Suuberg over the range that Tyler reported a decrease. Tyler's tar yields decrease because the hot surrounding gas cannot quench the "hot" tar molecule, hence the tar decomposes to light hydrocarbon gases and soot. The reason Tyler's light hydrocarbon yields exceed those of Suuberg is basically due to experimental technique.

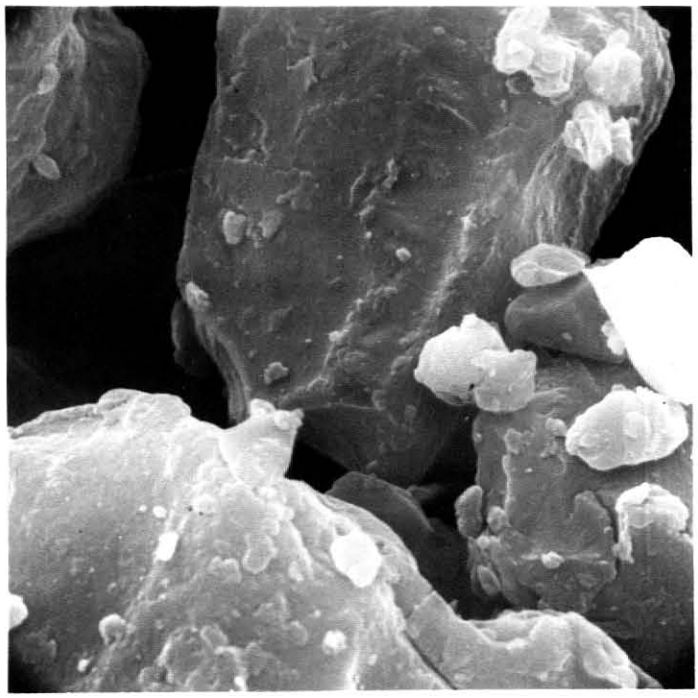

Fig. 36. Illinois #6 coal before shock heating. Full width of photograph corresponds to 9 microns.

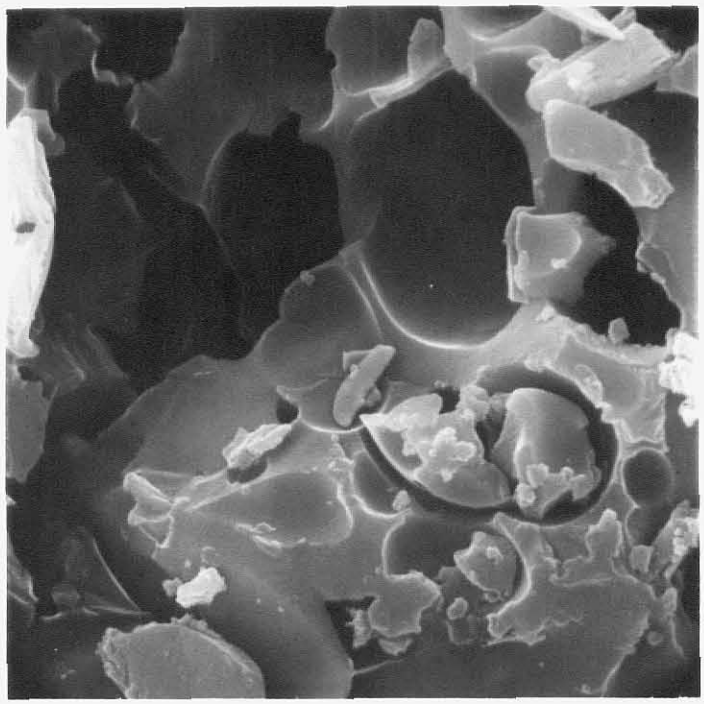

Fig. 37. Illinois #6 coal after shock heating. Full width of photograph corresponds to 9 microns.

Yields obtained in an hydrogen atmosphere exceeded those obtained in an argon atmosphere, and are shown in Fig. 38 along with yields obtained by Tyler and Coates in hydrogen atmospheres. As in the case of an inert atmosphere, Tyler's yields exceed those obtained in this study, but yields obtained by Coates are close to those obtained in this study. Based on the model given in Sec. 3.2, yields comparable to Tyler can be attained at 1500 °K in 7.9 milliseconds.

What specifically is the mechanism for increased yields in an hydrogen atmosphere over an inert atmosphere? Tyler[22] investigated pyrolysis of coal in both hydrogen and helium atmospheres. For Liddell B coal, Tyler observed an increase in methane to 11.5% in an hydrogen atmosphere compared to methane yields of 7% in an helium atmosphere. Since the yields obtained in helium were quite close to those obtained in nitrogen, Tyler concluded that the hydrogen influence was of a chemical nature because the thermal conductivities of hydrogen and helium are nearly the same. Based on the current experimentation, this appears incorrect. While thermal conductivity affects the heat up of solid particles in a hot suspension, residence times of 300 msec in a fluidized bed should be more than adequate for the particle to achieve the ultimate reaction temperature. Even at a heating rate of 10^4 K/sec, the particle reaches a final temperature of 900 °C in less than 100 msec. Thermal conductivity of gases has nothing to do with the ability of the gas to absorb energy, it reflects on its ability to transfer thermal energy. A gas molecule can absorb energy from an excited collision partner in a

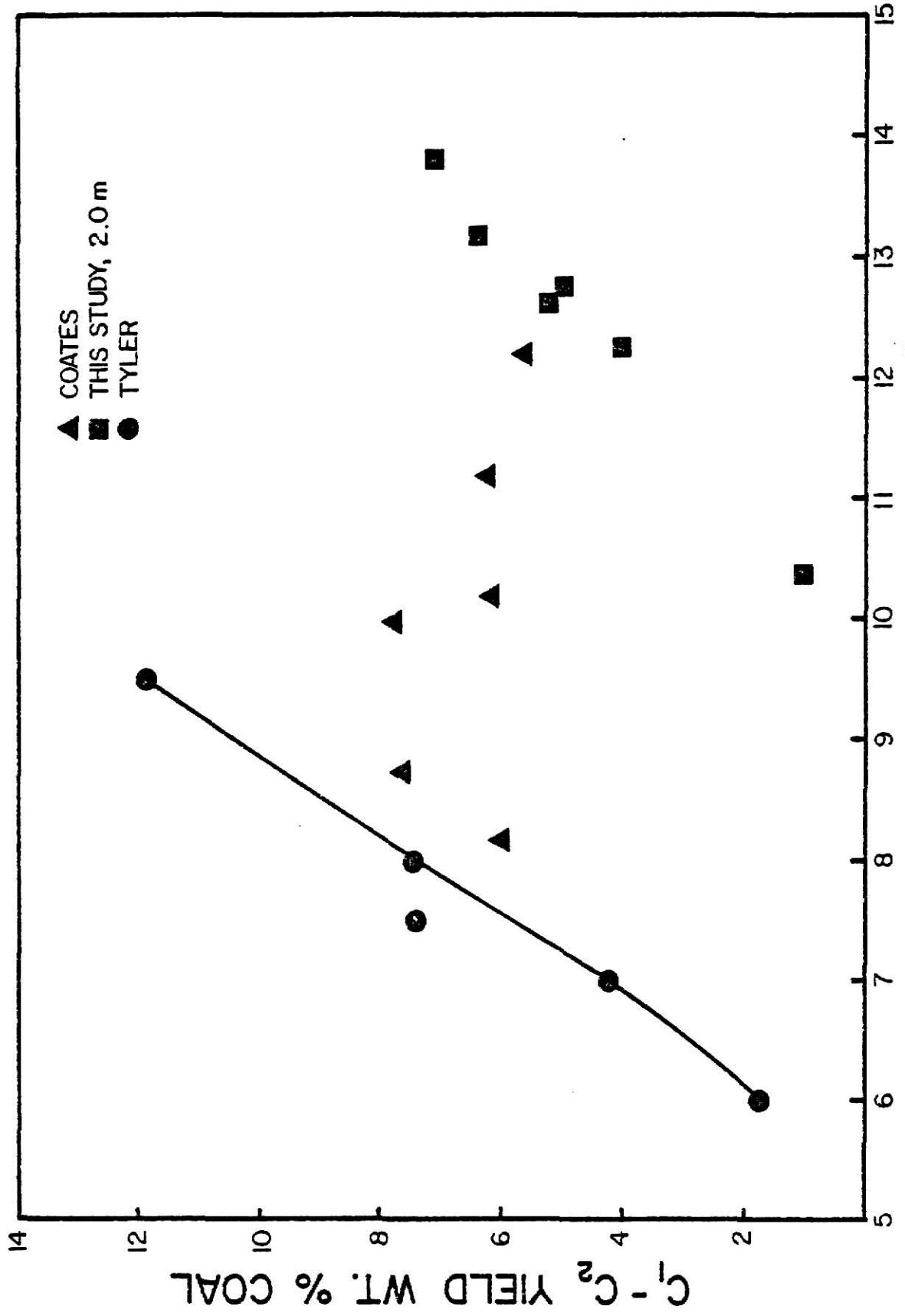

Fig. 38. C_1-C_2 hydrocarbon yields from pyrolysis in hydrogen atmospheres.

rotational mode, translational mode, or vibrational mode. The more available modes to absorb energy that a molecule possesses reflects on its ability as a third body. A third body enters into a chemical reaction by being the means by which the excess energy of the reaction is dissipated. For instance, if an excited methyl radical combines with an hydrogen atom to form methane, the methane will dissociate unless there is a means by which the excess energy can be removed.

In comparing the yields obtained by Tyler at 800 °C, methane yields are 8.6% in hydrogen, 4.2% in helium. The ratio of these values is 2.05. The third body efficiency of the hydrogen atmosphere (relative to a pure hydrogen atmosphere) is .77, while the third body efficiency of the helium atmosphere is .39. (Third body efficiencies are calculated for the gas mixture in the pyrolyser, hence they include any effects introduced by the nitrogen quench gas.) The ratio of the third body efficiencies is 1.97, quite close to the ratio of the yields. Thus, the effect of hydrogen on coal pyrolysis may be only a stabiliziation effect, not a chemical effect.

The fact that stabilization plays a dominant role in pyrolysis is displayed by the work of Banerjee et al.[66] Banerjee investigated coal pyrolysis at 1150 °C in atmospheres of nitrogen, argon, deuterated benzene, and in a vacuum. Pyrolysis yields obtained in all atmospheres exceeded those obtained *in vacuo*, with yields obtained in benzene exceeding those obtained in argon. Of more significance is that infrared spectrometry of the gaseous products obtained from pyrolysis in an atmosphere of benzene displayed no stretching modes characteristic of

the C-D bond. Thus, the increase in yields in the benzene atmosphere was apparently not due to chemical interaction.

In this investigation it has been noted that ethylene yields are unaffected by the hydrogen atmosphere. If the influence of hydrogen is mainly a chemical effect, ethane yields would be expected to increase at the expense of ethylene. This phenomena is not evident in the gas analysis. The reader is reminded of the benzene yields at low temperatures in an hydrogen atmosphere which are, perhaps, indicative of stabilization, but do not conclusively reject chemical interaction of hydrogen.

In summation, substantial gas and liquid conversions can be obtained at short residence times. Conversions of up to 50% of the volatile carbon to gases could theoretically be attained within 7 milliseconds at 1500 °K. Liquid yields are a strong function of time; optimal yields can be achieved in 1 millisecond. The maximum rate of benzene formation, 2.58×10^{-3} moles/sec occurred at 1386 K in an argon atmosphere. Benzene yields appeared in the pyrolysate at approximately 1000 K in hydrogen atmospheres; the maximum rate of benzene production, 1.50×10^{-3} moles/sec occurred at 1623 K and 2.0 milliseconds. Decomposition of benzene appeared to be inhibited by the presence of hydrogen.

4.0 RECOMMENDATIONS

Further studies to elucidate the role of hydrogen and other gaseous atmospheres on coal pyrolysis products and product distributions is warranted. Specifically, it is important to establish if third body stabilization plays a dominate role in coal pyrolysis or if chemical effects due to the surrounding atmosphere are most important. If third body stabilization is the dominate mode, greater pyrolysate yields and a change in pyrolysate product distributions could then be obtained by use of gases with better third body efficiencies (e.g., CO_2, H_2O).

Present technology is to maximize liquid yields by pyrolysing coal in hydrogen at short residence times. If increased liquid yields are attributed to third body effects, other less expensive gases could be substituted for hydrogen in these processes, while increasing or maintaining the liquid yield.

For conclusive proof to be obtained, it is suggested that further experiments be conducted with deuterium or deuterated water. Deuterium has a third body efficiency of approximately one, deuterated water approaches a third body efficiency of 15 (relative to hydrogen). Mass spectrometric analysis of the pyrolysate products will show if deuterium is being incorporated into the pyrolysis products (reflecting a chemical effect) or if deuterium is absent in the pyrolysate products (reflecting stabilization). To prevent random shuttling of hydrogen and deuterium in the pyrolysate products, experiments should be conducted at temperatures below 1400 K.

Liquid yields from coal pyrolysis appear to have a strong dependence on time, decreasing as time increases. It is suggested that a series of experiments be conducted at residence times less than or equal to one millisecond to determine maximum liquid yields. It has been postulated that liquid yields are a function of the aliphatic hydrogen content of the coal and that yields are independent of the surrounding gaseous atmosphere. If this is so, no deuterium will be present in the liquid yields obtained. To establish if liquid yields do correlate with aliphatic hydrogen content, experiments should be performed with coals of different rank.

REFERENCES

1. Ogden H. Hammond and Robert E. Baron, "Synthetic Fuels: Prices, Prospects, and Prior Art," American Scientist, 64, 407-417 (1976).

2. C. Y. Wen, R. C. Baile, C. Y. Lin, and W. S. O'Brien, in Coal Gasification, Advances in Chemistry Series, No. 131, (Am. Chem. Soc., Washington, D.C., 1974), pp. 9-28.

3. R. H. Essenhigh, Sixteenth Symposium (International) on Combustion (The Combustion Institute, PIttsburgh, Pa., 1977), p. 353.

4. Normand M. Laurendeau, "Heterogeneous Kinetics of Coal Char Gasification and Combustion," Prog. Energy Combust. Sci. 4, 221-270 (1978).

5. Donald B. Anthony and Jack B. Howard, "Coal Devolatilization and Hydrogasification," AIChE Journal, 22 (4), 625-656 (1976).

6. W. R. Seeker, "The Kinetics of Ignition and Particle Burnout of Coal Dust Suspensions Under Rapid Heating Conditions," Ph.D. Dissertation, Kansas State University, 1978.

7. Donald B. Anthony, "Rapid Devolatilization and Hydrogasification of Pulverized Coal," Sc.D. Thesis, Mass. Instit. Technol., 1974.

8. Stanley Badzioch and Peter G. W. Hawksley, "Kinetics of Thermal Decomposition of Pulverized Coal Particles," Ind. Eng. Chem. Process Des. Develop. 9 (4), 521-530 (1970).

9. American Society of Testing Materials, Designation ANSI/ASTM D3175-77, (1977).

10. David Gray, John G. Cogoli, and Robert H. Essenhigh, in Coal Gasification, Advances in Chemistry Series, No. 131, (Am. Chem. Soc., Washington, D.C., 1974), pp. 72-91.

11. D. C. Wegener, "The Production of Lower Molecular Weight Hydrocarbons During the Thermal Decomposition of Pulverized Coal in Air and Nitrogen," M.S. Thesis, Kansas State University, 1978.

12. M. Mentser, H. J. O'Donnell, S. Ergun, and R. A. Friedel, in Coal Gasification, Advances in Chemistry Series, No. 131, (Am. Chem. Soc., Washington, D.C., 1974), pp. 1-8.

13. D. W. Van Krevelen, Coal (Elsevier, Amsterdam, 1961), p. 266.

14. P. H. Given, Lecture notes prepared for the Short Course of Coal Characteristics and Coal Utilization at Pennsylvania State University, (1977).

References - Continued

15. John H. Campbell, "Pyrolysis of Subbituminous Coal Relation to In-situ Coal Gasification," Fuel 57 (4), pp. 217-224, (1978).

16. Irwin Glassman, Combustion, (Academic Press, New York, 1977), p. 245.

17. Eric M. Suuberg, William A. Peters, and Jack B. Howard, "Product Composition and Kinetics of Lignite Pyrolysis," Ind. Eng. Chem. Process Des. Develop. 17 (1), pp. 37-46 (1978).

18. Eric M. Suuberg, William A. Peters, and Jack B. Howard, Seventeenth Symposium (International) on Combustion, (The Combustion Institute, Pittsburgh, Pa., 1979), p. 117.

19. Mitsunori Makino and Yuzo Toda, "Relation Between Formation Rates of Methane and Hydrogen on Pyrolysis of Coal Under Pressure," Fuel 58 (8), pp. 573-576 (1979).

20. Ralph J. Tyler, "Flash Pyrolysis of Coals. 1. Devolatilization of a Victorian Brown Coal in a Small Fluidized Bed Reaction," Fuel 58 (9), pp. 680-686 (1979).

21. Ralph J. Tyler, "Flash Pyrolysis of Coals. Devolatilization of Bituminous Coals in a Small Fluidized Bed Reactor," Fuel 59 (4), pp. 218-226 (1980).

22. Soxhlet (trademark).

23. Peter R. Solomon and Meredith B. Colket, Seventeenth Symposium (International) on Combustion, (The Combustion Institute, Pittsburgh, Pa., 1979), p. 131.

24. Peter R. Solomon and Meredith B. Colket, "Evolution of Fuel Nitrogen in Coal Devolatilization," Fuel 57 (12), pp. 749-755 (1978).

25. J. M. Beer, "Drop Tube Experiments on Oils and Coals," presented at E.P.A. Fundamental Combustion Research Contractors Review Meeting, Newport Beach, Calif., January 1980.

26. Donald B. Anthony, Jack B. Howard, H. C. Hottel, and H. P. Meissner, Fifteenth Symposium (International) on Combustion, (The Combustion Institute, Pittsburgh, Pa., 1975), p. 1303.

27. Donald B. Anthony, Jack B. Howard, H. C. Hottel, and H. P. Meissner, "Rapid Devolatilization and Hydrogasification of Bituminous Coal," Fuel, 55, 121 (1976).

28. H. Jüntgen and K. H. Van Heek, Fortschritte der Chemischen Forshung, (Springer-Verlag, Berlin, 1970), 13, pp. 691-699.

References - Continued

29. Gary Breipohl, "Chemical Shock Tube Studies of Mechanisms of Grain Dust Ignition," M.S. Thesis, Kansas State University, 1979.

30. J. L. Johnson, in Coal Gasification, Advances in Chemistry Series, No. 131, (Am. Chem. Soc., Washington, D.C., 1974), pp. 145-178.

31. S. N. Vaughn, personal communication.

32. W. R. Seeker, M. P. Heap, G. S. Samuelsen, and J. D. Trolinger, "Thermaldecomposition of Pulverized Coal Particles," accepted for publication in Eighteenth Symposium (International) on Combustion, (The Combustion Institute, Pittsburgh, Pa., 1980).

33. Jayram Polavarapu, "Evolution of H_2S and SO_2 During Rapid Heating of Pulverized Coal and Sulfur Containing Model Compounds," M.S. Thesis, Kansas State University, 1979.

34. F. J. Dent, W. H. Blackburn, and H. C. Millet, Trans. Inst. Gas Eng., 88, 150 (1938-1939).

35. Herman F. Feldmann, J. A. Mima, and Paul M. Yavorsky, in Coal Gasification, Advances in Chemistry Series, No. 131, (Am. Chem. Soc., Washington, D.C., 1974), pp. 108-127.

36. E. J. Pyrcioch and H. R. Linden, Ind. Eng. Chem. 52, p. 590 (1960).

37. B. S. Lee, E. J. Pyrcioch, and F. C. Schora Jr., in Fuel Gasification, Advances in Chemistry Series, No. 69, (Am. Chem. Soc., Washington, D.C. 1967), p. 104.

38. Robert A. Graff, Samuel Dobner, and Arthur M. Squires, "Flash Hydrogenation of Coal. 1. Experimental Methods and Preliminary Results," Fuel 55, pp. 109-112 (1976).

39. Samuel Dobner, Robert A. Graff, and Arthur M. Squires, "Flash Hydrogenation of Coal. 2. Yield Structure for Illinois No. 6 Coal at 100 atm," Fuel 55, pp. 113-115 (1976).

40. A. L. Pelofsky, M. I. Greene, and C. J. LaDelfa, "Direct Production of Methane and Benzene from Coal," Energy Communications 3 (3), pp. 253-272 (1977).

41. J. A. Hamshar and S. J. Bivacca, "Evaluation of the Flash Hydropyrolysis Technique for Coal Gasification," Coal Processing Technology, Volume 5, (Am. Inst. Chem. Eng., New York, 1979) pp. 215-218.

42. Meyer Steinberg and Peter Fallon, "Flash Hydropyrolysis of Coal, Quarterly Report No. 4 for the period Oct. 1 to Dec. 31, 1977, NTIS #50821, (1978).

References - Continued

43. C. L. Oberg, "Partial Liquefaction of Coal by Direct Hydrogeneation," Quarterly report, April-June 1978, NTIS #2044-35 (1978).

44. A. I. Sass, "The Garrett Research and Development Co. Process for the Conversion of Coal into Liquid Fuels," presented at 65th Annual AIChE meeting, New York, November 29, 1972.

45. J. R. Martin, "Union Carbide Coalcon Process," presented at the Institute of Gas Technology Symposium on "Clean Fuels from Coal II," Chicago, Illinois, June 24, 1975.

46. "Char Oil Energy Development," U.S. Dept. of the Interior, Office of Coal Research, Report No. 73, prepared by FMC Corp., December, 1972.

47. R. L. Coates, C. L. Chen, and B. J. Pope, in Coal Gasification, Advances in Chemistry Series, No. 131, (Am. Chem. Soc., Washington, D.C. 1974), pp. 92-107.

48. R. L. Zahradnik and R. A. Glenn, "Direct Methanation of Coal," Fuel 50 (1), pp. 77-90 (1971).

49. F. Moseley and D. Paterson, Journal Inst. Fuel, 38 (288), p. 13 (1965).

50. S. Lewis, S. Friedman, and R. W. Hiteshue, in Fuel Gasification (Am. Chem. Soc., Washington, D.C., 1967) pp. 50-63.

51. R. A. Glenn, E. E. Donath, and R. J. Grace, in Fuel Gasification, (Am. Chem. Soc., Washington, D.C., 1967) pp. 81-103.

52. W. R. Seeker, "The Design, Assembly, and Testing of a Shock Tube for the Study of Coal Combustion Kinetics," M.S. Thesis, Kansas State University, 1977.

53. C. W. Kaufmann, P. Wolanski, E. Ural, J. A. Nichols, and R. VanDyk, in Proceedings of the International Symposium on Grain Dust, October 1979.

54. M. A. Field, D. W. Gill, B. B. Morgan, and P. G. W. Hawksley, Combustion of Pulverized Coal, (The British Coal Utilization Research Association, Leatherhead, England, 1967).

55. A. G. Gaydon and I. R. Hurle, The Shock Tube in High-Temperature Chemical Physics, (Reinhold Publishing Corporation, New York, 1963).

56. Ascher H. Shapiro, The Dynamics and Thermodynamics of Compressible Fluid Flow-Volume II, (Ronald Press Company, New York, 1954).

References - Continued

57. Russell R. Dutcher, personal communication, (1979).

58. Maurice J. Zuchrow and Joe D. Hoffman, Gas Dynamics Volume I, (John Wiley and Sons, New York, 1976).

59. S. L. Wittig, personal communication, (1979).

60. S. N. Vaughn, personal communication (1979).

61. Raymond H. Myers, Response Surface Methodology, (Allyn and Bacon, Inc., Boston, 1971).

62. S. N. Vaughn, "Isotopic Studies of the Chemical Mechanisms of Soot Formation," presented at the Central States Section/ The Combustion Institute, 1980 Spring Meeting, Baton Rouge, La.

63. P.S. Virk, L. E. Chambers, and H. N. Woebcke, in Coal Gasification, Advances in Chemistry Series, No. 131, (Am. Chem. Soc., Washington, D.C., 1974), pp. 237-258.

64. K. J. Laidler, Chemical Kinetics, (McGraw Hill, New York, 1965), pp. 187.

65. John R. Kershaw and Gordan Barass, "Deuterium Studies of Coal Hydrogenation," Fuel 56 (4), (1977).

66. Nara N. Banerjee, Gumma S. Murty, Hejamadi S. Rao, and Adinath Lahiri, Fuel 52 (4), pp. 168-170 (1973).

ACKNOWLEDGEMENTS

I wish to thank the departments of Mechanical and Nuclear Engineering for support provided in the form of a graduate research assistantship, and to extend my deepest appreciation to Dr. Paul Miller for encouraging me to pursue my studies for an advanced degree at Kansas State University.

This investigation would not have been possible without the support and guidance of Dr. Thomas Lester and Dr. J. Fred Merklin, to whom I wish to express my sincere graditude. I have the utmost respect for these two men whose friendly attitude makes for a most conducive learning atmosphere. Thank you for your patience and understanding, but more importantly, thank you for opening my eyes to the exciting world of research.

A very special note of thanks to Mr. Steve Vaughn, whose help has been invaluable. Steve not only taught me how to operate all the equipment, but always had time to listen to an idea and provide added insights.

Finally, I wish to thank Ms. Shelly Kemnitz for her skillful typing of this manuscript, and Mr. Charles O'Brien for his assistance in drafting the figures.

APPENDIX A

Experimental Procedure

To insure minimum contamination of solid products recovered and unambiguous gas samples, the following operational sequence is recommended.

1) Separate all shock tube segments at flanges and clean flanges of mylar particles. (Clean and re-grease O-rings if needed).
2) Open dump tank, remove aluminum blocks, clean dump tank of mylar particles. Clean tube length joining dump tank and shock tube with paper towels and acetone; blow out tube length with compressed helium. Clean aluminum blocks and replace in dump tank. Reassemble dump tank.
3) Reassemble shock tube segments to length desired.
4) Mount test section, place oxidation blocks in place, and mount end wall.
5) Insert aluminum diaphragm, check that all inlet valves are closed, open valves to pumps, and evacuate shock tube.
6) Check for leaks, re-tighten bolts at flanges if necessary.
7) When shock tube is evacuated to less than 10^{-3} torr, close valves to vacuum pumps.
8) Open valve on oxygen/argon gas mixture, open valve to gas inlet line, open gas inlet line valve to shock tube and fill low pressure section to 40 torr with oxygen/argon mixture.
9) Close all valves, and close valve to vacuum gauge.
10) Fill driver section with 225 psia helium gas.
11) Recheck all inlet valves; all valves must be closed.
12) Burst diaphragm.
13) Vent shock tube.

14) Repeat steps 5 through 13.

15) Remove end flange, and clean test section of any mylar particles.

16) Repeat steps 5 through 15 until there is no visible contamination by mylar.

17) Insert aluminum diaphragm.

18) Insert aluminum sleeve into test section.

19) Replace 2 μm stainless steel filter into gas venting line.

20) Replace 2 μm stainless steel filter into gas sampling line.

21) Mount gas venting saddle block on shock tube.

22) Mount end wall.

23) Mount gas sample bottle on gas sampling line.

24) Mount gas sampling line on shock tube.

25) Weigh dispersion plate.

26) Place 40 mg coal on dispersion plate.

27) Mount dispersion plate into saddle block, and mount saddle block on shock tube.

28) Close all inlet valves to shock tube, and open valve to gas sample bottle.

29) Evacuate shock tube to 10^{-3} torr.

30) Close valve to gas sample bottle, and close valve to pumps.

31) Fill low pressure section to desired pressure with argon gas.

32) Close off dump tank.

33) Re-evacuate shock tube and gas inlet line.

34) When shock tube is evacuated to less than 10^{-3} torr close valves to pumps.

35) Fill low pressure section to desired pressure with desired test gas mixture.

36) Check that all inlet valves to the shock tube are closed, and close valve to vacuum gauge.

37) Reopen dump tank to shock tube.

38) Fill driver section with helium to desired pressure.

39) Recheck that all valves are closed.

40) Reset digital timer and set trigger on oscilloscope.

41) Rupture diaphragm.

42) Shut isolation ball valve isolating test section from rest of shock tube.

43) Allow test section to remain isolated for one hour.

44) While test section is isolated mount activated charcoal filter into gas venting line.

45) Wrap heating tape around test section, and place thermocouple between heating tape and shock tube wall.

46) Place insulation over heating tape.

47) Vent shock tube upstream from ball valve.

48) Remove ruptured diaphragm.

49) Insert new diaphragm.

50) After test section has been isolated for one hour, heat test section to an outside wall temperature of 128 °C.

51) Immediately after reaching desired temperature, open valve to gas sample bottle. Allow time for gas sample bottle and test section to reach an equilibrium pressure.

52) Weigh fresh kim wipe† in preparation for cleaning saddle blocks and end flange.

---

†Trademark of Kimberly Clark Corporation.

53) Close valve to gas sample bottle.

54) Open valve on gas venting line, vent gas over charcoal filter at a flow rate of 1 liter/min using flow control valve.

55) After complete venting, remove activated charcoal filter and cap ends.

56) Remove gas sample bottle.

57) Remove 2 μm filter elements from venting line and sampling line.

58) Remove dispersion plate saddle block, and remove dispersion plate and weigh. Wipe off any residue on saddle block using kim wipe.

59) Remove gas venting saddle block, and wipe off any residue present using kim wipe.

60) Remove end flange, and wipe off residue on end flange.

61) Weigh filter elements.

62) Reweigh kim wipe, determine amount of residue that has been deposited on saddle blocks and end flange.

63) Using the sleeve extractor, gently remove aluminum sleeve from test section. Cap ends of sleeve.

64) Tape openings on sleeve, place sleeve in shipping cannister.

65) Reopen isolation ball valve.

66) Clean test section and ball valve with paper towels and acetone.

67) Replace end flange and saddle blocks.

68) Open valves to pumps, evacuate shock tube.

69) Repeat steps 6 through 13.

70) During (69) clean dispersion plate and weigh new coal sample.

71) Begin again at (17).

72) When shipping cannister is full, purge with argon gas.

APPENDIX B
Error Analysis

The global activation energies determined in Chapter 3.0 have an associated error due to uncertainties in experimental data used to determine these energies. The major source of error in the calculation of activation energies is due to the temperature measurement which can deviate as much as 50 K.[63] Using the method of progressive error as discussed by Breipohl,[29] a standard deviation for the activation energy is determined by the standard deviations of the parameters used in the activation energy calculation. The expression used to calculate the activation energy was given as

$$\ln\left\{\frac{1}{t}\left(-\ln\left(\frac{V^*-Vg}{V^*}\right)\right)\right\} = \ln A - \frac{E_A}{RT} \qquad (B1)$$

The independent variables are t, T, V* and Vg. Taking the partial derivative of E_A with respect to each of these variables yields

$$\frac{\partial E_A}{\partial T} = -R\left\{\ln\left[\frac{1}{t}\left(-\ln\frac{(V^*-Vg)}{V^*}\right)\right] - \ln A\right\} , \qquad (B2)$$

$$\frac{\partial E_A}{\partial t} = \frac{RT}{t} , \qquad (B3)$$

$$\frac{\partial E_A}{\partial V^*} = \left(\frac{-RT}{\ln\left(\frac{V^*-Vg}{V^*}\right)}\right)\left(\frac{Vg}{V_*^2 - VgV_*}\right) , \qquad (B4)$$

$$\frac{\partial E_A}{\partial Vg} = \left(\frac{-RT}{(V_*-Vg)}\right)\left(\frac{1}{\ln\left(\frac{V_*-Vg}{V_*}\right)}\right) . \qquad (B5)$$

The standard deviation σ_E of the activation energy is

$$\sigma_E = \left\{\left(\frac{\partial E_A}{\partial T}\right)^2 \sigma_T^2 + \left(\frac{\partial E_A}{\partial t}\right)^2 \sigma_t^2 + \left(\frac{\partial E_A}{\partial V_*}\right)^2 \sigma V_*^2 + \left(\frac{\partial E_A}{\partial V_g}\right)^2 \sigma Vg^2\right\}^{1/2} \qquad \text{(B6)}$$

where σ_T, σ_t, σ_{V*} and σ_{vg} are the standard deviations of the subscripted variables. The uncertainties in T and t are 50 K and 4.0×10^{-4} sec respectively, the uncertainty of V_* is assumed to be 10% of V_* and the uncertainty of V_g is 10% of the mean value obtained over the temperature range used in this experimentation. Solving Eq. (B6) at a time of 2 msec and a temperature of 1285 K yields a standard deviation of 1.09 kcal/mole.

SHORT RESIDENCE TIME PYROLYSIS AND HYDROPYROLYSIS OF BITUMINOUS COAL

by

Sharon Lee Szydlowski

B.S., University of Wisconsin-Milwaukee, 1978

AN ABSTRACT OF A MASTER'S THESIS

submitted in partial fulfillment of the
requirements for the degree

Master of Science

Department of Mechanical Engineering
KANSAS STATE UNIVERSITY
Manhattan, Kansas

1980

ABSTRACT

An investigation of the devolatilization behavior of a bituminous coal during short residence times in atmospheres of argon and argon/hydrogen mixtures was conducted in a single pulse shock tube. Devolatilization behavior was studied over the temperature range of 1000 to 1900 K and at residence times varying from .5 to 3.0 milliseconds. Total reaction pressure was maintained at 10 $\pm$ 1 atm; hydrogen partial pressures were varied from .62 to 4.1 atm. Gaseous and liquid pyrolysis products were collected and analyzed by gas chromatography for lower C_1-C_2 hydrocarbons, benzene, and toluene. Solid samples were recovered and analyzed by infrared spectrometry.

Major devolatilization products from pyrolysis in an argon atmosphere were methane, ethylene, acetylene and benzene. Methane and ethylene yields increased with increasing temperature up to 1550 K where they reached their maximum values of 3.6 and 2.5 w/w (carbon in coal) before declining. Acetylene yields increased with increasing temperature, never declining over the temperature range studied. Maximum acetylene yields were 3.0 w/w at 1732 K and 2.0 milliseconds. Maximum benzene yields occurred at 1593 K and 2.0 milliseconds; however benzene production displayed a strong dependence on time, generally displaying increased yields at very short residence times.

Major devolatilization species from pyrolysis in hydrogen/argon mixtures were also methane, ethylene, acetylene, and benzene. Acetylene and ethylene yields showed little or no increase over yields obtained in an argon atmosphere. Above 1400 K methane yields began

exceeding those obtained in an argon atmosphere, reaching a maximum value of 4.45 w/w at 1509 K, 3.0 milliseconds, and an hydrogen partial pressure of .98 atm. Benzene yields did not greatly exceed those obtained in an argon atmosphere; however, benzene began appearing in the pyrolysate at lower temperatures than in an argon atmosphere.

Global activation energies and pre-exponential factors were determined using a decomposition model, first order in light hydrocarbon gases yet to be evolved. Argon pyrolysis yielded a global activation energy of 24.7 kcal/mole with a pre-exponential factor of 2.93×10^5 sec^{-1}. Hydrogen/argon pyrolysis yielded a global activation energy of 21.9 kcal/mole and pre-exponential factor of 1.50×10^5 sec^{-1}. Of primary importance is the finding that given sufficiently fast heating rates, yields of volatile products comparable to those observed in previous studies at much longer residence times can be obtained in only 3 msec. Although the effect of an hydrogen atmosphere is to increase product yields, it has not yet been conclusively shown whether the hydrogen influence is a chemical effect or a stabilization effect. Comparison of the results of this study with those of previous investigators suggests the increase in product yields in an hydrogen atmosphere to be due to more effective stabilization of the devolatilization products by third body collisions with hydrogen.